



2016-03-01

Evaluation of the Accuracy of Approach Volume Counts and Speeds Collected by Microwave Sensors

Gregory Hans Sanchez
Brigham Young University - Provo

Follow this and additional works at: <https://scholarsarchive.byu.edu/etd>

 Part of the [Civil and Environmental Engineering Commons](#)

BYU ScholarsArchive Citation

Sanchez, Gregory Hans, "Evaluation of the Accuracy of Approach Volume Counts and Speeds Collected by Microwave Sensors" (2016). *All Theses and Dissertations*. 5850.
<https://scholarsarchive.byu.edu/etd/5850>

This Thesis is brought to you for free and open access by BYU ScholarsArchive. It has been accepted for inclusion in All Theses and Dissertations by an authorized administrator of BYU ScholarsArchive. For more information, please contact scholarsarchive@byu.edu, ellen_amatangelo@byu.edu.

Evaluation of the Accuracy of Approach Volume Counts and Speeds

Collected by Microwave Sensors

Gregory Hans Sanchez

A thesis submitted to the faculty of
Brigham Young University
in partial fulfillment of the requirements for the degree of

Master of Science

Mitsuru Saito, Chair
Grant G. Schultz
Dennis L. Eggett

Department of Civil and Environmental Engineering

Brigham Young University

March 2016

Copyright © 2016 Gregory Hans Sanchez

All Rights Reserved

ABSTRACT

Evaluation of the Accuracy of Approach Volume Counts and Speeds Collected by Microwave Sensors

Gregory Hans Sanchez
Department of Civil and Environmental Engineering, BYU
Master of Science

This study evaluates the accuracy of approach volumes and free flow approach speeds collected by the Wavetronix SmartSensor Advance sensor using the field data collected by JAMAR counter boards for free flow approach volumes and a TruCam LiDAR gun for approach speeds. The Advance sensor is primarily designed for dilemma zone reduction. It does not have the capability to differentiate between lanes, but the Advance sensor currently used has a detection range of up to 600 ft. and has the capability to track vehicles approaching the intersection. The Utah Department of Transportation (UDOT) wanted to use this capability to get added values from their investment in the Advance sensors.

The approach volume accuracy was analyzed with three factors: sensor position, number of approach lanes, and approach volume level. The results showed that the high accuracy is achieved when the number of approach lanes is low, or closer to one-lane, and the approach volume level is low. It was found that the accuracy of the approach volume counts was not affected by the sensor position. As a result of the sensor's inability to differentiate lanes, the more cars travel alongside each other, the more likely they are to be detected together as one vehicle. The overall range of accuracy for the approach volume counts was found to range from approximately 76% (24% undercount) to 106% (6% overcount).

The accuracy of approach speeds was analyzed with two factors: the number of lanes and offset position of the lanes relative to the location of the speed gun. First, the lane position and offset were tested to see if any effect exists on the difference between the measurements of the speed by the LiDAR gun and the Advance sensor. Then the difference between mean speeds was tested. Each site was analyzed individually and there were some sites which had a statistically significant difference while there were others which did not. However, the difference was considered not to be practically significant because of the difference in mean speeds of the sample being approximately ± 2 mph. The speeds were also used to calculate the 85th percentile speed for all sites with more than 50 samples. For these sites, the average difference in 85th percentile speed was -0.43 mph, the biggest negative difference was -1.6 mph, and the biggest positive difference was 1.5 mph. Because of the limited number of samples taken at each site, a statistical resampling method called Bootstrapping was performed to predict the expected distribution of speed differences in 85th percentile speeds. The results of this analysis also showed the 85th percentile speeds by the LiDAR gun and the Advance sensor were not significantly different for practical traffic engineering applications. However, it is recommended that more research be performed to better understand the applicability of 85th percentile speed measurements.

Keywords: Wavetronix SmartSensor Advance, approach volume, approach speed, 85th percentile speed, accuracy, Signal Performance Metrics

ACKNOWLEDGEMENTS

The author would like to acknowledge Dr. Mitsuru Saito for his support and advice throughout the entire course of the research project, as well as all the members of the Technical Advisory Committee (TAC), especially Mark Taylor, Jamie Mackey, and Adam Lough from UDOT, and Roger Sun, Brad Giles, and Bryan Jarrett from Wavetronix, for their invaluable input and assistance during the entire course of the data collection and analysis process. The author would also like to recognize Dr. Grant Schultz from the BYU Civil Engineering Department for his input in this project and Dr. Dennis Eggett from the BYU Statistics Department for his guidance and assistance in performing the statistical analysis of this research. Also a special thanks to my parents and my wife, Emily, for their endless support and for encouraging me to pursue a Master's degree.

TABLE OF CONTENTS

LIST OF TABLES.....	vii
LIST OF FIGURES.....	ix
1 Introduction.....	1
1.1 Problem Statement.....	1
1.2 Objectives.....	2
1.3 Thesis Organization.....	2
2 Literature Review.....	3
2.1 Digital Wave Radar.....	3
2.1.1 Features.....	4
2.1.2 Mounting.....	7
2.1.3 Physical Properties.....	8
2.2 Other Speed Detection Methods.....	9
2.2.1 Laser Speed Measurement.....	9
2.2.2 In-Road Speed Measurement.....	10
2.3 Chapter Summary.....	13
3 Methodology.....	15
3.1 UDOT Signal Performance Metrics Website and the Factors Tested.....	15
3.1.1 UDOT Application of the Advance Sensor.....	19
3.1.2 Factors Tested for Approach Volumes.....	20
3.1.3 Factors Tested for Approach Speeds.....	22
3.2 Approach Volume Data Collection.....	23
3.2.1 Volume Data Collection.....	23
3.2.2 Data Reduction.....	26

3.2.3	Hi-res Data	26
3.3	Speed Data Collection	34
3.3.1	TruCam Speed Gun.....	34
3.3.2	Calibration of the LiDAR Speed Gun.....	40
3.3.3	Data Collection	43
3.3.4	Data Reduction.....	61
3.4	Chapter Summary	74
4	Results	76
4.1	Approach Volume Accuracy	76
4.1.1	Raw Data.....	77
4.1.2	Statistical Test Performed	77
4.1.3	Analysis Results.....	78
4.2	Mean Approach Speed Comparison	83
4.2.1	Cosine Effect.....	84
4.2.2	Raw Data.....	84
4.2.3	Statistical Tests Performed	85
4.2.4	Results of Statistical Analyses	87
4.3	85 th Percentile Approach Speed Comparison	89
4.3.1	Raw Data.....	89
4.3.2	Statistical Test Performed	91
4.3.3	Results of Statistical Analysis.....	92
4.4	Chapter Summary	98
5	Applications	101
5.1	Approach Volume.....	101
5.2	Approach Speed.....	104

5.3	Chapter Summary	105
6	Conclusions and Recommendations	106
6.1	Summary of Findings.....	106
6.1.1	Approach Volume.....	107
6.1.2	Approach Speed.....	107
6.2	Conclusion	108
6.3	Recommendations.....	109
	List of Acronyms	110
	References.....	111
	Appendix A: Speed Gun Calibration Data.....	113
	Appendix B: Raw Volume Data.....	116
	Appendix C: Raw Approach Speed Data	119
	Appendix D: Results of Paired t-Test for Means	153
	Appendix E: Results of Bootstrapping Method on 85th Percentile Speeds.....	161

LIST OF TABLES

Table 3-1: Event Codes Used in Approach Volume Reduction	20
Table 3-2: Measured Speed Compared to True Speed by Angle of Measurement	36
Table 3-3: Percentage of True Speed Measured Given the Distance Offset from the Vehicle's Path and the Distance to the Target Vehicle.....	36
Table 3-4: Factors for the Eastbound Approach.....	38
Table 3-5: Factors for the Westbound Approach.....	38
Table 3-6: True Speed for the Eastbound Approach Based on Measured Speed and the Lane Number.....	39
Table 3-7: True Speed for the Westbound Approach Based on Measured Speed and the Lane Number.....	39
Table 3-8: Speed Gun Calibration Sample Results.....	43
Table 3-9: Paired t-Test for Means for LiDAR Calibration	44
Table 3-10: The Detection Zone Distance and Number of Lanes of Each Sample Site.....	56
Table 3-11: Data Reduction Summary Table	75
Table 4-1: The Sample Compiled Approach Volume Data.....	78
Table 4-2: Number of Samples (# of sites / # of total samples taken).....	80
Table 4-3: Mean Accuracy for Factor Combinations	80
Table 4-4: Standard Deviation of Accuracy	80
Table 4-5: 95 Percent Confidence Interval of the Mean.....	81
Table 4-6: Results of Tests on Fixed Effects on Approach Volume	81
Table 4-7: Results of the Tukey-Kramer Test	82
Table 4-8: Sample Approach Speed Data.....	86
Table 4-9: Assigned Treatments	86
Table 4-10: Results of Mixed-Model ANOVA on Mean Approach Speed.....	87
Table 4-11: Least Squares Means Result for Approach Speed.....	88

Table 4-12: Paired Two-Sample for Means t-Test	90
Table 4-13: Numbering of Approaches Used in 85th Percentile Analysis.....	93
Table 4-14: 85th Percentile Speeds and Differences	93
Table 5-1: Combined Sample Size	103
Table 5-2: Combined Mean Accuracy.....	103
Table 5-3: Combined Standard Deviation of Accuracy.....	103
Table 5-4: Combined 95% Confidence Interval of the Mean.....	103
Table 5-5: Mean Multiplication Factors	104
Table 5-6: 95% Confidence Interval Multiplication Factors	104

LIST OF FIGURES

Figure 2-1: Virtual loops created by the sensor for vehicle tracking	5
Figure 2-2: The dilemma zone.....	7
Figure 2-3: Possible mounting locations of SmartSensor Advance.....	8
Figure 2-4: Exterior view of Advance sensor.....	9
Figure 2-5: LiDAR technology used to measure speed.....	10
Figure 2-6: Sensitivity of inductive loops to vehicles of various heights.....	11
Figure 2-7: Inductive loop in relation to a traveling vehicle.....	12
Figure 3-1: UDOT's SPMs website	16
Figure 3-2: Graphical representation of the approach volume counts.....	17
Figure 3-3: Graphical representation of the speed data.....	18
Figure 3-4: Description of the sensor positions	22
Figure 3-5: JAMAR counter board.....	24
Figure 3-6: Data collection sheet.....	25
Figure 3-7: JAMAR counter output table.....	28
Figure 3-8: Count spreadsheet input table.....	29
Figure 3-9: Count spreadsheet output table.....	30
Figure 3-10: SQL output with controller events.....	31
Figure 3-11: Spreadsheet used to find start time based on time gap between vehicles.....	32
Figure 3-12: Spreadsheet used to find start time based on a green phase start.....	33
Figure 3-13: Spreadsheet used to find the number of vehicles counted by the sensor.....	33
Figure 3-14: Image of the speed gun	35
Figure 3-15: Image portraying painted lines used in LiDAR calibration	42
Figure 3-16: Graphical representation of the results from the LiDAR calibration.....	44

Figure 3-17: Flowchart of the approach speed data collection process.....	46
Figure 3-18: Traffic video recorded of an approach with timestamp	47
Figure 3-19: Image of the inside of a traffic controller box	47
Figure 3-20: Double taped Advance cables with bridge ports above the cables	48
Figure 3-21: Computer connected to the sensor for data collection	48
Figure 3-22: Data collector connecting the computer to the sensor	49
Figure 3-23: SSM Advance program opening window.....	50
Figure 3-24: SSM Advance connection window.....	51
Figure 3-25: SSM Advance sensor selection window.....	51
Figure 3-26: SSM Advance sensor connecting window.....	52
Figure 3-27: SSM Advance sensor options window.....	52
Figure 3-28: SSM Advance sensor tracking display.....	53
Figure 3-29: SSM Advance log file window.....	53
Figure 3-30: SSM Advance sensor screen ready for recording.....	54
Figure 3-31: Graph of the approach speed with sensor information from the SPMs website.....	55
Figure 3-32: Speed data collection page.....	57
Figure 3-33: The screen of the gun while collecting data.....	59
Figure 3-34: Measuring out the distance to place the cone.....	60
Figure 3-35: Collecting speed data (front view).....	60
Figure 3-36: Collecting speed data (back view).....	61
Figure 3-37: Flowchart of the approach speed data reduction process.....	62
Figure 3-38: Final combined video.....	64
Figure 3-39: Image provided by the LiDAR gun.....	65
Figure 3-40: The sensor video and traffic video to match the LiDAR picture.....	66
Figure 3-41: Spreadsheet matching picture and sensor video data.....	67

Figure 3-42: Example of a log file as recorded by the SmartSensor Advance.	68
Figure 3-43: SQL server approach speed output.	70
Figure 3-44: Spreadsheet showing the log file data along with the Hi-res data.	73
Figure 3-45: Spreadsheet showing completed data reduction of speed data.	73
Figure 4-1: Speed distributions created by Bootstrapping for approach 1.	95
Figure 4-2: 85 th percentile speed distributions created by Bootstrapping for approach 1. ...	96
Figure 4-3: Expected 85 th percentile speed difference distribution created by Bootstrapping for approach 1.....	96
Figure 4-4: Speed distributions for approach 5.....	97
Figure 4-5: 85 th percentile speed distributions for approach 5.	97
Figure 4-6: Expected 85 th percentile speed difference distribution for approach 5.....	98

1 INTRODUCTION

Performance metrics are a way for traffic engineers, roadway designers, and the Utah Department of Transportation (UDOT) engineers to observe and evaluate the condition of highways. Approach volume and speed are important metrics in evaluating the performance of their highways and streets. Wavetronix has developed the SmartSensor Advance™ (hereafter referred to as an Advance sensor), which is a microwave radar sensor that was originally developed for dilemma zone control at signalized intersections. Added functions to this sensor are the ability to count the number of approaching vehicles and measure the approach speed at an intersection. UDOT has purchased and installed many Advance sensors at various signalized intersections throughout the state. The approach volume and speed data obtained by these sensors are placed in the UDOT Signal Performance Metrics (SPMs) website, which became public in 2012 (UDOT 2015).

In this Introduction the problem statement, objectives of the study, and the thesis organization are presented.

1.1 Problem Statement

Now that the SPMs website has been made available to the public, UDOT desired to calibrate the accuracy of approach volumes and speeds collected by Advance sensors to determine if an adjustment factor needs to be applied to the metric values reported by Advance sensors so these metrics can be used for traffic engineering applications.

1.2 Objectives

The first objective of this study was to collect the ground truth approach volume counts and approach speeds and statistically compare them with the approach volumes and speeds collected by Advance sensors to evaluate if any of the factors selected by UDOT engineers, including sensor position, level of traffic volume, number of approach lanes, and lane position, would significantly affect the accuracy of approach volume and speed. The second objective was to use the results from the statistical analysis to recommend a calibration factor, if needed, and recommend how the results could be incorporated in UDOT's SPMs.

1.3 Thesis Organization

This thesis consists of six chapters: 1) Introduction, 2) Literature Review, 3) Methodology, 4) Results, 5) Applications, and 6) Conclusions, followed by a list of references and several appendices, which contain all of the raw data and raw outputs from the statistical analysis performed in this study.

Chapter 1 presents the problem statement, objectives, and report organization. Chapter 2 contains the results of literature review, consisting of a description of the Advance sensor and descriptions of various other methods of speed data collection. Chapter 3 discusses the procedure and methods used in collecting the ground truth data, collecting the sensor data, downloading the data from the UDOT database, and reducing both the ground truth and sensor data. Chapter 4 presents the results from the statistical analyses performed on approach volume and speed. Chapter 5 discusses the potential applications of the sensor data, based on the results of the statistical analyses for approach volume and speed. Chapter 6 then presents the concluding remarks, key findings from the study of the Advance sensor, and recommendations for further research.

2 LITERATURE REVIEW

The device to be discussed in this thesis is the Wavetronix SmartSensor Advance™ (also referred to as the Advance sensor) version 3.2.0 for approach volume and speed data collection. The various SmartSensor devices designed by Wavetronix are for use in arterial, intersection or rail crossing management. The Advance sensor is the companion to the SmartSensor Matrix™ sensor used for intersection traffic management. The features and functions of the Advance sensor, although in some aspects are similar to the Matrix, are unique in its application. For information about the various types of volume detection devices and counting methods, refer to sections 2.1 and 2.2 of the Volume 1 report of this study (Saito et al. 2015). Please note that the Advance sensor was used as a representative of microwave sensors in this study because it is the sensor currently used by UDOT for collecting approach volume and speed data for the SPMs. This study is not intended to endorse the use of a particular microwave sensor for data collection.

In this chapter the results and findings of the literature review on digital wave radar and other speed detection methods are presented.

2.1 Digital Wave Radar

The Wavetronix SmartSensor Advance™ sensor is a traffic detection device which uses Digital Wave Radar (DWR) technology to collect traffic data. This type of radar is digitally created so that the bandwidth is maintained at the desired level without being adversely affected by changes

in temperature or deterioration over time. The DWR has the ability to produce “a stable signal that continues to perform accurately over time without being reconfigured” (Wavetronix 2015c).

2.1.1 Features

The various features of the Advance sensor include a detection range of 600 feet, continuous vehicle tracking; dynamic virtual sensing zones; criteria-based signaling, meaning the dynamic adjustment of signal timing as needed; and safe arrival, which is used in eliminating the dilemma zone of approaching vehicles (Wavetronix 2015a). The Advance sensor has the ability to track and collect data from the approaching vehicle for a longer distance than other sensors developed by Wavetronix, providing more useful and accurate data than the data collected in the field by human data collectors. Because of the greater sensing range, larger vehicles can be detected at even greater distances than smaller vehicles.

The continuous vehicle tracking feature allows the sensor to collect data from an approaching vehicle which includes the range, or distance from the stop bar, of each vehicle, as well as the speed and the estimated time of arrival (ETA) of a vehicle to the stop bar. The Advance sensor can be used to “determine the time, location and size of gaps in flowing traffic” (Wavetronix 2015a). The data collected by the Advance sensor using this feature is dynamic in that it can calculate a change in speed and in ETA as the approach vehicle nears the stop bar.

The dynamic sensing zones of the Advance sensor allow for various zones to be assigned to the approach and they each can be assigned to be activated based on the vehicle’s range, speed and ETA. This is unique when compared to inductive loops. The “virtual loops” created within the sensor range can be activated selectively based on the setup and user defined criteria. Figure 2-1 shows how the virtual loops can track an approaching vehicle at an intersection as shown in the bottom image, as opposed to the top image, that has standard inductive loop detectors that only

detect a smaller range. Because the Advance sensor can have up to 8 channels, an intersection can accommodate up to 8 different approach directions or movements for each approach. It is important to note that for the Advance sensor, the virtual loops do not differentiate between lanes (Wavetronix 2015a). This can also be seen in Figure 2-1. As the second vehicle is being detected, the entire width of the count zone, being three-lanes, is illuminated, including the area before and after the vehicle. As the vehicle continues to move forward, the detection zones behind the vehicle turn off and the ones in front turn on.

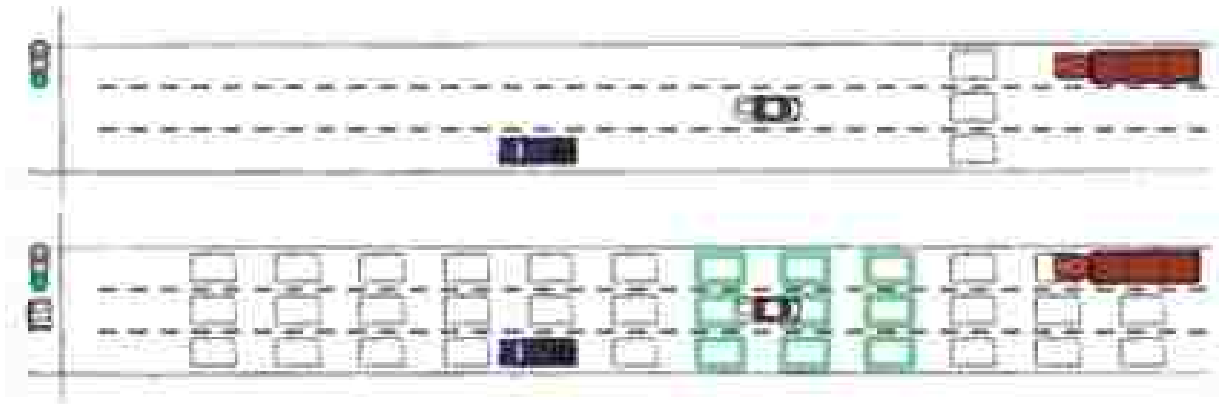


Figure 2-1: Virtual loops created by the sensor for vehicle tracking (Wavetronix 2015a).

The Advance sensor uses the information collected from the approaching vehicles, such as selected ranges, speeds, ETAs or the number of vehicles counted as the parameters to extend a green light. This ability to change the signal timing based on the conditions at the intersection approach is referred to as criteria-based signaling and it allows the use of user-defined criteria to allow the signal to respond accordingly in certain situations, such as a fast moving vehicle approaching an intersection, depending on how the signal is programmed to respond to particular vehicle-moving patterns. This ability allows for each intersection to safely and effectively manage traffic as desired by the traffic engineer (Wavetronix 2015a).

The Safe Arrival feature is the main purpose and function of the Advance sensor. Though it is outside the scope of this research, this main feature of the Advance sensor is briefly described here as background information. The feature refers to the sensor's ability to calculate the dilemma zone of approach vehicles. The dilemma zone is defined by Wavetronix as "an area approximately 2.5 to 5 seconds away from the intersection stop bar in which a driver, when faced with a yellow light, must decide whether to stop or proceed through the intersection and try to beat the red light: stopping increases the risk of a rear-end collision and proceeding to enter the intersection increases the risk for right-angle crashes" (Wavetronix 2015c). Reducing the dilemma zone is important and the Advance sensor assists in doing so by calculating the time the green light can be extended to allow the oncoming vehicles that would have trouble slowing down to make it through the intersection before the commencement of the red phase. Figure 2-2 shows a graphical representation of the likeliness of a vehicle to stop or continue through an intersection upon seeing the traffic signal change from green to yellow. The area in the middle in red is classified as the dilemma zone where the driver is unsure if they will be able to make it through the intersection or if they can stop. The sensor would incorporate the various features of this system to ensure that the green lights are not extended for slower traveling vehicles but that they are extended for faster traveling vehicles that do need more time and space in order to safely slow down and stop. The sensor would take into account the actual speeds of the car as opposed to the commonly used design speed which is generally based on the 85th percentile of a sample of the traveling speeds of vehicles through that intersection. Using the actual speeds, the sensor is able to use more accurate ETA calculations to reduce the dilemma zone and ensure the safe approach of the traveling vehicles to the intersection.

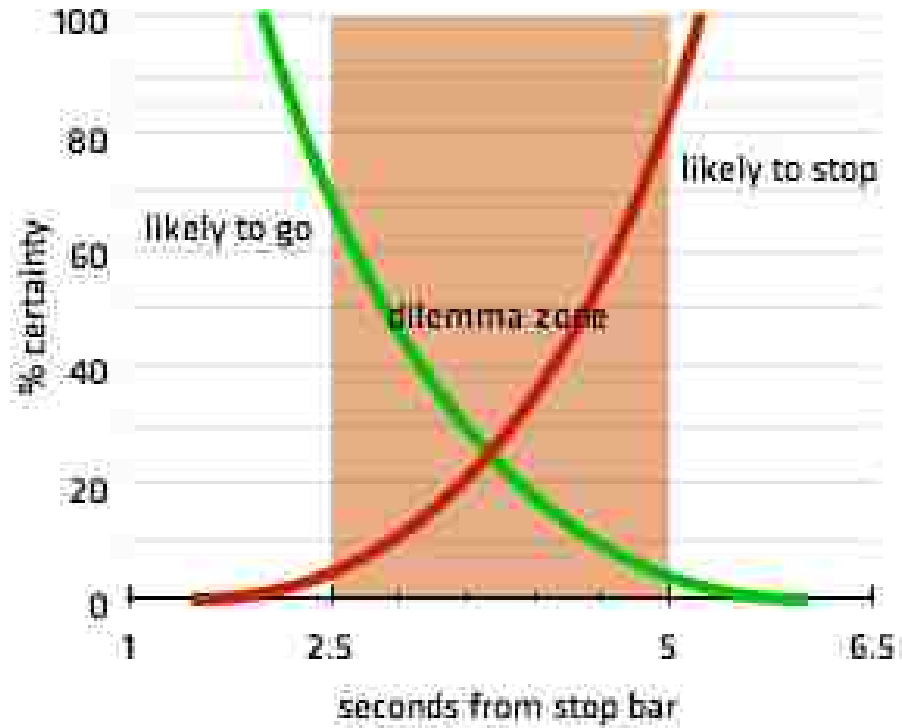


Figure 2-2: The dilemma zone (Wavetronix 2015c).

2.1.2 Mounting

While mounting, or installing, the sensor, it is important to ensure that there are no physical barriers that may block the radar from reaching the approaching vehicles. The Advance sensor has various mounting and installation options. It can be mounted at a maximum distance of 50 feet from the center of the approach lanes and an installation height range of 17 to 40 feet. It can be mounted on either a vertical pole or horizontal mast arm. Figure 2-3 shows the possible mounting locations of Advance sensors, which are shown as blue circles (Wavetronix 2015b).

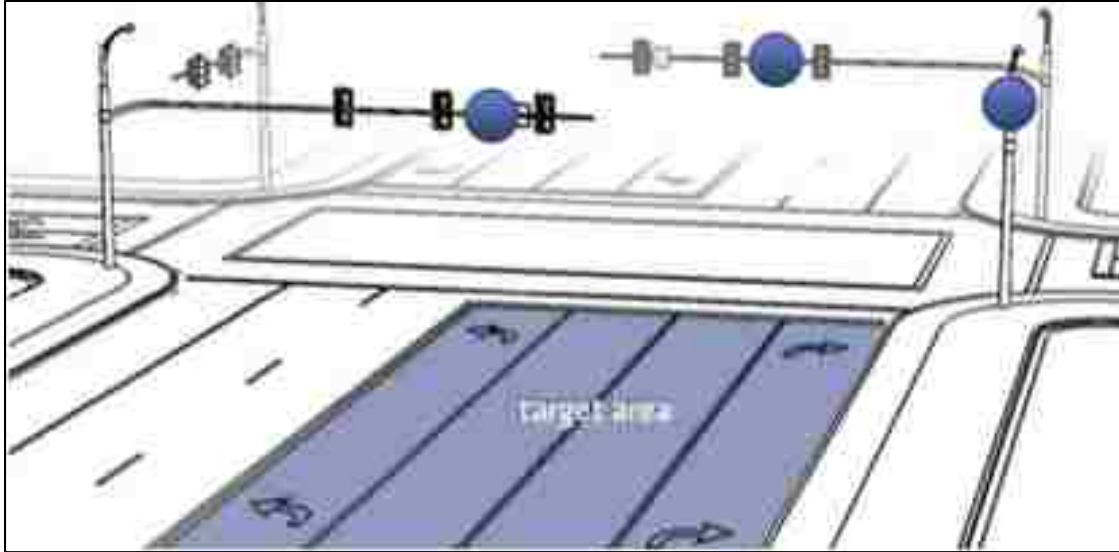


Figure 2-3: Possible mounting locations of SmartSensor Advance (Wavetronix 2015b).

2.1.3 Physical Properties

The Advance sensor is built to withstand the effects of weather and sunlight. The sensor is resistant to various temperatures from a range of -40°F to 165°F (Wavetronix 2015b). The various climates have little effect on the box and it can withstand changing light including direct sunlight during dawn and dusk. It is designed for long-life, being resistant to corrosion, fungus, moisture deterioration and ultraviolet rays which can eventually destroy the functionality of the sensor. The exterior is made of lexan polycarbonate and the sensor itself is lightweight, weighing only 3.9 lbs. The sensor is relatively small, with dimensions of a width of 13.2 in., a height of 10.6 in., and a thickness of 3.8 in (Wavetronix 2015b).



Figure 2-4: Exterior view of Advance sensor (Wavetronix 2015b).

2.2 Other Speed Detection Methods

Apart from microwave radar detectors, there are other forms of speed measuring devices that are used by human data collectors. This section will compare two of the more common forms of speed data collection: laser and in-road speed measurement devices.

2.2.1 Laser Speed Measurement

Light Detection and Ranging (LiDAR) is a method used by law enforcement agencies to visually track and capture the speed of an oncoming vehicle. The technology used in the LiDAR speed guns is that of pulses of lasers being emitted from the gun, reflected off the target, and returned to the gun. Laser Technology Incorporated designs guns which emit as many as 60 pulses in a measurement period, which allows for increased accuracy in the measurement of speed (Laser Technology 2015b). Using the difference in time to return to the gun, the distance the vehicle traveled can be calculated and then using the time elapsed between laser emissions the speed of the vehicle can be calculated. The issue with this technology is that there needs to be an unblocked

line of sight from the gun to the target and the target must have a form of reflective surface to allow the laser to reflect off the target and return to the gun as shown in Figure 2-5. While accurate, the specific conditions in which the LiDAR gun successfully works, such as lighting, and a trigger used to emit laser beams makes this speed data collection method effective only in certain cases such as in law enforcement or speed data collection when compared to other methods such as microwave sensors or inductive loops (Laser Technology, Inc. 2015a).

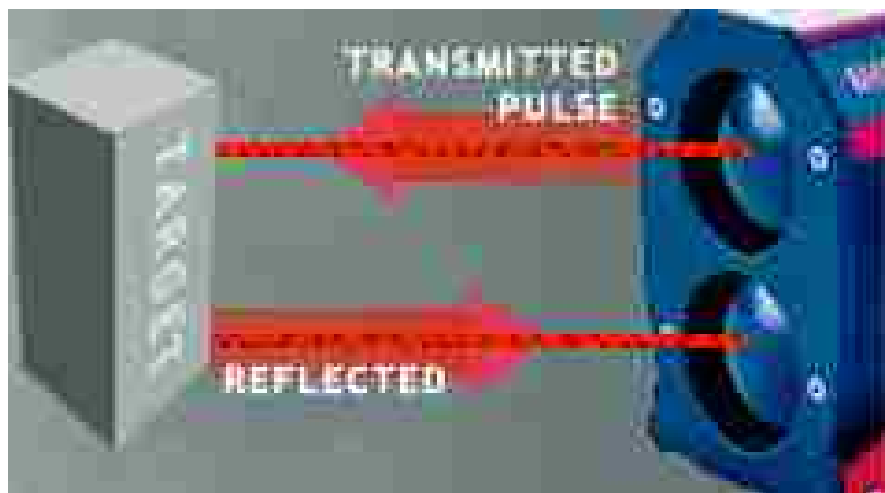


Figure 2-5: LiDAR technology used to measure speed (Laser Technology, Inc. 2015a).

2.2.2 In-Road Speed Measurement

In-road speed measurement methods can include inductive-loop detectors, magnetic detectors and magnetometers. The detector is placed into a sawed-out groove in the road and the current which runs through the cable creates a magnetic field which can detect the presence of a vehicle by the disturbance of a surface area of metal being at close proximity (Marsh Products 2000). These devices may be placed mid-block for approach volume counts and free flow speeds. These

detectors are effective for presence detection, but there are some issues with their maintenance and the detection capability. According to one publication, the detector detects a stronger frequency change for sports cars, which ride closer to the road, than for the taller sport utility vehicles (SUVs) or trucks, as shown in Figure 2-6 (Marsh Products 2000). The detector will sense the front of the vehicle entering at one edge of the detector and will record when the tail end leaves the other end of the detector loop. Figure 2-7 shows the position of a vehicle over a loop in an application of the technology to a fast food restaurant. This application allows the employees to be notified inside the restaurant so that the driver can place their order into the speaker post. Similar applications can be made at intersections with actuated signals that respond to vehicle presence or in measuring the speed of vehicles (Marsh Products 2000).

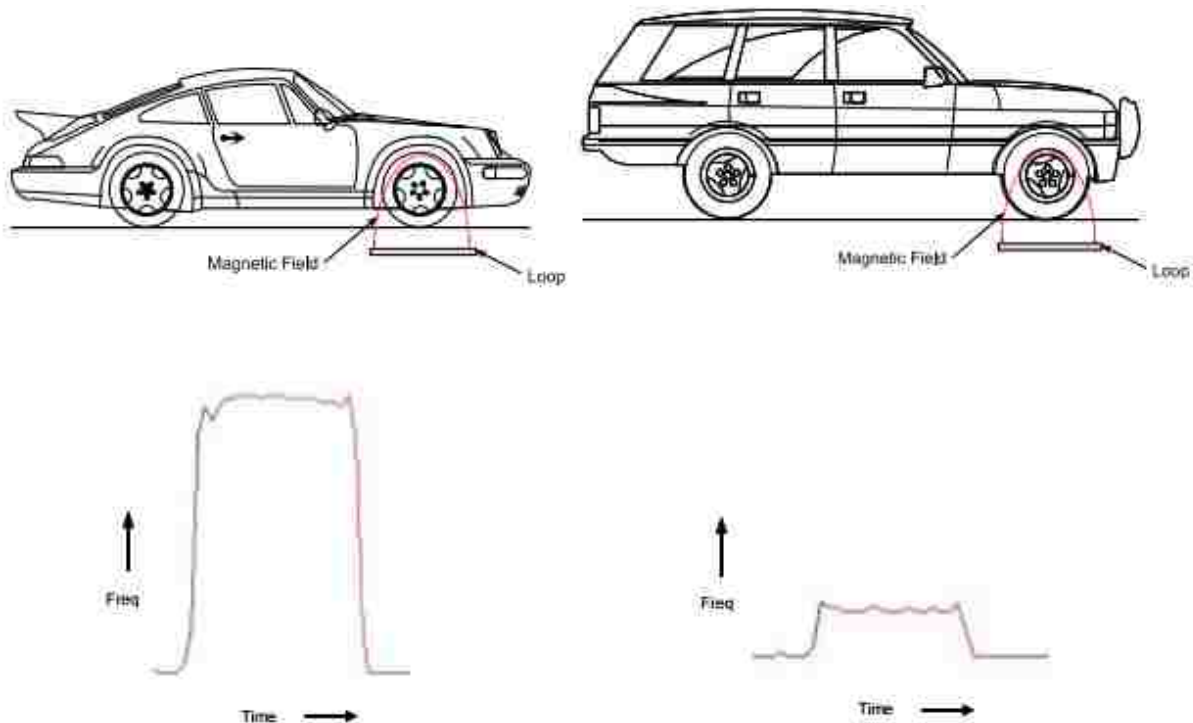


Figure 2-6: Sensitivity of inductive loops to vehicles of various heights (Marsh Products 2000).

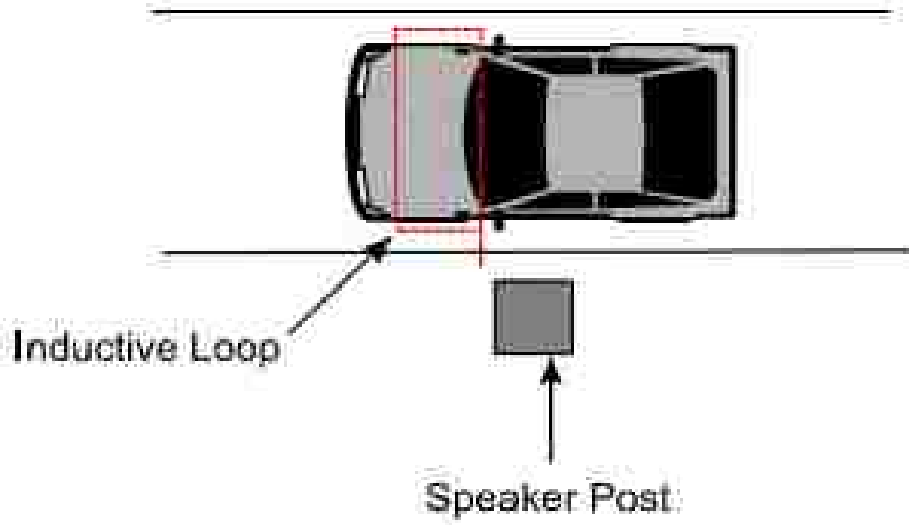


Figure 2-7: Inductive loop in relation to a traveling vehicle (Marsh Products 2000).

In order to approximate the traveling speed of vehicles, the detector will use the time the presence of the vehicle is sensed on the sensor, or dwell time, and an average length of vehicle. To better calculate the speed of the vehicles, two loop detectors may be used in tandem and using the distance between the sensors as a factor they can be used to determine vehicle length and calculate vehicle speed. In terms of installation and maintenance, the inductive loop requires a groove to be cut into the pavement, and in areas where it snows, the salt that is used to melt the snow and ice could seep into the groove and damage the inductive loop and the freeze-thaw action could damage both the roadway pavement and the inductive loop. To reduce the effects of deterioration due to weather, inductive loops may be installed in deeper grooves in the pavement, at no significant expense to the detection capabilities. Some tests concluded that “with high sensitivity, proper installation, and calibration, the depth at which a loop is buried should have little effect on automobile detection” (Marsh Products 2000). To obtain accurate data, it is recommended that separate loops be installed in each lane so as to prevent simultaneous counts of multiple vehicles.

The inductive loops are effective for presence detection and speed measurements, but are

vulnerable to weather conditions and various electrical interferences. For this reason, the inductive loops need to be designed to withstand the potential damaging effects. For instance, they are more vulnerable to lightning strikes due to their magnetic field than mounted microwave sensors (Marsh Products 2000).

2.3 Chapter Summary

There are various methods for automated traffic data collection. The method to be tested in this study is a form of microwave radar sensor, which detects the presence of vehicles and measures speeds. The various features of this sensor include a detection range of 600 feet, continuous vehicle tracking, dynamic virtual sensing zones, criteria-based signaling or the application of changing the signal timing based on the dynamic traffic conditions at the intersection, and the realization of safe arrival of vehicles at the intersections which is the sensor's ability to calculate the dilemma zone of the approach vehicles. What the Advance sensor was designed for originally is dilemma zone reduction. By reducing the dilemma zone, drivers are ensured a sufficient time to clear the intersection during the end of the green phase and during the yellow phase prior to the commencement of the green phase for the conflicting vehicles. The two features of the Advance sensor which will be applied to this study are the dynamic zone feature used in counting approaching vehicles and the continuous vehicle tracking to measure the speeds of approaching vehicles.

The radar-based data collection is one of many data collection methods used in the field. Examples of common data collection methods are laser and in-road measurements. The laser technology applied in data collection in this study is a LiDAR gun, which emits rapid pulses of laser that reflect off of the surface of the approaching object. It uses two sets of laser emissions and the difference time between the times when each pulse was emitted and received is used for

calculating the distance the vehicle has traveled over the period between laser emissions. This method allows for the speed of the vehicle to be calculated as well. The LiDAR gun is accurate, but requires a clear, unobstructed line of sight, which may be difficult to achieve in rain or snow. In order to collect continuous data, the LiDAR must have lasers emitted constantly and in specific areas, which would be difficult and safety concern to approaching traffic. In comparison, the microwave sensor can have microwave radar that can be constantly emitted over a period of time and does not require a reflective surface to collect data.

In-road vehicle detectors are used both to count the number vehicles and measure the speed of the vehicles. For approach volumes and free flow speed measurements, these devices may be placed midblock to allow for the vehicles to be away from intersections on either side where they may be accelerating or decelerating. These devices are effective in detecting the presence of a vehicle and can be used in tandem to measure speed more accurately than a single detector. The installation requires that grooves be cut into the pavement and hence traffic must be stopped in the lanes where these inductive loops are installed. While effective, this device is more prone to weather-caused damage and the grooves created in the road could accelerate the deterioration of pavement by freeze-thaw action and salt penetration.

3 METHODOLOGY

This chapter discusses the methods used in retrieving the data collected by the Advance sensor and the process undertaken in reducing approach volume and speed data from the Hi-res data created by the Advance sensor. Included in this chapter is also the method used to compare the ground truth approach volumes and speeds collected by the Brigham Young University (BYU) team with the approach volumes and speeds reported in the Hi-res data collected by the Advance sensor.

3.1 UDOT Signal Performance Metrics Website and the Factors Tested

The calibration of the Wavetronix SmartSensor Advance version 3.2.0 required data collection of both the approach volume and approach speed. The data collected from the field counts were compared with the data presented by UDOT in their SPMs website (UDOT 2015). Figure 3-1 shows the website with the various options of the metrics used to measure the performance at various signalized intersections. Using the map or signal ID number, an intersection is found and the specific metric, whether it be speed or approach volume, is selected for a particular day and the results are presented in graphic format. For example, Figure 3-1 shows where a site would be selected by signal number, or on the map, a specific date and time would be selected, the type of metrics would be selected, and then the metrics for that site would be created.

Figure 3-2 shows the approach volume of one of the sites where ground truth data were collected. This site is located on US-89 and 1500 North, in Lehi, UT. The data are from August 4,

2015 and show the northbound and southbound approaches of this intersection. The horizontal axis shows the time of day and the vertical axis shows the volume of vehicles which are approaching the intersection, in vehicles per hour. At this location it can be observed that the volume of traffic is very low during the late night and early morning, but increases during the morning peak at around 8:00 a.m. and again during the evening peak at around 6:00 p.m.

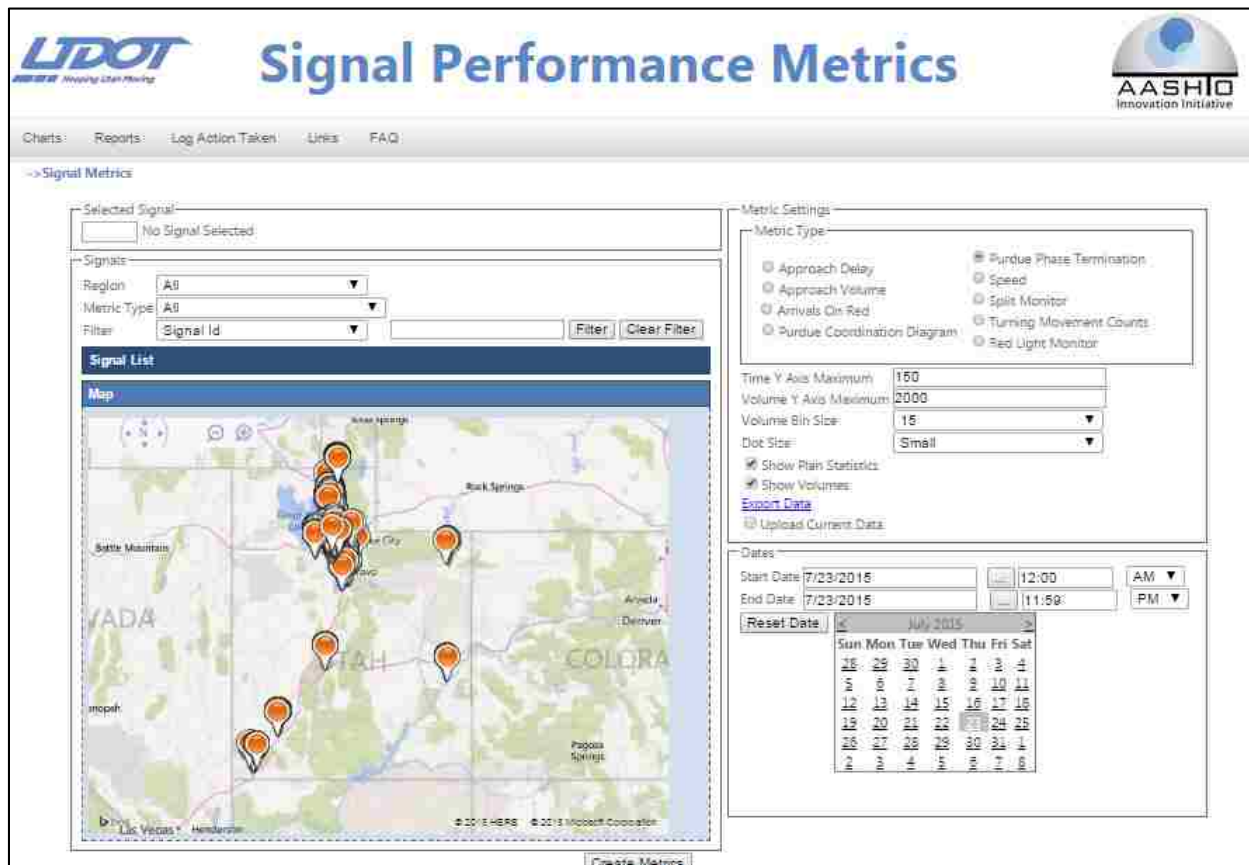


Figure 3-1: UDOT's SPMs website (UDOT 2015).

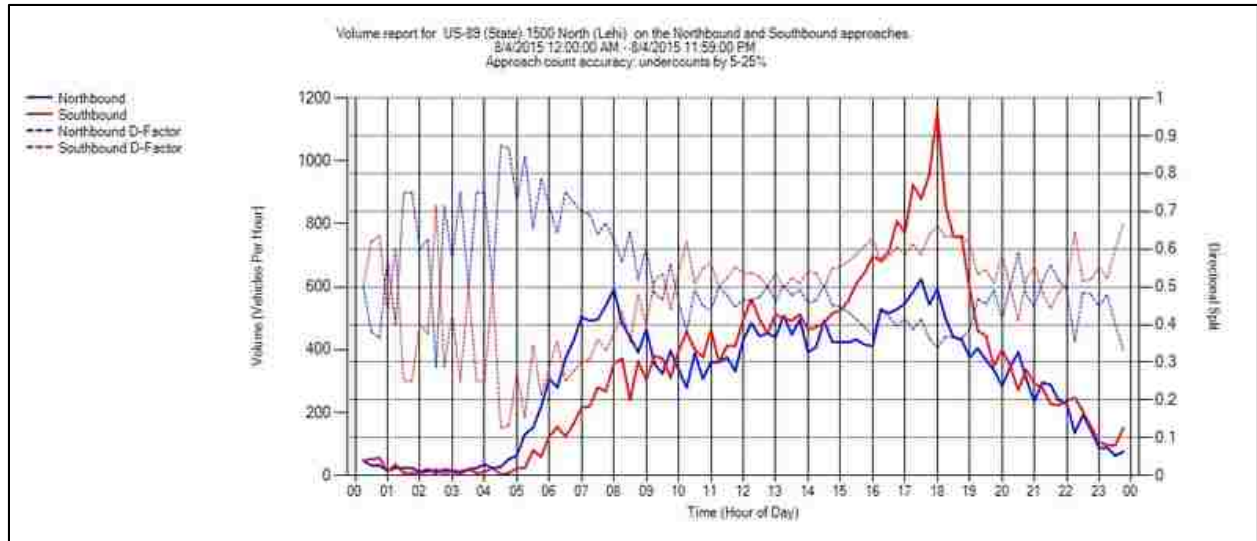


Figure 3-2: Graphical representation of the approach volume counts (UDOT 2015).

Figure 3-3 shows the approach speeds at one of the study sites where speed data were collected. This site is located on 3300 North and University Avenue, in Provo, UT. The data are from July 14, 2015 and show the northbound and southbound directions. The horizontal axis shows the time of day and the vertical axis shows the speed of the vehicles, in miles per hour (mph). The graphs show the posted speed limit as a solid line at 50 mph, the average speed of the approaching vehicles as the lower of the two lines, and the 85th percentile speed as the higher of the two lines. At this location, the speed appears relatively constant during the course of the day and drops significantly during the late night and early morning when there are no vehicles on the road. To investigate the accuracy of both metrics, data were collected for both the ground truth measurements and the measurements reported by the Advance sensor.

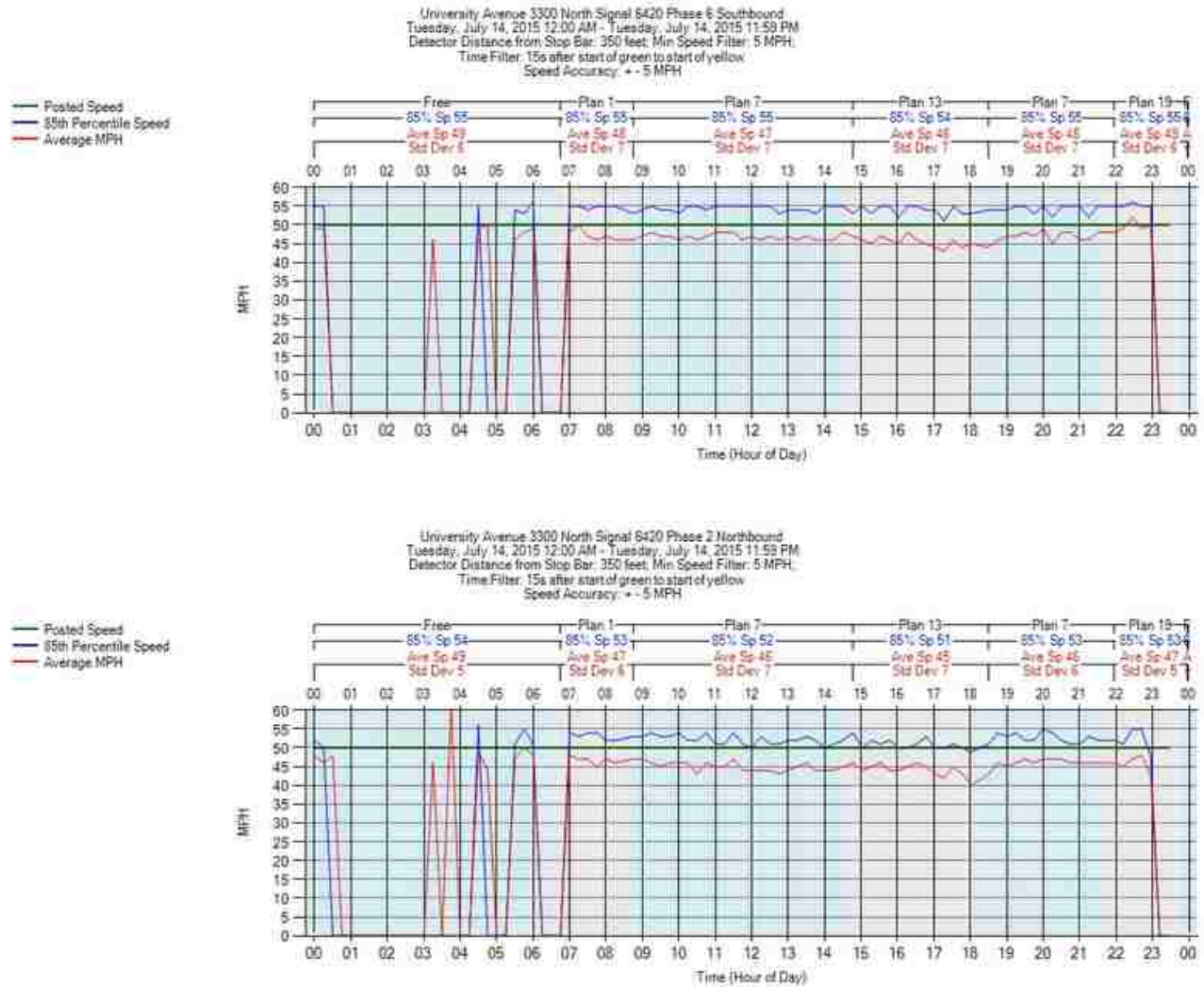


Figure 3-3: Graphical representation of the speed data (UDOT 2015).

Accuracy is expressed as the quotient of the measurements by the sensor divided by the ground truth measurements expressed in percentage in this study. If an accuracy value is less than 100%, the Advance sensor undercounted the measurements and if an accuracy value is greater than 100%, the Advance sensor overcounted the measurements. Using the accuracy values, a statistical analysis was then performed to analyze the effect of the factors on accuracy level. Both of the data were collected during ideal ambient conditions, meaning that there was no precipitation, no strong

winds, and no external factors, such as construction and incidents, which may alter the traffic flow. In the subsequent sections in this chapter the methodologies used to calibrate the accuracy of approach volume counts and approach speeds recorded by the Advance sensor are presented.

3.1.1 UDOT Application of the Advance Sensor

UDOT documents all the activities that the Advance sensor records in a database and through the use of the Structured Query Language (SQL) server the data acquired by Advance sensors can be downloaded. The SQL server was queried by searching the time and frequency of every event that was recorded in the controller box at an intersection. Events that are recorded include the beginning and end of the green, yellow, and red intervals. The data that are retrieved from the SQL server are called “Hi-res” data by UDOT engineers, a short term for high resolution data. There are various datasets which can be retrieved using the SQL. For this study, only two were used, the event log and the speed data.

The event log is the Hi-res data used for approach volume counts. The data consist of a pair of numbers for each time stamp. These numbers are used to describe and match the events which occur at the intersection to a specific phase or detector channel. The numbers are derived from the Indiana Traffic Signal Hi-resolution Data Logger Enumerations (Sturdevant et al. 2012). By using these enumerations, an event can be identified as an active phase event, active pedestrian event, barrier/ring event, phase control event, overlap event, detector event, preemption event, coordination event, and cabinet and/or system event. In this study, only the active phase event and the detector event were needed for the approach volume calibration. Table 3-1 shows the event codes used in the approach volume calibration study. The active phase event is used to denote the exact starting time of a green interval. The phase event number 1 signifies that the green interval began for a corresponding phase as the parameter. The detector event is used to denote when the

presence of a vehicle is detected within the specified range of the detector, or a virtual detector set in the Advance sensor. The detector event 82 means that a vehicle was detected and the 81 means that the vehicle was no longer detected. As each event is recorded, so is the detector channel assigned to the approach, or a phase number for the phase event.

The Hi-res data for the speeds does not use the event log, but rather a search of the location and approach of the intersection in question. The Hi-res speed data outputs consist of the speed in both mph and kilometers per hour (kph), and the timestamp for the corresponding speed. When the Advance sensor detects a vehicle, it records in the Hi-res the time and speed as the vehicles cross the detection zone.

Table 3-1: Event Codes Used in Approach Volume Reduction

Event Code	Event Descriptor	Parameter	Description
Active Phase Events:			
1	Phase Begin Green	Phase # (1-16)	Set when either solid or flashing green indication has begun. Do not set repeatedly during flashing operation.
Detector Events:			
81	Detector Off	Detector Channel # (1-64)	Detector on and off events shall be triggered post any detector delay/extension processing.
82	Detector On	Detector Channel # (1-64)	

3.1.2 Factors Tested for Approach Volumes

The variables that were tested in the calibration of the approach volume were sensor position, approach size in terms of the number of approach lanes, and volume level. In Utah, the Advance sensors are primarily installed in two positions. The first position is on the mast arm, at a location

close to the middle of the road, facing approaching traffic. The second position is on the right side of approaching traffic, high on the mast pole, or on the right side of the mast arm, facing approaching traffic. These are general sensor position descriptions because upon installation the Advance sensors are not installed exactly at the same position at every intersection. Several factors affect sensor positions including trees, signs, or power lines which create visual barriers, or existing sensors and signs which are already installed at those general positions. For these reasons the Advance sensors must be installed wherever space is available on the mast or pole.

The common and preferred location of installing an Advance sensor is the first position, or position 1. The second position, or position 2, is used when position 1 is deemed ineffective due to the reasons stated above. Figure 3-4 shows a diagram of the general Advance sensor installation locations of position 1 and position 2. The purpose for looking at the two different positions is to test if the installation location affects the accuracy of approach volume.

In order to observe the effect that traffic volume level would have on the accuracy of the Advance sensor, approach volume data were collected during various times of the day. The data had samples that could be labeled as high, medium, and low volume levels. These volume levels were decided by observing patterns of approach volume on the UDOT SPMs website. The same method used in the Volume 1 report of this study (Saito et al. 2015) on Matrix sensors to select the volume thresholds was also used in this study. The volume levels chosen were less than 175 vehicles per hour per lane (vphpl), between 175 vphpl and 350 vphpl, and above 350 vphpl as the low, medium, and high volumes, respectively. These levels ensured a variety of density from which the accuracy of the Advance sensors can be better calibrated.

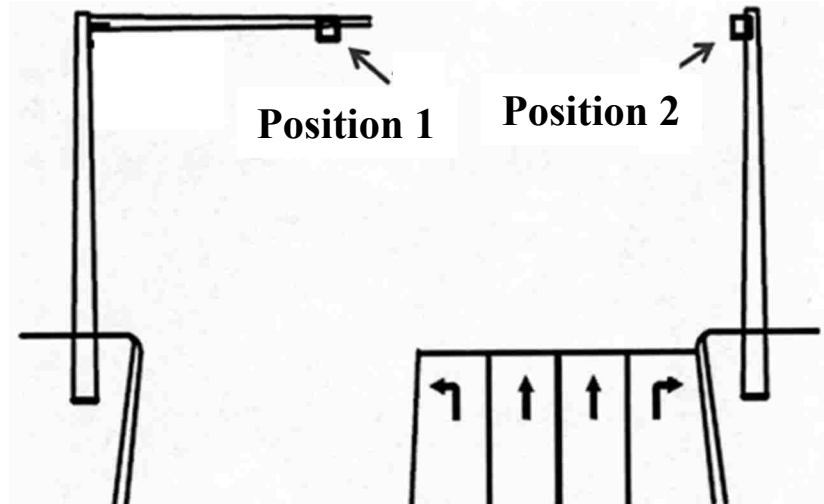


Figure 3-4: Description of the sensor positions.

As stated in Chapter 2, the design of the Advance sensor does not incorporate the ability to differentiate between lanes. For this reason it was important to find various sample sites that consisted of one, two, or three through lanes, which are the common number of approach lanes at the signalized intersections where the Advance sensors are installed.

3.1.3 Factors Tested for Approach Speeds

The factors that were evaluated in calibrating the accuracy of the approach speed feature of the Advance sensor were the number of through lanes and the lane's position relative to the location from which the LiDAR gun was aimed at approaching vehicles. The sensor location was not studied in the calibration of accuracy in speed reading due to the small number of study sites. The volume levels in this case were irrelevant because the purpose of collecting speed data was to collect speed of vehicles in free flow as they approached intersections. Hence, low volume traffic was preferred for data collection.

3.2 Approach Volume Data Collection

The accuracy of approach volume was calibrated using the ground truth approach volume counts that were made on site by the BYU team and comparing them to the approach volume counts made by the Advance sensors as recorded in the Hi-res data.

3.2.1 Volume Data Collection

The approach volume data collection consisted of two stages. In the first stage, JAMAR counting boards were used to count the passenger vehicles. The original purpose of using a JAMAR counter was to count turning movements, but by denoting each through lane as a specific turning movement, the JAMAR counter was effectively used to count the approach volume separated by specific through lanes. When a passenger vehicle passed the specified distance to which the SmartSensor Advance was configured to count, the user would push the button that corresponds to that lane. The JAMAR counter used for this study has the ability to break up counts into timed intervals that the user specifies (JAMAR 2015). For this study, a total of twelve 5-minute intervals were used. Figure 3-5 shows a JAMAR counter used in counting the approach volume.

The second stage consisted of using pencil and paper to record the location, approach, volume level, date, and start time of the count which was either the beginning of a green phase or a gap of time between cars. The 12 tables were prepared and used to count the trucks, trucks with trailers, semi-trucks, and motorcycles. Each table represented a 5 minute count interval. Figure 3-6 shows an image of the data collection sheet. A lane was assigned to each column ranging from T1 to T3, with the T signifying a “through” lane, and a number was then assigned to each through lane as decided by the BYU team as they used the JAMAR board.

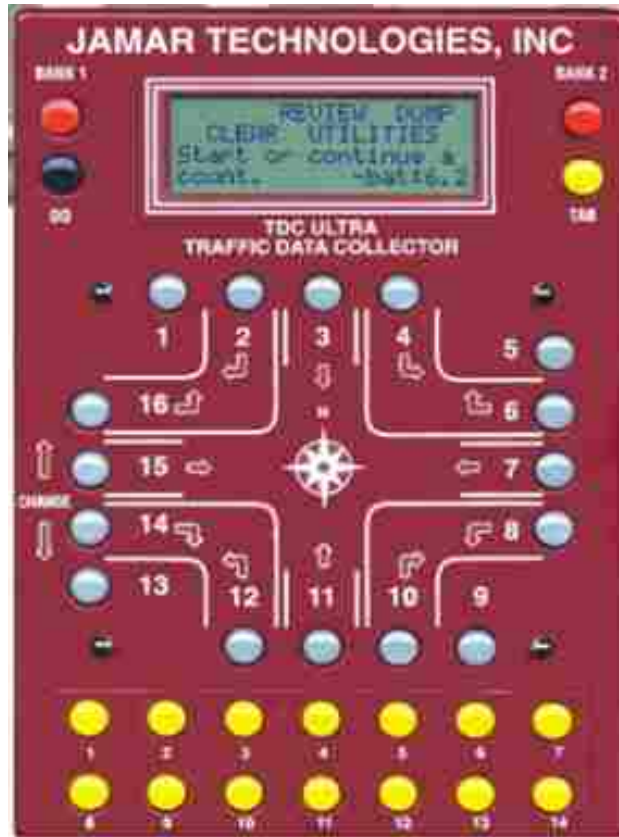


Figure 3-5: JAMAR counter board (JAMAR 2015).

The BYU team was stationed close to the specified count zone and would press the corresponding lane button on the JAMAR board for passenger vehicles or would mark the number of non-passenger vehicles, being trucks, vehicles towing trailers, and motorcycles, on the data collection sheet, according to the vehicle type.

Prior to counting, it was necessary to determine what type of reference time should be used to match the time from the manual count with the timestamp as given in the Hi-res data. The timestamp of each controller box has a few seconds of delay from the time the vehicles are counted and the data are sent to the Hi-res database. For this reason, the time from the smartphone of the data collectors was assumed as the correct time and used as the reference time for analyzing the data.

Intersection: _____ Date: _____		Start Time		Classification		Lanes	
Direction: _____ Start Time: _____							
Volume: _____ Time Counted: _____							
Start Time		Classification		Lanes			
	Truck						
	Truck w/ Trailer						
	Semi						
	Motorcycle						
	Truck						
	Truck w/ Trailer						
	Semi						
	Motorcycle						
	Truck						
	Truck w/ Trailer						
	Semi						
	Motorcycle						
	Truck						
	Truck w/ Trailer						
	Semi						
	Motorcycle						
	Truck						
	Truck w/ Trailer						
	Semi						
	Motorcycle						
	Truck						
	Truck w/ Trailer						
	Semi						
	Motorcycle						
	Truck						
	Truck w/ Trailer						
	Semi						
	Motorcycle						
Notes:							

Figure 3-6: Data collection sheet.

To assist in finding the exact starting time when the count began, the reference times that were used were the beginning of the green phase of the through movement being counted or a time gap between vehicles as they cross the count zone. Using the green light was found to be the preferred method because the exact start time of the green interval could also be found in the Hi-res data and each green phase was separated by a large number of seconds, which would ensure that the correct start time was used in the analysis stage. The time gap between approaching vehicles was used when the traffic signal was out of view. The reason that a time gap would be used was that as vehicles crossed the count zone, they were assigned a time stamp. Recording the time gap between two approaching vehicles, as precisely as possible, would allow the data collectors to find the start time by looking for an instance where the sensor detected two vehicles with the same or similar

time gap in the Hi-res data as the time gap recorded for the two approaching vehicles recorded in the field.

3.2.2 Data Reduction

The JAMAR counter saves each count with a date and time stamp. When the data are imported to a computer via a USB cable using the software Petra Pro by JAMAR Technologies, an output table that resembles the one shown in Figure 3-7 is produced. The far left column shows the 5 minute intervals used in counting the approach volume and the numbered columns correspond to a turning movement as numbered on the JAMAR counting board.

A spreadsheet was made to combine the counts produced by the JAMAR counter and the counts recorded on the data collection sheet. Figure 3-8 shows the portion that shows the final summary of the counts by time interval and by lane. This sheet allowed for the entry of the data of number of vehicles by type for each 5 minute counting period. The counts by the JAMAR counter were entered into the spreadsheet using the number the lane was assigned to during the field data collection. These totals were summed and then presented in four 15-minute totals and a 1-hour total. Figure 3-9 shows the portion of the count data prepared for comparison with the Hi-res data.

3.2.3 Hi-res Data

Similar to the process used for the Matrix sensors as described in Chang (2015) and Saito et al. (2015), the date, time, and intersection number were used to identify the number of vehicles counted by the Advance sensor. After counting the approach volume collected manually at the study sites the Hi-res data were downloaded from the UDOT SQL server. Two types of code were used to extract the data. The first code provided the sensor information and the detector channel. They allowed for an efficient sorting of the data. The intersection number was found using the map

feature of the SPMs website, by simply locating the intersection on the map. Upon selection of an intersection, the intersection name, number, and the various metric options would appear in a text box above the selected intersection. The information provided by some of the metrics was used to find the start time of the count. When the time gap was used to identify the start time, the detector channel number assigned to the Advance sensor for its respective approach was noted. When the count began at the beginning of a green interval, the phase number for that corresponding to the approach direction that received the green interval was noted. To collect the approach volume data from the Hi-res data, the detector channel was also needed so that the correct sensor data were analyzed. The second set of data was downloaded from the SQL server using the code that searched for events at the controller box, as previously explained in section 3.1.1. Entering the signal ID and the timestamp range in question, the Hi-res data for all events at the intersection were extracted. The data that resulted from extracting the second set of data were similar to the data shown Figure 3-10. This dataset contained timestamps, event codes, and event parameters. To begin data extraction, it was necessary to figure out if the count began or not, using a time gap or the beginning time of a green phase.

When the data collection began, if a gap of time between vehicles was used as the method to determine starting time, the spreadsheet shown in Figure 3-11 was used, where the results from Figure 3-10 were pasted into the top part of the spreadsheet. The detector channel was then entered in the highlighted cell in Figure 3-11 and the “Find” button was clicked, which extracted the events that would activate the Advance sensor. The events of interest were the ones which denoted a vehicle entering the sensor’s detection zone. The first few minutes of vehicle

Unshifted		Bank 1		Bank 2		Site Code: 01201504												Number of Intervals: 5 Interval Length: 15 Minutes							
Start Date: 1/20/2015 Start Time: 4:30:00 PM		From North						From East						From South						From West					
Start Time	Right	Thru	Left	Peds	Right	Thru	Left	Right	Thru	Left	Right	Thru	Left	Right	Thru	Left	Right	Thru	Left	Right	Thru	Left	Peds		
04:30 PM	0	0	0	0	14	6	13	0	9	0	252	15	0	0	0	0	0	0	0	0	0	0	0		
04:45 PM	0	0	0	0	8	7	12	0	6	0	271	19	0	0	0	0	0	0	0	0	0	0	0		
05:00 PM	0	0	0	0	18	6	16	0	10	0	280	19	0	0	0	0	0	0	0	0	0	0	0		
05:15 PM	0	0	0	0	10	9	17	0	10	0	269	12	0	0	0	0	0	0	0	0	0	0	0		
05:30 PM	0	0	0	0	12	5	12	0	8	0	266	24	0	0	0	0	0	0	0	0	0	0	0		
05:45 PM	0	0	0	0	11	3	19	0	7	0	248	16	0	0	0	0	0	0	0	0	0	0	0		

Figure 3-7: JAMAR counter output table.

Intersection: Eastbay		Gap: 64 seconds								
Date: 13-May										
Time: 5:17:23AM										
Matrix										
		Counts				Summary				
Time Interval	Classification	Left (1)	Left (2)	Through (1)	Through (2)	Through (3)	Right (1)	Right (2)	5 Min Summary	15 Min Summary
5	Cars	0	0	7	6	2	0	0	15	
	Trucks			1		1			2	
	Trucks w/ Trailers								0	
	Semi						1		1	
	Motorcycles								0	
	Totals	0	0	8	6	4	0	0	18	
10	Cars	0	0	7	8	4	0	0	19	
	Trucks								0	
	Trucks w/ Trailers								0	
	Semi								0	
	Motorcycles								0	
	Totals	0	0	7	8	4	0	0	19	
15	Cars	0	0	9	10	3	0	0	22	
	Trucks			1					1	
	Trucks w/ Trailers								0	
	Semi			2		1			3	
	Motorcycles					1			1	
	Totals	0	0	12	10	5	0	0	27	64
20	Cars	0	0	15	13	7	0	0	35	
	Trucks			1					1	
	Trucks w/ Trailers								0	
	Semi								0	
	Motorcycles								0	
	Totals	0	0	16	13	7	0	0	36	
25	Cars	0	0	22	22	7	0	0	51	
	Trucks								0	
	Trucks w/ Trailers								0	
	Semi				1				1	
	Motorcycles								0	
	Totals	0	0	22	23	7	0	0	52	
30	Cars	0	0	20	16	16	0	0	52	
	Trucks			1	1				2	
	Trucks w/ Trailers								0	
	Semi								0	
	Motorcycles								0	
	Totals	0	0	21	17	16	0	0	54	142
35	Cars	0	0	22	20	12	0	0	54	
	Trucks			1					1	
	Trucks w/ Trailers				2	1			3	
	Semi					1			1	
	Motorcycles								0	
	Totals	0	0	23	22	14	0	0	59	
40	Cars	0	0	19	12	17	0	0	48	
	Trucks								0	
	Trucks w/ Trailers								0	
	Semi					2			2	
	Motorcycles								0	
	Totals	0	0	19	12	19	0	0	50	
45	Cars	0	0	17	8	14	0	0	39	
	Trucks			1	1				2	
	Trucks w/ Trailers								0	
	Semi								0	
	Motorcycles								0	
	Totals	0	0	18	9	14	0	0	41	150
50	Cars	0	0	12	8	12	0	0	32	
	Trucks					1			1	
	Trucks w/ Trailers			1	1				2	
	Semi				1	1			2	
	Motorcycles								0	
	Totals	0	0	13	10	14	0	0	37	
55	Cars	0	0	14	13	11	0	0	38	
	Trucks			2					2	
	Trucks w/ Trailers								0	
	Semi								0	
	Motorcycles			1					1	
	Totals	0	0	17	13	11	0	0	41	
60	Cars	0	0	22	18	9	0	0	49	
	Trucks			3	1	1			5	
	Trucks w/ Trailers								0	
	Semi				1				1	
	Motorcycles								0	
	Totals	0	0	25	20	10	0	0	55	133
Total:										489

Figure 3-8: Count spreadsheet input table.

detection data were separated with their timestamps. A sample output from this process is shown in the spreadsheet in Figure 3-11. From the first few minutes of vehicle detection data, the closest time difference, or gap, between the first two vehicles that were recorded by the data collectors in the field were used to match the vehicles used to begin the data collection period. The timestamp of the first vehicle of the two vehicles used to determine the starting time was considered as the start time of the data collection period.

Visual Counts										
Time Interval	Left (1)	Left (2)	Through (1)	Through (2)	Through (3)	Right (1)	Right (2)	5 Min Summary	15 Min Summary	
5	0	0	8	6	4	0	0		18	
10	0	0	7	8	4	0	0		19	
15	0	0	12	10	5	0	0		27	64
20	0	0	16	13	7	0	0		36	
25	0	0	22	23	7	0	0		52	
30	0	0	21	17	16	0	0		54	142
35	0	0	23	22	14	0	0		59	
40	0	0	19	12	19	0	0		50	
45	0	0	18	9	14	0	0		41	150
50	0	0	13	10	14	0	0		37	
55	0	0	17	13	11	0	0		41	
60	0	0	25	20	10	0	0		55	133
Total	0	0	201	163	125	0	0	489	489	veh/hr
Hi-res Data Counts										
Start Time: 12:03:15 AM					Date: 42137					
Time Interval	Left (1)	Left (2)	Through (1)	Through (2)	Through (3)	Right (1)	Right (2)	5 Min Summary	15 Min Summary	
5								17		94%
10								19		100%
15								24	60	89% 94%
20								33		92%
25								50		96%
30								43	126	80% 89%
35								50		85%
40								53		106%
45								39	142	95% 95%
50								40		108%
55								38		93%
60								48	126	87% 95%
Total	0	0	0	0	0	0	0	454	454	94% 93%
	#DIV/0!	#DIV/0!	0	0	0	#DIV/0!	#DIV/0!			

Figure 3-9: Count spreadsheet output table.

When the green interval was used to find the start time for data reduction, a spreadsheet shown in Figure 3-12 was used. Similarly, the data were pasted into the spreadsheet and the phase number was entered into the highlighted cell in Figure 3-12. Clicking the “Find” button would show the starting times of the first few green intervals for that approach. Using the starting time of the green

SignalID	Timestamp	EventCode	EventParam
6305	2015-04-28 07:30:00.400	43	1
6305	2015-04-28 07:30:00.400	81	11
6305	2015-04-28 07:30:02.300	44	6
6305	2015-04-28 07:30:02.300	81	9
6305	2015-04-28 07:30:02.400	44	2
6305	2015-04-28 07:30:02.400	82	11
6305	2015-04-28 07:30:02.600	43	6
6305	2015-04-28 07:30:02.600	82	12
6305	2015-04-28 07:30:03.100	81	12
6305	2015-04-28 07:30:03.200	150	1
6305	2015-04-28 07:30:03.600	82	12
6305	2015-04-28 07:30:03.900	81	12
6305	2015-04-28 07:30:04.000	82	12
6305	2015-04-28 07:30:04.300	81	12
6305	2015-04-28 07:30:04.400	82	12
6305	2015-04-28 07:30:04.700	81	12
6305	2015-04-28 07:30:04.800	82	12
6305	2015-04-28 07:30:06.100	81	12

Figure 3-10: SQL output with controller events.

interval closest to the starting time of manual approach volume count in the field allowed for a start time to be properly selected and recorded by the analyst. The spreadsheet shown in Figure 3-13 allowed the analyst to use the starting time found, either by the time gap or green interval start time method and to insert the spreadsheet row number of the start time in the rows in the table underneath the label “Beginning.” Beginning with the row number of the starting time, the analyst would find the row number for an event that occurred 5 minutes after the starting time and insert that number into the table. This process continued until the twelve 5 minute intervals’ beginning and end row numbers were accounted for. Entering the beginning and end row numbers allowed the analyst to count the number of vehicles between those specified row numbers which specify a specific 5 minute interval. Underneath the “Intersection Codes” cell there is a cell where the analyst

enters the detector channel number found in the previous step. After all these data were entered, the analyst would click the “Start” button to get approach volume counts.

	A	B	C	D	E	F	G	H	I	J	K	L	M
1	8305	2015-04-30 15:55:02.000	2	2									
2	8305	2015-04-30 15:55:02.000	2	6									
3	8305	2015-04-30 15:55:02.000	43	1									
4	8305	2015-04-30 15:55:02.000	82	9									
5	8305	2015-04-30 15:55:02.000	83	2									
6	8305	2015-04-30 15:55:02.300	2	2									
7	8305	2015-04-30 15:55:03.700	2	6									
8	8305	2015-04-30 15:55:03.700	44	1									
9	8305	2015-04-30 15:55:03.700	81	2									
10	8305	2015-04-30 15:55:03.700	81	9			start						
11	8305	2015-04-30 15:55:03.900	82	11			2015-04-30 15:55:30.600	82	2				
12	8305	2015-04-30 15:55:06.600	82	9			2015-04-30 15:56:34.600	82	2				
13	8305	2015-04-30 15:55:06.700	82	12			2015-04-30 15:57:40.300	82	2				
14	8305	2015-04-30 15:55:07.200	81	12			2015-04-30 15:58:39.900	82	2				
15	8305	2015-04-30 15:55:07.400	81	9			2015-04-30 15:58:44.100	82	2				
16	8305	2015-04-30 15:55:08.300	81	5			2015-04-30 15:58:44.500	82	2				
17	8305	2015-04-30 15:55:09.300	44	4			2015-04-30 16:00:34.500	82	2				
18	8305	2015-04-30 15:55:09.300	82	7			2015-04-30 16:00:51.300	82	2	Start			
19	8305	2015-04-30 15:55:09.700	23	8			2015-04-30 16:00:53.600	82	2				
20	8305	2015-04-30 15:55:09.700	43	8			2015-04-30 16:01:04.500	82	2				
21	8305	2015-04-30 15:55:09.700	82	9			2015-04-30 16:01:42.100	82	2				
22	8305	2015-04-30 15:55:10.000	3	8			2015-04-30 16:02:24.100	82	2				
23	8305	2015-04-30 15:55:10.000	81	11			2015-04-30 16:03:46.500	82	2				
24	8305	2015-04-30 15:55:10.000	82	12			2015-04-30 16:04:11.100	82	2				
25	8305	2015-04-30 15:55:10.100	48	8			2015-04-30 16:04:34.600	82	2				
26	8305	2015-04-30 15:55:10.100	81	12			2015-04-30 16:04:49.600	82	2				
27	8305	2015-04-30 15:55:10.100	82	11			2015-04-30 16:05:01.300	82	2				
28	8305	2015-04-30 15:55:10.200	81	9			2015-04-30 16:07:06.700	82	2				
29	8305	2015-04-30 15:55:10.900	81	7			2015-04-30 16:07:41.600	82	2				
30	8305	2015-04-30 15:55:12.200	44	8			2015-04-30 16:08:21.200	82	2				
31	8305	2015-04-30 15:55:12.200	82	12			2015-04-30 16:08:30.900	82	2				
32	8305	2015-04-30 15:55:12.600	81	12			2015-04-30 16:09:37.300	82	2				
33	8305	2015-04-30 15:55:12.700	7	4			2015-04-30 16:11:26.100	82	2				
34	8305	2015-04-30 15:55:13.100	4	4			2015-04-30 16:11:51.000	82	2				

Figure 3-11: Spreadsheet used to find start time based on time gap between vehicles.

The spreadsheet macro sorted the events by the detector channel to separate all the events that occurred at that specific sensor and counted all the events which would indicate that the detector was turned on, which were events with code 82. When the Advance sensor’s detection zone was activated, or turned on, it was assumed that the Advance sensor counted the vehicle. After running the spreadsheet macro attached to this spreadsheet, the output counts from the Hi-res data were presented in a table underneath the column named ‘5-min summary’ in the spreadsheet in Figure 3-9. A percent accuracy was then given, representing the percent of the ground truth approach volume counts the sensor was able to capture. Accuracy was determined

	A	B	C	D	E	F	G	H	I	J	K
2	6402	2015-05-05 20:45:00.200	81	49							
3	6402	2015-05-05 20:45:00.200	82	49							
4	6402	2015-05-05 20:45:00.400	82	34							
5	6402	2015-05-05 20:45:01.100	81	34							
6	6402	2015-05-05 20:45:01.300	82	23							
7	6402	2015-05-05 20:45:01.600	82	10							
8	6402	2015-05-05 20:45:01.800	81	23							
9	6402	2015-05-05 20:45:01.800	82	9							
10	6402	2015-05-05 20:45:02.000	3	1			2015-05-05 20:45:13.800	1	2		
11	6402	2015-05-05 20:45:02.000	81	10			2015-05-05 20:46:55.600	1	2		
12	6402	2015-05-05 20:45:02.200	3	5			2015-05-05 20:49:04.900	1	2		
13	6402	2015-05-05 20:45:02.200	82	10			2015-05-05 20:51:08.300	1	2		
14	6402	2015-05-05 20:45:02.400	81	10			2015-05-05 20:52:57.300	1	2		
15	6402	2015-05-05 20:45:02.500	82	22			2015-05-05 20:55:03.000	1	2		
16	6402	2015-05-05 20:45:02.700	81	22			2015-05-05 20:57:23.200	1	2		
17	6402	2015-05-05 20:45:02.800	82	12			2015-05-05 20:58:50.600	1	2		
18	6402	2015-05-05 20:45:03.100	81	12			2015-05-05 21:01:08.700	1	2		
19	6402	2015-05-05 20:45:03.300	82	36			2015-05-05 21:02:69.700	1	2		
20	6402	2015-05-05 20:45:03.600	82	23			2015-05-05 21:05:03.600	1	2		
21	6402	2015-05-05 20:45:03.800	81	36			2015-05-05 21:06:51.900	1	2		
22	6402	2015-05-05 20:45:03.800	81	49			2015-05-05 21:09:15.200	1	2		
23	6402	2015-05-05 20:45:03.800	82	49			2015-05-05 21:11:31.300	1	2		
24	6402	2015-05-05 20:45:04.000	81	9			2015-05-05 21:12:45.600	1	2		
25	6402	2015-05-05 20:45:04.100	81	23			2015-05-05 21:14:55.600	1	2		
26	6402	2015-05-05 20:45:04.100	82	34			2015-05-05 21:17:06.200	1	2		
27	6402	2015-05-05 20:45:04.200	81	34			2015-05-05 21:19:13.900	1	2		
28	6402	2015-05-05 20:45:04.400	82	22			2015-05-05 21:20:59.300	1	2		

Figure 3-12: Spreadsheet used to find start time based on a green phase start.

	A	B	C	D	E	F	G	H	I	J	K	L	M	N	O	P	Q
1	6305	2015-04-30 15:55:02.000	2	2													
2	6305	2015-04-30 15:55:02.000	2	6													
3	6305	2015-04-30 15:55:02.000	43	1													
4	6305	2015-04-30 15:55:02.000	82	9													
5	6305	2015-04-30 15:55:02.000	83	2													
6	6305	2015-04-30 15:55:02.300	2	2													
7	6305	2015-04-30 15:55:03.700	2	6													
8	6305	2015-04-30 15:55:03.700	44	1	Example	Beginning	Ending										
9	6305	2015-04-30 15:55:03.700	81	2	5			2384									
10	6305	2015-04-30 15:55:03.700	81	9	10			3158									
11	6305	2015-04-30 15:55:03.900	82	11	15			4076									
12	6305	2015-04-30 15:55:06.600	82	9	20			5015									
13	6305	2015-04-30 15:55:06.700	82	12	25			5954									
14	6305	2015-04-30 15:55:07.200	81	12	30			6945									
15	6305	2015-04-30 15:55:07.400	81	9	35			7845									
16	6305	2015-04-30 15:55:08.300	81	5	40			8766									
17	6305	2015-04-30 15:55:09.300	44	4	45			9715									
18	6305	2015-04-30 15:55:09.300	82	7	50			10663									
19	6305	2015-04-30 15:55:09.700	23	8	55			11622									
20	6305	2015-04-30 15:55:09.700	43	8	60			12577									
21	6305	2015-04-30 15:55:09.700	82	9	30			99									
22	6305	2015-04-30 15:55:10.000	3	8	35			113									
23	6305	2015-04-30 15:55:10.000	81	11	40			104									
24	6305	2015-04-30 15:55:10.000	82	12	45			113									
25	6305	2015-04-30 15:55:10.100	48	8	50			103									
26	6305	2015-04-30 15:55:10.100	81	12	55			100									
27	6305	2015-04-30 15:55:10.100	82	11	60			115									
28	6305	2015-04-30 15:55:10.200	81	9													
29	6305	2015-04-30 15:55:10.900	81	7													

Figure 3-13: Spreadsheet used to find the number of vehicles counted by the sensor.

by dividing the sensor counts by the ground truth counts expressed in percentage. This percentage was the accuracy that was recorded and used for calibrating the accuracy of the sensor. This data extraction process was repeated for each volume level and approach size combinations for the intersections under study.

3.3 Speed Data Collection

To collect speed data at the study sites, a LiDAR speed gun was used. The LiDAR gun was pointed at the license plate of an approaching vehicle and as the trigger was pulled, a laser beam was emitted to the vehicle and a speed was calculated, as explained in Section 2.2.1. The resulting speed data collected were classified as a spot speed, or the speed measured at that specific point on the road.

3.3.1 TruCam Speed Gun

The LiDAR speed gun used in the ground truth speed data collection was the TruCam LiDAR speed gun, manufactured by Laser Technology, Inc. This gun combines the laser technology of measuring speed with a video camera that allows for the user to visually match the object speed to the image of the particular vehicle. The purpose of using this function was to provide the link among the video of approaching vehicles to UDOT's closed circuit television (CCTV) in the BYU Transportation Lab, the Advance sensor Hi-res data, and the LiDAR speed data. Figure 3-14 shows an image of the LiDAR speed gun used in this study.



Figure 3-14: Image of the speed gun (Officer.com 2015).

There is a potential for error when the speed gun is used at an angle, creating what is called the cosine effect. This effect is caused by the fact that the gun is not used directly in front of an oncoming vehicle, but rather the gun is generally offset a few feet from the edge of the road. The user's manual of the LiDAR gun presents an accuracy tables for the user to show the effects the cosine effect can cause on the calculated speed. Table 3-2 shows what the true speeds are compared to the measured speeds of the approaching vehicles and Table 3-3 shows the percent accuracy based on the gun's perpendicular distance to the road and the distance away from the center of the lane where the vehicle speeds are measured.

Table 3-2: Measured Speed Compared to True Speed by Angle of Measurement (Laser Technology, Inc., 2009)

IMPERIAL					
Angle (degrees)	True Speed				
	30 mph	40 mph	50 mph	60 mph	70 mph
	Measured Speed (mph)				
0	30.00	40.00	50.00	60.00	70.00
1	29.99	39.99	49.99	59.99	69.99
3	29.96	39.94	49.93	59.92	69.90
5	29.89	39.85	49.81	59.77	69.73
10	29.54	39.39	49.24	59.09	68.94
15	28.98	38.64	48.30	57.94	67.61
20	28.19	37.59	46.99	56.38	65.78
45	21.21	28.28	35.36	42.43	49.50
90	0.00	0.00	0.00	0.00	0.00

Table 3-3: Percentage of True Speed Measured Given the Distance Offset from the Vehicle's Path and the Distance to the Target Vehicle (Laser Technology, Inc., 2009)

IMPERIAL					
Distance off the roadway (feet)	Range to Target Vehicle				
	100 ft.	250 ft.	500 ft.	1000 ft.	2000 ft.
	fraction of the True Speed that will be measured				
10	0.9950	0.9992	0.9998	0.9999	1.0000
25	0.9682	0.9950	0.9987	0.9997	0.9999
50	0.8660	0.9798	0.9950	0.9987	0.9997
100	0.0000	0.9165	0.9798	0.9950	0.9987
200	0.0000	0.6000	0.9165	0.9798	0.9950

In order to compare the speeds measured by the Advance sensor and the ground truth speed collected by the LiDAR gun, a test data collection was performed. A test site where the offset would be large was selected, which was a site with the maximum number of through lanes for the study. The largest number of approach lanes available for data collection was three, and the site was the intersection at 400 E 800 N, Orem. This site consisted of an east and west approach with three approach lanes in both directions. Using the Advance sensor, each approach's individual detector distance was recorded. The gun's offset distance, or the distance from the center of the

approach lane to the location where the LiDAR gun was held during data collection, was also recorded. Using large range of speeds collected during the data collection process, the true speed for each sample was calculated using Equation 1. This equation uses the measured speed, the offset, and measured distance. The measured velocity, or V_m , is the speed that the LiDAR gun records. The measured distance is how far the speed gun is from the vehicle at the time of the picture is taken. This distance is what is recorded by the speed gun, but it is not the distance the car is located from the stop bar due to the angle created by the offset. This distance includes the width of the right turn lane, the distance away from the edge of the right turn lane, the location where the data collector is standing, and one-half of the width of an approach lane, because the distance measured is to the center of the approach lane. If the vehicle is traveling in the middle, or the second, of three approaching lanes, the distance between the vehicle and the data collector is one and a half lanes plus the right turn lane and the standing offset distance from the curb. The dimensions used in the equation for this test were a standard lane width for urban streets of 11 ft. and the 18 ft. which was the distance from the data collector's standing spot to the first lane. Using these dimensions, the speeds were calculated for a range of speeds that were likely to be observed at the study sites. Table 3-4 and Table 3-5 contain the distances used in calculating the true speed for the eastbound and westbound approaches, respectively. Note that the distance used was 280 ft. for eastbound and 180 ft. for westbound at the test site. This difference occurred because the two sites had the sensor detection zone setup at different distances by the technicians. These two distances would represent any variation found at the various sites during data collection. The distances at the actual site locations may vary due to the installation process where the UDOT technicians adjust the range of the sensors as needed in order to provide the sensor an unobstructed view of the traffic. The true speeds were then calculated using measured speeds ranging from 25

mph to 60 mph with a 5 mph increment and with offset totals where the vehicles were in 1st, 2nd, or 3rd lanes away from the speed gun. Table 3-6 and Table 3-7 show the resulting true speeds for the eastbound and westbound approaches at the test site, respectively.

$$V_t = V_m \times \cos\left(\sin^{-1}\left(\frac{\text{Offset}}{\text{Measured Distance}}\right)\right) \quad \text{Equation 1}$$

Where:

V_t = true velocity

V_m = measured velocity

Offset = distance from the standing spot to the center of the travel lane

Measured Distance = distance of vehicle measured by the LiDAR gun

Table 3-4: Factors for the Eastbound Approach

Eastbound	Distance (ft.)
Offset to first lane:	18
Standing Distance:	50
Lane Width:	11
Goal distance:	350
Example Measured Distance:	280

Table 3-5: Factors for the Westbound Approach

Westbound	Distance (ft.)
Offset to first lane:	18
Standing Distance:	50
Lane Width:	11
Goal distance:	250
Example Measured Distance:	180

Table 3-6: True Speed for the Eastbound Approach Based on Measured Speed and the Lane Number

True Speed (mph)			
Measured Speed (mph)	# of Lanes away from the speed gun		
	1	2	3
25	24.91	24.81	24.67
30	29.89	29.77	29.60
35	34.88	34.73	34.53
40	39.86	39.70	39.47
45	44.84	44.66	44.40
50	49.82	49.62	49.34
55	54.81	54.58	54.27
60	59.79	59.54	59.20

Table 3-7: True Speed for the Westbound Approach Based on Measured Speed and the Lane Number

True Speed (mph)			
Measured Speed (mph)	# of Lanes away from the speed gun		
	1	2	3
25	24.79	24.54	24.19
30	29.74	29.44	29.03
35	34.70	34.35	33.86
40	39.66	39.26	38.70
45	44.61	44.17	43.54
50	49.57	49.07	48.38
55	54.53	53.98	53.21
60	59.49	58.89	58.05

The results of this comparison showed that over all, the difference between the true speed and measured speed was greatest for vehicles traveling in the farthest lane from the speed gun, being the 3rd lane in this study. For the eastbound approach, the measured distance was 100 ft. longer than the westbound approach. This result shows that with a greater measured distance, the error would be less. This agrees with the LiDAR user's manual. While the actual speed data collection was not be collected at a distance as short as 180 ft. in this study, it provided an upper bounds to

the cosine effect in that the difference in speed will be less than or equal to 2 mph at the third lane with an approach speed of at least 35 mph and for the second lane with an approach speed of at least 55 mph, as is shown in Table 3-5. The standing distances that were planned on being used in this study were maintained at or above 250 ft. in the speed data collection for this study, ensuring that the speed difference remains within the ± 1 mph margin of error of the LiDAR gun.

3.3.2 Calibration of the LiDAR Speed Gun

The LiDAR speed gun used in this study, although was new, needed to be calibrated to ensure its accuracy and to test the effectiveness of the speed data collection method to be used in collecting speed data for the study. This LiDAR gun used for the study provides the user with the speed of the approaching vehicle and the distance at which the speed was recorded.

The distance measuring capability of the LiDAR gun was tested using the distance measured by a distance measurement wheel. At the test site, a traffic cone was placed at the desired location of speed data collection. From the stop bar, the LiDAR gun was shot at the traffic cone. The distance recorded by the gun was then compared with the distance measured by the measuring wheel. The distances collected by the LiDAR gun were always within ± 1 ft. of the distances recorded by the measuring wheel.

The speed measuring feature of the LiDAR speed gun was tested in order to confirm the accuracy of the speed gun. The site selected for the test was the southbound approach of the intersection at 800 North and Geneva Road, Orem, UT. This site was selected for its lack of visual obstructions, such as trees and signs, for its long green intervals, and for its straight horizontal alignment, which would provide consistent and representative results of ideal conditions. The site had two through lanes and a left-turn lane. The lack of a right-turn lane allowed the data collectors to stand close to the stop bar without a large offset usually created by the right-turn lane. The test

at this site involved filming from a vantage point that showed the detection zone of the Advance sensor, where the vehicles would be detected and counted by the sensor. UDOT painted lines perpendicular to the movement of traffic, beginning at the Advance sensor's detection zone. Additional lines were painted as a buffer of 40 feet on either side of the detection zone. The first 20 feet were marked at every 10 feet, and then the last 20 feet consisted of one marking 20 feet away from the other lines. The idea behind marking the lines at the detection zone distance was to simulate the data collection scenario where the speed gun would be aiming to collect data at the location where the Advance sensor detects and counts vehicles. Figure 3-15 shows a capture of the video recorded in the calibration process showing the painted lines used to denote the distance from the detection zone, as marked by a cone and a line, in the center of the image. Then vehicles were videotaped using a GoPro camera which filmed at a rate of 30 frames per second to assist with the testing.

After the data collection, the video created by the GoPro camera was played back in slow-motion and then an approximate speed was calculated using the number of frames it took for the vehicle to travel along the painted lines. The GoPro camera was attached at a high position to avoid any visual interference from vehicles travelling in the opposing direction. The LiDAR speed gun was placed near the stop bar of the approach, which provides for a more direct shot at an approaching vehicle at a smaller angle so that the resulting speed value would be as accurate as possible.



Figure 3-15: Image portraying painted lines used in LiDAR calibration (taken by a GoPro camera).

Upon finishing the data collection, the video created by the GoPro camera was reviewed frame by frame and the number of frames was counted from the location where a reference point on a car would pass over two separate, painted lines. The distance between the lines and the duration of time represented by the number of frames were used to compute a speed that the vehicle was traveling at. A total of 75 speed samples were collected from both of the two through lanes. Table 3-8 contains a sample of the results of the calibration. All the speed data collected for the LiDAR gun calibration can be found in Appendix A: Speed Gun Calibration Data. The difference between the speed as provided by the LiDAR gun and the speed calculated using the video was used to calibrate the accuracy of the LiDAR gun speeds. Figure 3-16 shows a graphical representation of the differences between the speeds by the two means for all the samples. The resulting differences do show a difference of ± 2 mph for the majority of the samples. Table 3-9 shows the results of a paired two-sample t-test. The difference between the mean speeds is 1.04 mph, with a p-value of 0.00015, which shows evidence of there being a significant difference in mean speeds. This difference is not significant for practical applications considering the ± 1 mph margin of error of

the LiDAR gun. The results of this test showed that the LiDAR speed gun could provide the accuracy level that was required for the speed analysis conducted in this study.

Table 3-8: Speed Gun Calibration Sample Results

Sample No.	Lane#	Distance (ft.)	LiDAR Speed (mph)	Video Speed (mph)	LiDAR Speed – Video Speed (mph)
1	2	331	55	56	1
2	1	331	48	49	1
3	1	395	59	57	-2
4	1	291	59	60	1
5	1	324	55	56	1
6	2	282	46	48	2
7	2	312	56	55	-1
8	2	346	52	56	4
9	1	324	51	51	0
10	2	343	54	59	5
11	2	367	54	56	2
12	1	331	48	50	2
13	2	323	53	55	2
14	2	346	48	50	2
15	2	317	50	50	0
16	1	272	38	39	1

3.3.3 Data Collection

This section discusses the steps involved in collecting speed data. These steps were performed at every site. Figure 3-17 shows a flowchart of the data collection process.

For each speed data sample that was taken at a site, a video of the traffic at the site was prepared for the duration of field data collection. Figure 3-18 shows a sample image of the traffic video recorded for the intersection of 400 E 800 N, Orem, UT. In this case the eastbound (EB) direction was observed. Similar to the approach volume data collection, a digital clock was used to create a relative timestamp for the video recording.

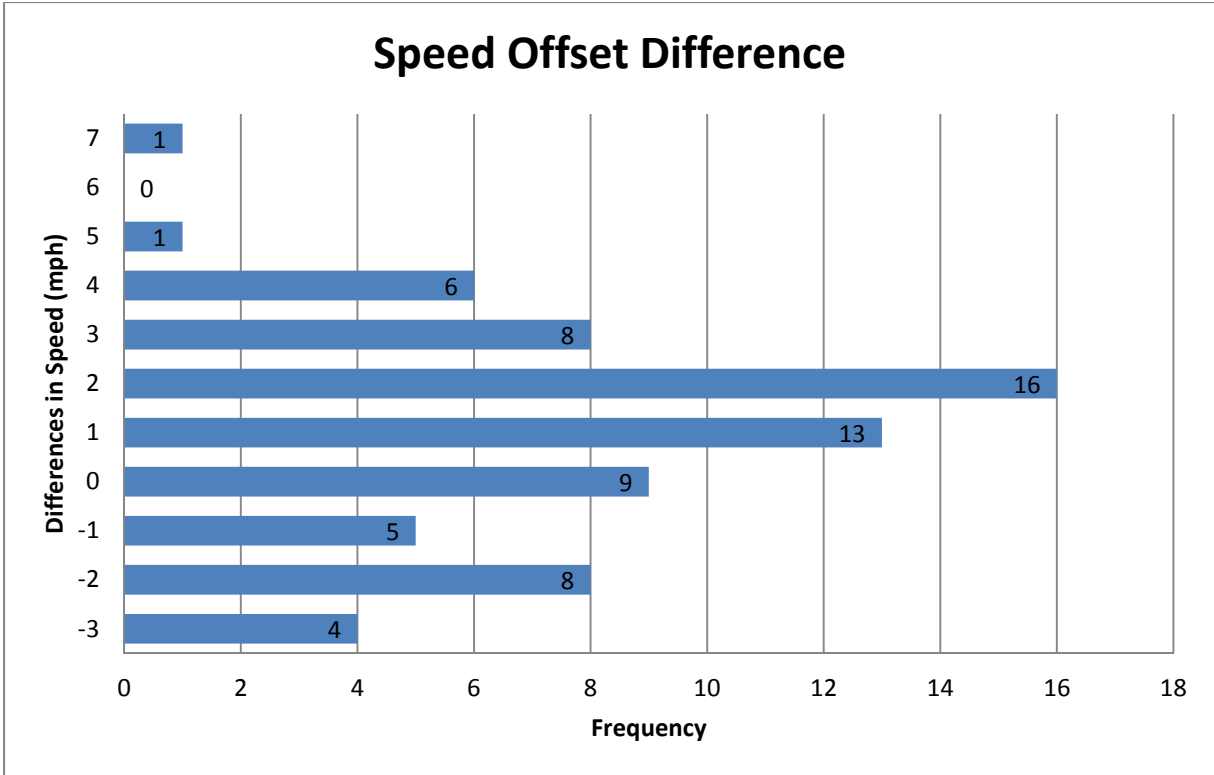


Figure 3-16: Graphical representation of the results from the LiDAR calibration.

Table 3-9: Paired t-Test for Means for LiDAR Calibration

	LiDAR Speed	Video Speed
Mean	48.42	49.44
Variance	24.62	26.68
Hypothesized Mean Difference	0	
df	70	
t Stat	-4.00282	
P(T<=t) two-tail	0.00015	
t Critical two-tail	1.99444	

The next step in the data collection process was to visit the site and to connect the laptop to the detector rack cards in the control box. Figure 3-19 shows an image of the inside of the controller box at one of the study sites. Connecting the laptop required a cable that would connect the bridge port of the detector rack card to the USB port of the laptop. Connecting the bridge port to the laptop allowed the collection of the information recorded by the Advance sensor. The sensor cards in the controller box collected data and then passed the data to the UDOT server. The bridge allowed for a data collector at the site to connect to the sensor and adjust or observe the performance without impeding the flow of data to the server. Figure 3-20 shows the bridge port above the double taped cables on each of the sensor cards. The double colored tapes on the cables, at the top of the image, show where to connect the laptop into the SmartSensor Advance™. The SmartSensor Matrix™ uses the single taped cables at the bottom of the figure. The colors of the tape on the cables are used to denote approach direction

Blue, red, yellow, and orange signify north, south, east, and west, respectively. Figure 3-21 shows the laptop successfully connected to the Advance sensor via the bridge port. The laptop needed to be connected to the right port before opening the program SmartSensor Manager (SSM) Advance v3.2.0, which allows the user to check the sensor's activity and the settings can be viewed on the monitor. Figure 3-22 shows a data collector preparing the computer prior to opening the SSM Advance software from which the speed data information can be recorded.

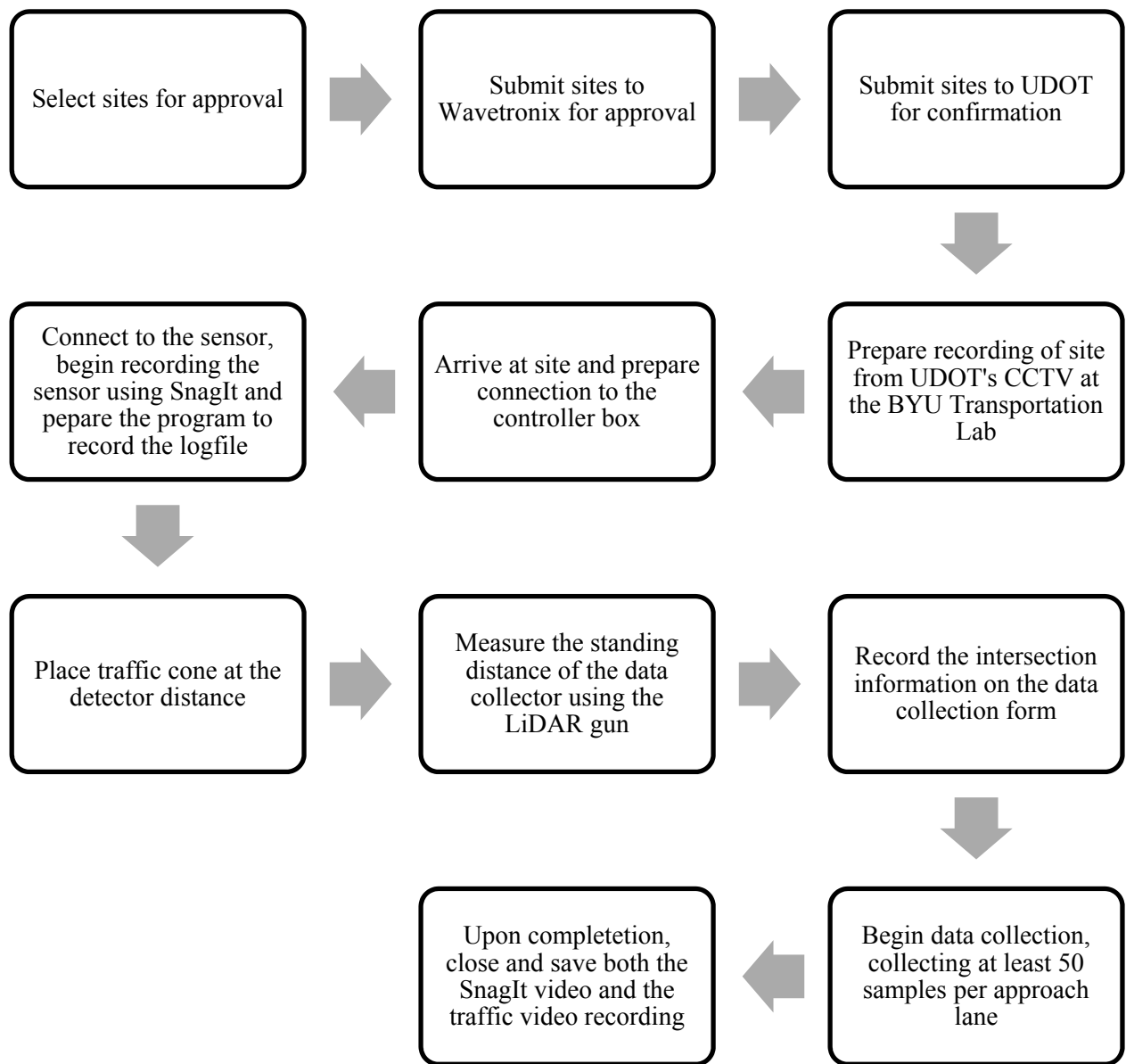


Figure 3-17: Flowchart of the approach speed data collection process.



Figure 3-18: Traffic video recorded of an approach with timestamp (photo by Greg Sanchez).



Figure 3-19: Image of the inside of a traffic controller box (photo taken by Greg Sanchez).



Figure 3-20: Double taped Advance cables with bridge ports above the cables (photo taken by Greg Sanchez).



Figure 3-21: Computer connected to the sensor for data collection (photo taken by Greg Sanchez).



Figure 3-22: Data collector connecting the computer to the sensor (photo taken by Greg Sanchez).

After the laptop has been connected the next step is to setup the software program to collect the data. Opening the SSM program brings the data collector to the program window as shown in Figure 3-23. Selecting the Communication option brings the user to the window as shown in Figure 3-24. Selecting the Serial option and the port as AutoDetect for a Multi-drop Network prepares the program to search for the sensors, which is done by selecting the Connect option. From there the software program searches for Advance sensors and the ones which it can connect to appear on the screen. Figure 3-25 shows the Advance sensors that are available for selection. Selecting the desired approach and pressing the select button begins the connection process. Figure 3-26 shows the connection window screen of the SSM program as the Advance sensor is being connected to the laptop. When the connection has been successful, the screen shown in Figure 3-27 appears.

Then the option “Channels-Alerts-Zones” is selected. Figure 3-28 shows the SSM program displaying the vehicles approaching the sensor. Each bar represents what the sensor reads as a vehicle. The numbers represent, from left to right, the vehicle’s distance from the stop bar, approach speed, and estimated time of arrival. The method to collect the data presented by the moving bars on the screen is to create a log file of the activity of the Advance sensor as displayed by the SSM program. A log file is created by selecting the folder icon on the left side of the program window. Figure 3-29 shows a new folder being created with the name of ‘Sample Site’ to which all the speed data running through the screen can be saved. Figure 3-30 shows the sensor Advance screen which shows the ‘on’ switch on the left side of the screen. When this option is selected, the data begins to be stored in the log file.

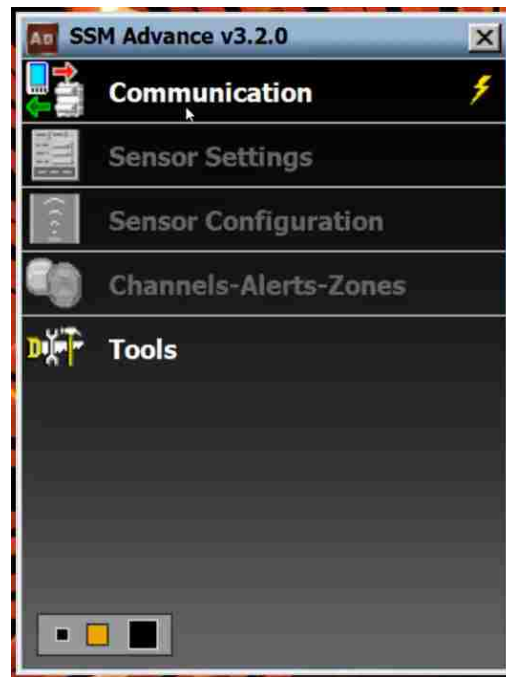


Figure 3-23: SSM Advance program opening window.

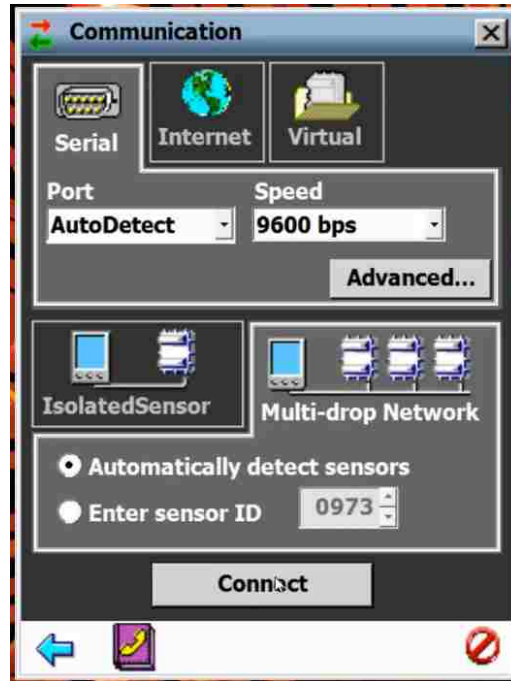


Figure 3-24: SSM Advance connection window.

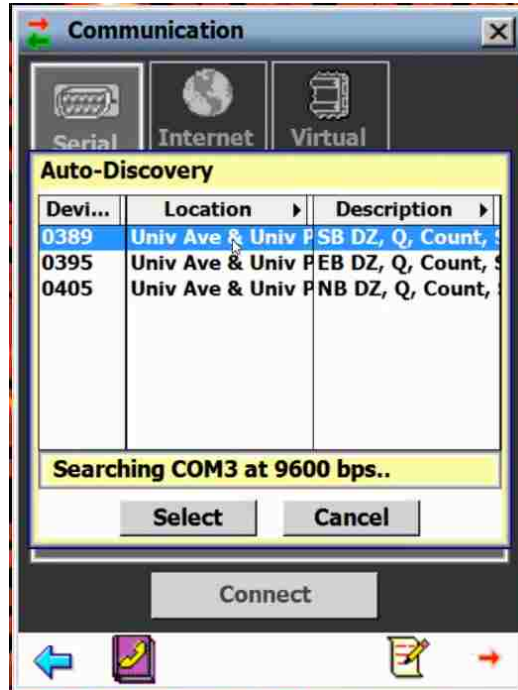


Figure 3-25: SSM Advance sensor selection window.

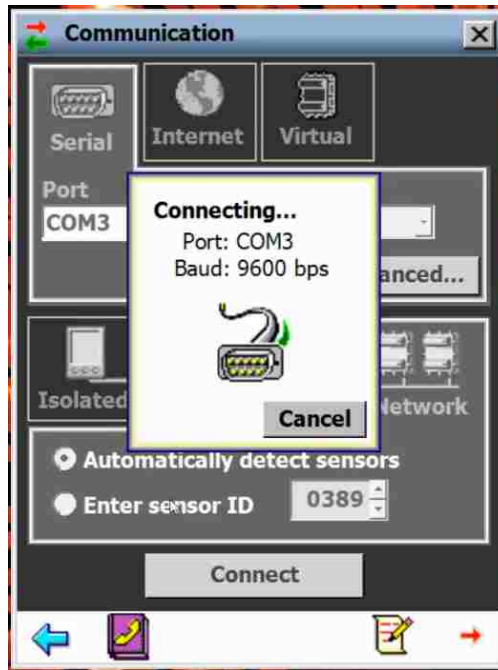


Figure 3-26: SSM Advance sensor connecting window.

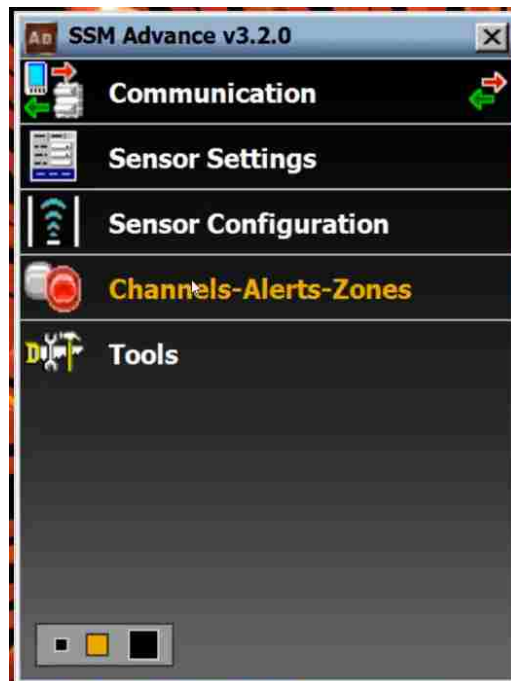


Figure 3-27: SSM Advance sensor options window.

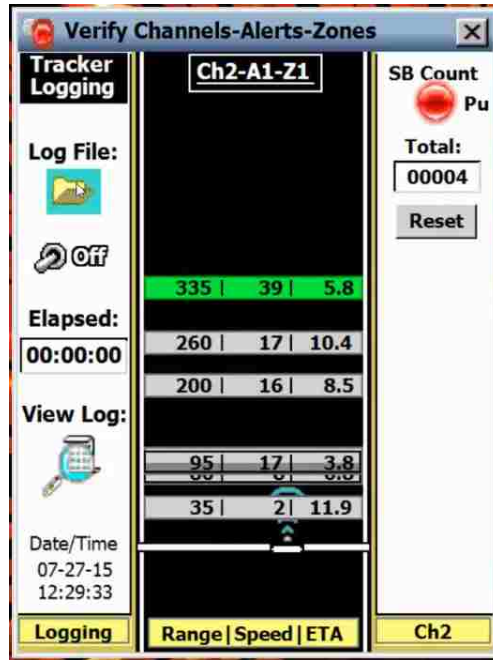


Figure 3-28: SSM Advance sensor tracking display.

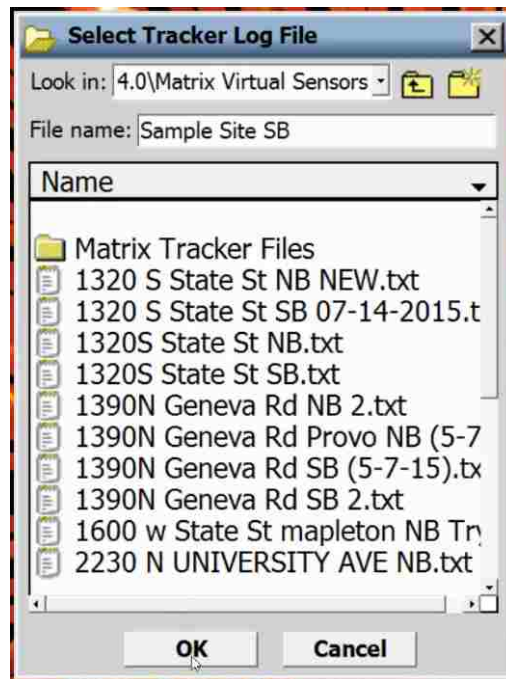


Figure 3-29: SSM Advance log file window.

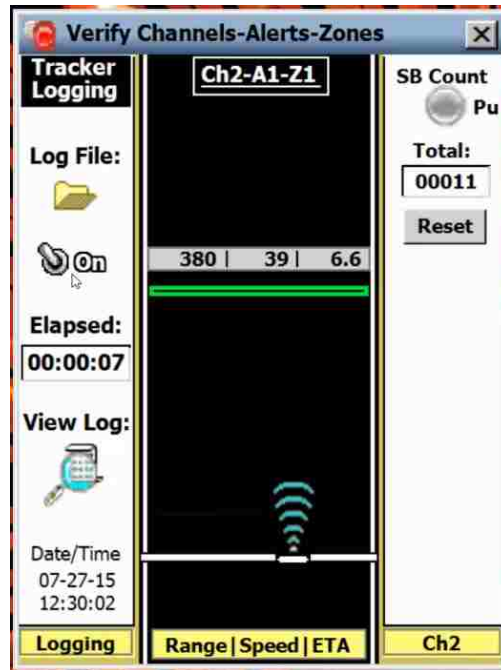


Figure 3-30: SSM Advance sensor screen ready for recording.

Apart from recording the data which the Advance sensor collected, the entire screen of the laptop monitor was recorded as well to visually show what the sensor was recording for later use in data reduction and for comparing the speeds collected by the sensor to the traffic video. Using the program SnagIt 11 (TechSmith 2014), the window of the SSM program showing the sensor display was recorded and saved as a video to refer to during the data reduction phase.

After finishing the setup inside the controller box, the next step was to prepare the area where the speed gun was placed to collect data. This included placing a traffic cone at the recommended distance at which the sensor's detection zone was set up. The purpose of placing the cone was to assist the data collectors to more effectively collect data using the LiDAR speed gun at the desired distance from the stop bar. The detector distance information can be found in the SPMs website; at the top of each approach speed graph shown in the SPMs website, the detector distance from the stop bar can be found, as shown in the circle area in Figure 3-31.

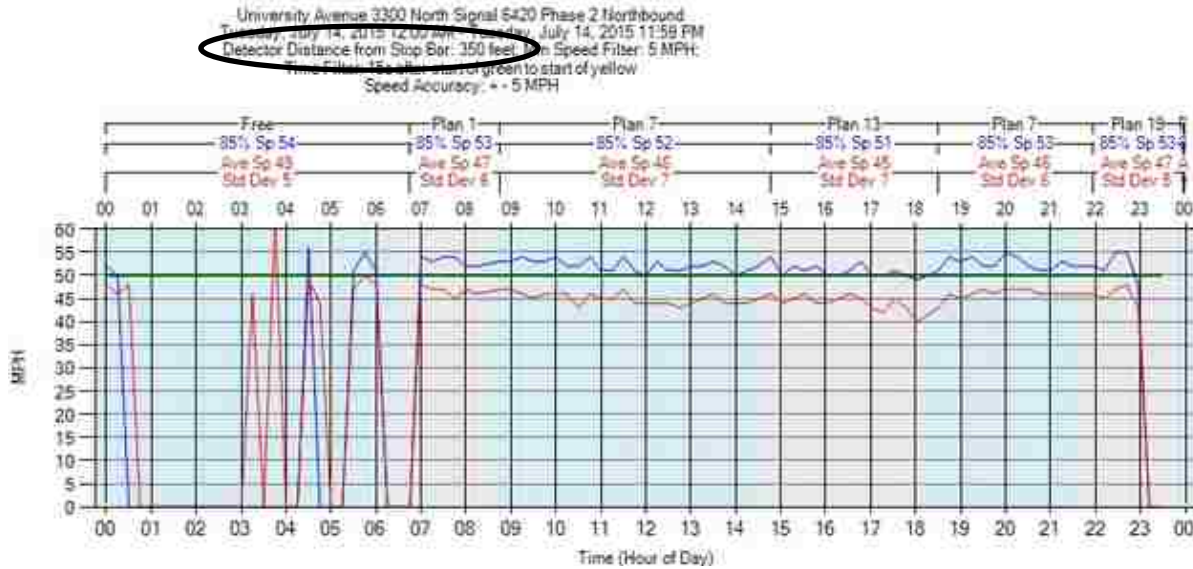


Figure 3-31: Graph of the approach speed with sensor information from the SPMs website.

Each sensor's detection zone distance can vary depending on how the sensor was installed by UDOT. UDOT uses a detection zone of 10 feet in width and generally at about 350 feet back from the stop bar. This setting is used because the primary purpose of the sensor's approach speed feature is to collect speed data of the vehicles traveling at free-flow speed. In order to effectively collect free-flow speeds the virtual detection distance is adjusted to avoid any obstructions, such as overhead cables, buildings, or trees. Another goal in adjusting the virtual detection zone is to ensure that during peak hours, the queue will not extend into the detection zone. In areas with high traffic volumes, the detection zone is generally placed farther upstream to ensure the free-flow speed of the vehicles. In areas where there are overhead obstructions, the detection zone may be placed closer to the stop bar Table 3-10 shows the studied intersections, their approaches for which speed data were collected (being the EB, westbound (WB), northbound (NB), or southbound (SB) directions), the distance away from the stop bar where the virtual detector zone was placed, and the number of lanes found in each approach.

After placing the cone at the specified distance away from the stop bar, or the goal distance, the data collectors measured how far away from the stop bar they would be standing while collecting speed data using the speed gun. These distances were recorded on the data collection page created by the BYU team to assist in data collection, which is shown in Figure 3-32. As agreed on by UDOT and Wavetronix, ± 20 ft. range from the detection zone distance were permitted to expedite speed data collection. Getting speed data by a LiDAR gun exactly at the distance of the detection zone was difficult.

Table 3-10: The Detection Zone Distance and Number of Lanes of Each Sample Site

Intersection	Approach	Distance from Stop bar	Number of Lanes
400 E 800 N, Orem	EB	350	3
	WB	250	3
800 N Geneva Rd, Orem	NB	360	2
1320 N State St, Provo	NB	400	2
	SB	350	2
Geneva Rd University Pkwy, Orem	NB	360	1
	SB	360	2
	WB	360	3
9000 S 700 W, Sandy	EB	350	3
	WB	350	3
University Ave University Pkwy, Provo	SB	350	2
3500 S 2200 W, West Valley	EB	350	3
	WB	350	3
3300 N University Ave, Provo	NB	350	2

Intersection: _____

Direction: _____

Date: _____

Starting time: _____

Range: _____ to _____

Standing distance from Stop bar: _____

Goal Distance: _____

Notes:

T1	T2	T3

Figure 3-32: Speed data collection page.

After the site and the detection zones were properly set up at the site, the data collection began. Using the LiDAR gun, speed data were collected by aiming and shooting at the license plate, or other reflective material of the approaching vehicle. There was a limitation on which vehicles can be shot at. Since the ideal sample vehicle was one that was isolated while moving, a successful sample vehicle could not have any vehicles traveling adjacent to or near them. This ensured that the sensor reading was not altered by the presence of another vehicle nearby. There was a 15 second delay from the time when the green interval began to the time when the sensor began to record the data; that is, speed data collected 15 seconds after the start of a green interval were sent to UDOT's server. The purpose of this arrangement was to ensure that there was no interference from a queue that might prevent the vehicles from travelling at free flow speed. Data collectors were instructed to collect data at any time between the 15 seconds into the green interval until the beginning of the yellow interval. After each time the LiDAR speed gun had shot at a vehicle, its image appears on the main screen of the LiDAR speed gun. Figure 3-33 shows a vehicle image taken by the LiDAR gun. The screen of the LiDAR gun displays the image of the vehicle whose speed was measured, the speed of the vehicle and the distance the vehicle was located from the LiDAR gun at the time its speed was recorded. By looking at this image, the data collectors could tell if the vehicle was within the ± 20 ft. range from the designated distance for the site. If the distance fell within the range, then the data collectors considered the vehicle as a valid speed sample. The goal for the data collectors was to acquire 50 speed samples per lane per site for this study. If 50 speed samples per lane per site were not possible in one visit, extra visits were made to the site. Additional samples were also taken when possible at the study intersections to ensure that there would be more samples that would be usable for a statistical analysis. Figure 3-34 shows a data collector measuring the distance needed to place the cone before beginning data collection.

Figure 3-35 and Figure 3-36 show a data collector using the LiDAR speed gun to collect speed data.



Figure 3-33: The screen of the gun while collecting data (photo taken by Greg Sanchez).



Figure 3-34: Measuring out the distance to place the cone (photo taken by Greg Sanchez).



Figure 3-35: Collecting speed data (front view) (photo taken by Greg Sanchez).



Figure 3-36: Collecting speed data (back view) (photo taken by Greg Sanchez).

After collecting the speed data, the SnagIt video recording of the SSM program window was stopped and saved. Then, the log file collection was turned off and the SSM program was closed. Upon returning to the BYU Traffic Lab, the video recording of the traffic underway in the Traffic Lab using the CCTV while speed data were collected in the field was turned off and saved.

3.3.4 Data Reduction

This section discusses the process involved in reducing the speed data collected by the LiDAR speed gun, the traffic video recorded in the Transportation Lab, the video of the SSM program recorded by SnagIt, and the Hi-res data. The process was followed at each site. Figure 3-37 shows a flowchart of the speed data reduction process.

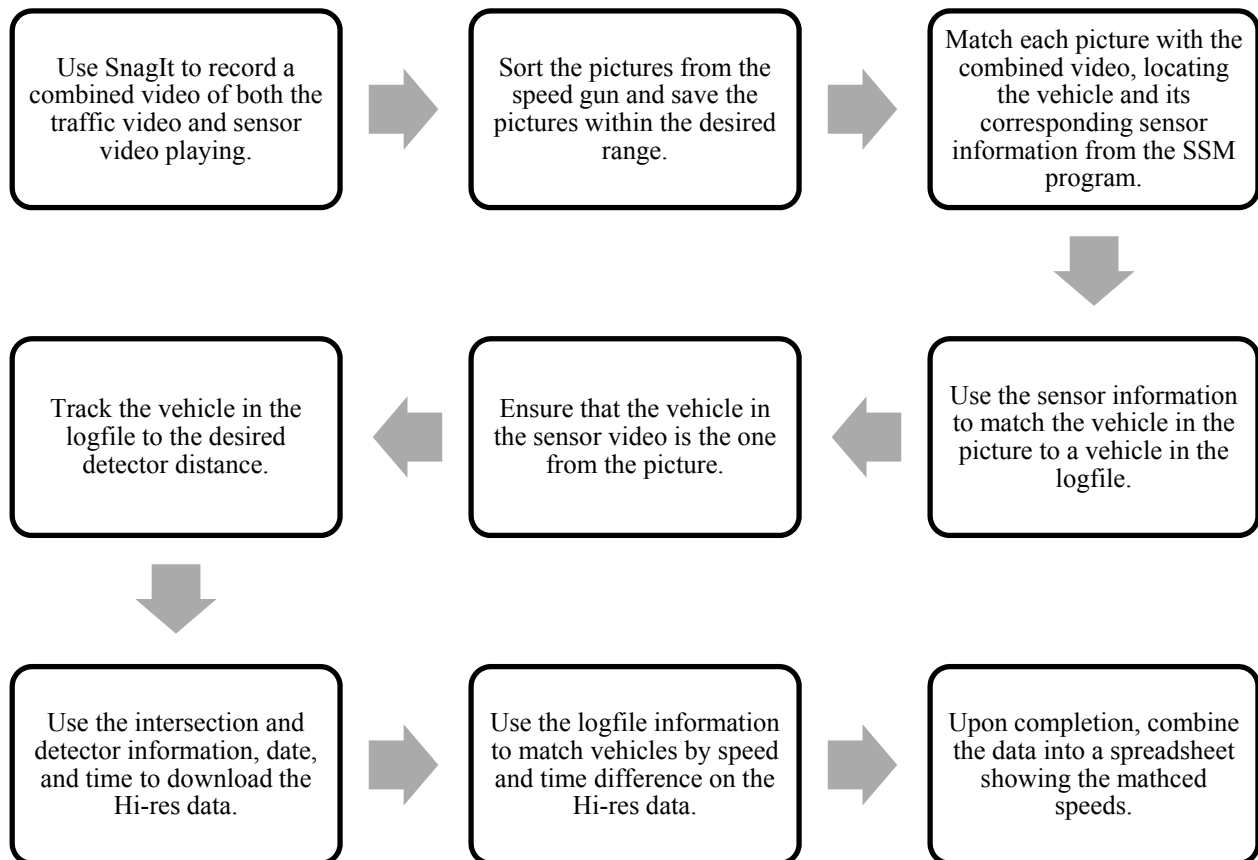


Figure 3-37: Flowchart of the approach speed data reduction process.

The process for reducing the data consisted of many steps, preparatory to the comparative analysis of the speed data. The first thing to do was to create a usable video of the traffic. The camcorder used in recording the intersections for this study split the recording into smaller segments. Using the Windows Movie Maker (Microsoft 2015), those segments were combined and made into one video. After this task, the next step was to synchronize the traffic and SSM

program recordings so that they could play simultaneously. This was done by matching a moving bar representing a vehicle movement from the recording of the SSM program window that showed the virtual detectors of the vehicles as they moved across the screen in the recording of the traffic video. The techniques used in finding the difference in time between both videos are either finding a long gap between two cars in the sensor video and then finding a similar gap on the traffic video or using a certain number of vehicles as seen on the SSM program recording as a reference and then finding the same situation in the traffic video where the same number of cars pass by during the same time interval. The purpose of this step was to ensure that the approaching vehicles and sensor movements were synchronized. A SnagIt video was created of the SSM recording and the traffic videos being played simultaneously. Figure 3-38 shows a screen capture of a finished, combined and synchronized video with the traffic video on the left and the video of the SSM program on the right.

Upon completion of the creation of the combined video, the data collected from the speed gun were sorted. The pictures that were found within the desired range were saved using the Snipping Tool available on a typical PC. The sorting consisted of finding the vehicles whose data had been collected within the range of ± 20 feet from the designated virtual detector location and vehicles that were traveling at more than 25 to 35 mph, depending on the speed limit of the road. This vehicle selection method helped the analyst to ensure that the vehicle was traveling at free flow speed as opposed to being in the middle of acceleration or deceleration. The information contained in the saved picture was an image of the sampled vehicle, the speed at which it was approaching, and the distance away from the LiDAR speed gun when the vehicle was located at the time its picture was taken. Figure 3-39 shows a sample image that was saved using the Snipping Tool with

the information located above the image of the vehicle. The process of sorting the pictures resulted in the number of potential usable speed samples.



Figure 3-38: Final combined video.

After the traffic and sensor videos had been combined and the speed gun pictures sorted, the next step was to match the vehicle in the speed gun picture to the vehicle in the combined video. This was done by selecting a picture of a sample vehicle and finding it on the combined video. The technique used was choosing a picture of a vehicle that was unique or large, such as a truck or a bus. After finding the reference vehicle in the combined video, the next task was to match the distance shown in the picture added to the distance away from the stop bar where the data collectors were standing, with the distance or range shown in the SSM program recording. This value was the first of three numbers shown on the solid bar in the SSM sensor portion of the combined video. For example, the picture in Figure 3-39 shows in the box at the lower left-hand corner a vehicle at

a distance of 188.5 feet travelling at a speed of 45 mph. Adding the standing distance of 50 feet made the resulting distance from the stop bar to be 238.5 feet. As shown in Figure 3-40, the closest sensor position to that distance was 245 feet, thus the picture was matched with the time and information displayed on the sensor portion of the video.

The speed, distance and time from the picture taken by the LiDAR gun, and the range, speed, ETA and time taken from the sensor video of each sample were recorded in a spreadsheet shown in Figure 3-41 along with any reasons or explanations if the sampled speed was not valid.

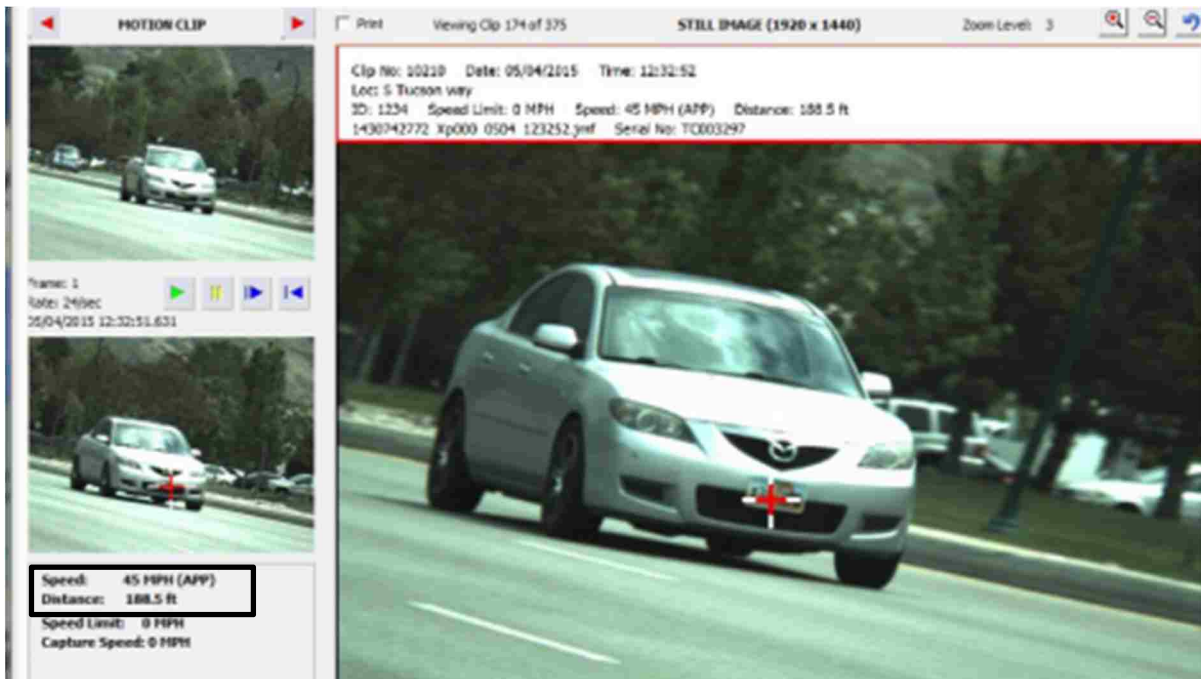


Figure 3-39: Image provided by the LiDAR gun.



Figure 3-40: The sensor video and traffic video to match the LiDAR picture.

After the pictures had been matched, the next task was to find the log file that had been saved from the time when the data collection took place. Figure 3-42 shows an example of a log file. The information included were the date, time, id number assigned to a vehicle, speed, distance from the stop bar, and the discovery range or distance at which the vehicle was first discovered by the sensor. The log file information is the data shown in the sensor video as each bar or vehicle was first discovered and then as the bar moves down the screen. Note that ETA is not part of the log file according to the current log file setup.

T2	Sensor				Picture				Log				High-res			
	Picture #	Range	Speed	ETA	Time	Speed	Distance	Time	Dif	Speed	Distance	Time	Dif	Speed	Real Time	Comp Time
1	4	370	49	5.1	11:28:14	59	361.1	10:27:35								
2	5	360	33	7.4	11:29:29	35	364.8	10:28:50	0:01:15				0:00:00			
3	7	345	43	5.4	11:31:35	45	351.7	10:30:56	0:02:06				0:00:00			
4	8	360	36	6.8	11:36:09	34	362.3	10:35:30	0:04:34				0:00:00			
5	9	365	48	5.1	11:37:21	56	367.3	10:36:42	0:01:12				0:00:00			
6	10	365	38	6.5	11:38:29	34	350.5	10:37:50	0:01:08				0:00:00			
7	12	365	43	5.7	11:39:20	45	362.2	10:38:41	0:00:51				0:00:00			
8	13	365	48	5.1	11:40:28	50	356	10:39:49	0:01:08				0:00:00			
9	14	355	45	5.3	11:40:49	46	353.3	10:40:10	0:00:21				0:00:00			
10	17	360	42	5.8	11:44:37	39	350.4	10:43:58	0:03:48				0:00:00			
11	18	370	37	6.8	11:44:56	38	360.6	10:44:17	0:00:19				0:00:00			
12	19	350	40	5.9	11:45:05	38	352.1	10:44:26	0:00:03				0:00:00			
13	23	345	41	5.7	11:49:28	41	348.9	10:48:48	0:04:22				0:00:00			
14	24	340	37	6.2	11:50:29	36	344.9	10:49:50	0:01:02				0:00:00			
15	25	340	40	5.7	11:50:35	39	336.9	10:49:57	0:00:07				0:00:00			
16	26	345	37	6.3	11:50:53	40	340.8	10:50:14	0:00:17				0:00:00			
17	28	340	45	5.1	11:54:03	44	336.6	10:53:25	0:03:11				0:00:00			
18	30	340	39	5.9	11:54:41	40	339.1	10:54:02	0:00:37				0:00:00			
19	31	340	44	5.2	11:55:29	46	336.8	10:54:50	0:00:48				0:00:00			
20	33	360	44	5.5	11:58:45	45	352.9	10:58:05	0:03:15				0:00:00			

accelerating

Figure 3-41: Spreadsheet matching picture and sensor video data.

```
FileVersion=SSMAv3.2, 12
Traffic=Toward
FirmwareVersion=3,10.01.12,0032
```

```
Serial Number:    SS200 V100001112
Location:         800n-400e, Orem
Description:      EB DZQ45
```

DATE (yyyy-mm-dd)	TIME (hh:mm:ss.ms)	ID (#)	SPEED (mph)	DISTANCE (ft)	DISCOVERY RANGE(ft)
2015-04-28	12:12:09.725	37	32	360	480
2015-04-28	12:12:09.852	37	32	350	480
2015-04-28	12:12:10.010	37	32	345	480
2015-04-28	12:12:10.132	37	32	335	480
2015-04-28	12:12:10.979	38	39	330	330
2015-04-28	12:12:11.199	38	24	325	330
2015-04-28	12:12:11.261	38	24	325	330
2015-04-28	12:12:11.504	38	25	325	330
2015-04-28	12:12:11.591	38	26	325	330
2015-04-28	12:12:11.827	38	26	320	330
2015-04-28	12:12:11.918	38	25	320	330
2015-04-28	12:12:12.151	38	24	320	330
2015-04-28	12:12:12.242	38	22	320	330
2015-04-28	12:12:12.447	38	20	315	330
2015-04-28	12:12:12.574	38	19	315	330
2015-04-28	12:12:12.771	38	18	310	330
2015-04-28	12:12:12.854	38	16	310	330
2015-04-28	12:12:13.062	38	15	305	330
2015-04-28	12:12:13.177	38	14	305	330
2015-04-28	12:12:13.387	38	14	300	330
2015-04-28	12:12:13.507	38	13	300	330
2015-04-28	12:12:13.699	38	12	295	330
2015-04-28	12:12:13.794	38	11	295	330
2015-04-28	12:12:13.991	38	9	295	330
2015-04-28	12:12:14.115	38	8	295	330
2015-04-28	12:12:14.307	38	7	295	330
2015-04-28	12:12:14.445	38	6	295	330
2015-04-28	12:12:14.627	38	5	295	330
2015-04-28	12:12:14.773	38	5	295	330

Figure 3-42: Example of a log file as recorded by the SmartSensor Advance.

Since the information from the sensor video was a visual representation of the data collected in the log file, the speed and range of a vehicle from one of the samples was used to confirm that the time shown in the sensor video and in the log file were the same. After confirming or noting the time difference, if there was any, the log file was then used to find the speed of the vehicle as close as possible to the distance away from the stop bar where the virtual detector was located. The technique used in finding the speed at the detector was to find and note the vehicle id number of the sample vehicle using the speed and range, as provided by the sensor. Using the vehicle id

number, the sampled vehicle was tracked either backward or forward until the range that was closest to the detector distance was found and the range, speed and time were recorded. This procedure was repeated for every vehicle sampled. The SSM program video could be used to confirm if a sample was not a good one, that is, if the speed was significantly different or if the vehicle in the log file data did not show speed data near the detector range distance. Such discrepancies might have been caused by the following reasons. First, there might have been multiple vehicles traveling alongside each other or when the sensor could not decipher the effect of a truck and trailer, recording it as two vehicles. When there was a reason why the sample should not be used, the speed cell was shaded with a different color and a note was placed next to the sampled vehicle to explain why it was not used.

After matching each sample to the speed calculated by the sensor using the log file, the final step in the speed data reduction was to use the Hi-res data to match and confirm the speeds provided by the log file, Advance sensor picture and LiDAR speed gun picture. Similar to the volume counts, the Hi-res data were downloaded from UDOT's SQL server. The process for the approach speed was to download from the SQL server the information about a signalized intersection so that the detector id number could be found. The detector id was then entered into the SQL server along with the date and time from the time the speed data collection was performed. The output from the SQL server was the Hi-res data used in the final step of the speed data reduction. Figure 3-43 shows a speed data output from the SQL server obtained from this step.

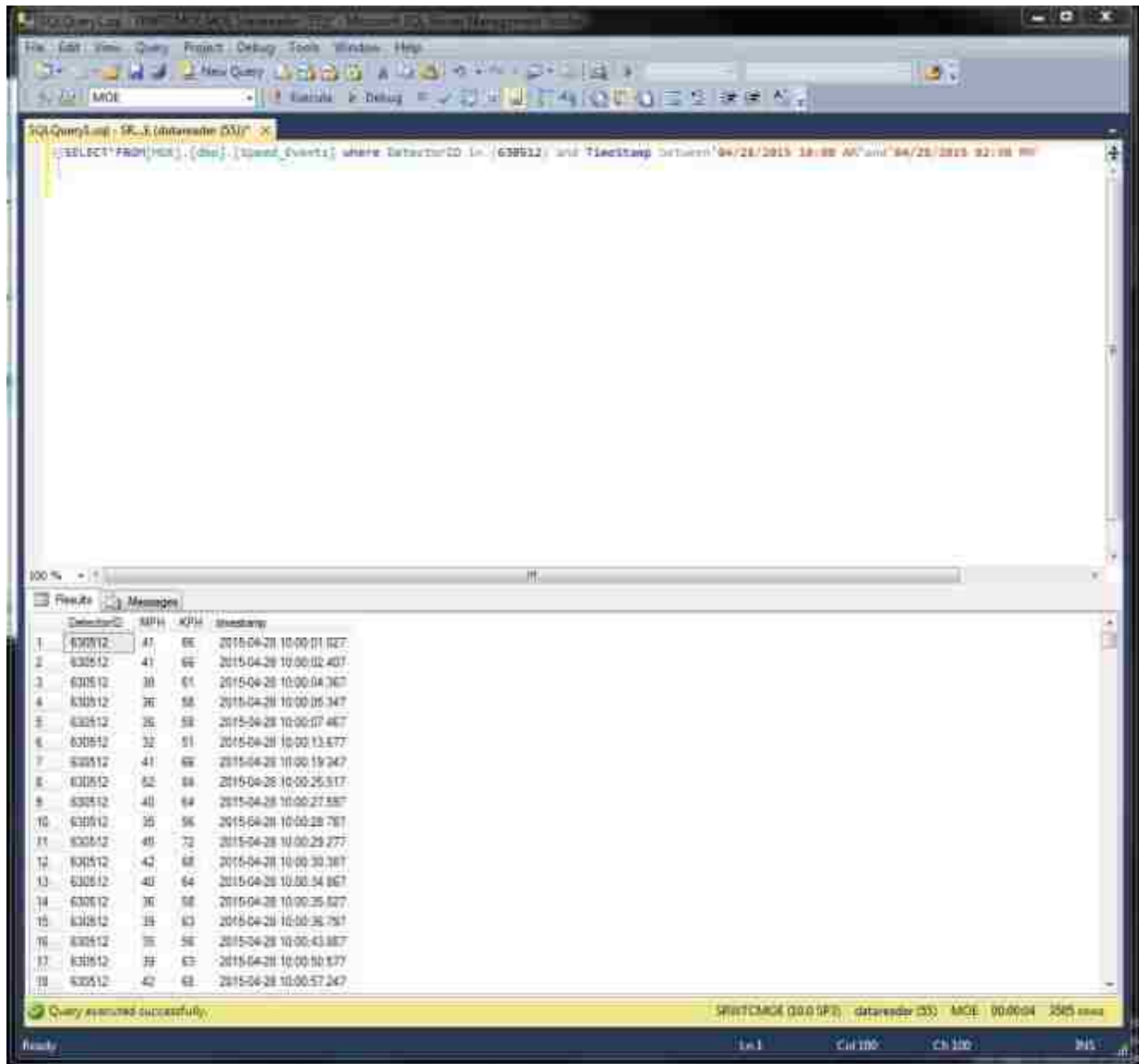


Figure 3-43: SQL server approach speed output.

The speed data were then exported into an Excel spreadsheet from where they were matched to the speed samples from the log files. The Hi-res output only provides time and speed in mph and kph. The process used in order to find the specific sample vehicles in the Hi-res was to use the time differences between samples in the log file. Since the Hi-res data shows the speeds of the vehicles at the detector locations, it can be assumed that the log file shows speeds similar, if not

exactly equal, to those in the Hi-res data. Before matching speed data from the log file to the speeds in the Hi-res data, the time difference between speed data in the log file and in the Hi-res data needed to be determined. The reason for performing this task was that the log file used the time of the laptop while recording speed data, which is updated via the Internet. The Hi-res data uses the UDOT server time because these speeds are the speeds that eventually appear on UDOT's SPMs website. The time that is reported by the Hi-res data is based on UDOT's central system's internal time clock, which is controlled by a server located at the Utah State Capitol building. The time in the controller boxes gets updated every 4 hours along with the Hi-res time clock. Since this update is happening remotely, there is a delay which results in a time difference between the actual time, and the times shown at the controller box and the Hi-res file.

To find the Hi-res speed data which corresponded to the log file speed data, two speed samples in the log file were found which had the same speed in mph at the detector distance. Using those speeds, the difference in arrival time between the vehicles were used to find corresponding speeds in the Hi-res data. This process was repeated until a successful match was made. Figure 3-44 shows a sample of how the speeds in the log file on the left were matched with the speeds in the Hi-res data on the right. The assumption that was made with the data was that the vehicle was traveling at constant, free flow speed; thus, the speed in the log file and the speed recorded in the Hi-res data would be the same. If this assumption was correct, the difference in time between the two selected speed samples in the log file and in the Hi-res file would be used as a reference to help the analyst match the log file speeds to the Hi-res speeds. By finding the difference in time between the sampled vehicle in the log file and in the Hi-res, the log file timestamps for the log file would be adjusted to become the same relative time as in the Hi-res data. After adjusting the time, the other sampled vehicles were checked to see if the time difference was accurate. It is important to note

that the speeds as recorded in the Hi-res data file and the log file may not be the same. As discussed in the literature review, while the speed data represent the same event, two separate processes are used to acquire the speed data and they may have slightly different values. Hence, if the first attempt at using the difference in time was not successful, the process needed to be repeated until speeds in the Hi-res data file and log file were matched. When the matching vehicles were found, their speeds and times were recorded. Figure 3-45 shows the results of data reduction using the log file and the Hi-res data and their corresponding Advance sensor and LiDAR gun picture data. In the figure, the “Sensor” column displays the data shown in the sensor video, the “Picture” column shows the speed of that specific vehicle according to the LiDAR gun, the “Log file” column shows the speed of that vehicle from the log file, and the Hi-res column shows the data that were successfully matched from the log file to the Hi-res data. In the case of the shaded row number 7, the sensor, log file and Hi-res shows the same vehicle as being measured to have been traveling at 48 mph, while the LiDAR gun measured the speed to be 45 mph. This vehicle was retained for statistical analysis because the information from the LiDAR gun, sensor video, and log file data for the sample vehicle were successfully matched in the data reduction.

Each lane was analyzed separately, as speed samples were taken by lane at each approach studied. The results of data reduction were compiled into a spreadsheet where a comparison of the speeds taken from the vehicle image from the LiDAR speed gun, Advance sensor, log file, and Hi-res could be easily analyzed.

1	DATE	TIME	ID	SPEED	DISTANCE	DISCOVERY
21247	5/4/2015	14:33:34	1183	45	85	340
21248	5/4/2015	14:33:34	1180	33	40	520
21249	5/4/2015	14:33:34	1183	44	75	340
21250	5/4/2015	14:33:34	1180	32	35	520
21251	5/4/2015	14:33:34	1183	43	70	340
21252	5/4/2015	14:33:34	1180	32	25	520
21253	5/4/2015	14:33:34	1183	44	55	340
21254	5/4/2015	14:33:34	1183	43	50	340
21255	5/4/2015	14:33:35	1183	43	40	340
21256	5/4/2015	14:33:35	1183	43	30	340
21257	5/4/2015	14:33:36	1184	46	280	280
21258	5/4/2015	14:33:36	1184	48	280	280
21259	5/4/2015	14:33:36	1184	48	270	280
21260	5/4/2015	14:33:36	1184	48	245	280
21261	5/4/2015	14:33:36	1184	47	240	280
21262	5/4/2015	14:33:36	1184	45	230	280
21263	5/4/2015	14:33:37	1184	44	220	280
21264	5/4/2015	14:33:37	1184	44	210	280
21265	5/4/2015	14:33:37	1184	45	195	280
21266	5/4/2015	14:33:37	1184	46	185	280
21267	5/4/2015	14:33:37	1184	47	170	280
21268	5/4/2015	14:33:37	1184	47	160	280
21269	5/4/2015	14:33:38	1184	48	150	280
21270	5/4/2015	14:33:38	1184	48	140	280
21271	5/4/2015	14:33:38	1184	46	130	280
21272	5/4/2015	14:33:38	1184	46	120	280
21273	5/4/2015	14:33:38	1184	45	115	280
21274	5/4/2015	14:33:38	1184	45	105	280
21275	5/4/2015	14:33:38	1184	45	95	280

1	DetectorID	MPH	KPH	timestamp
809	630510	46	74	2015-05-04 13:32:26.210
810	630510	49	79	2015-05-04 13:32:27.100
811	630510	45	72	2015-05-04 13:32:30.110
812	630510	45	72	2015-05-04 13:32:32.430
813	630510	43	69	2015-05-04 13:32:32.430
814	630510	43	69	2015-05-04 13:32:33.820
815	630510	38	61	2015-05-04 13:32:35.370
816	630510	28	45	2015-05-04 13:32:40.420
817	630510	38	61	2015-05-04 13:32:44.530
818	630510	37	60	2015-05-04 13:32:46.190
819	630510	46	74	2015-05-04 13:32:48.010
820	630510	48	77	2015-05-04 13:32:52.720
821	630510	55	89	2015-05-04 13:32:56.200
822	630510	54	87	2015-05-04 13:32:59.930
823	630510	43	69	2015-05-04 13:33:03.480
824	630510	49	79	2015-05-04 13:33:17.920
825	630510	41	66	2015-05-04 13:33:19.710
826	630510	38	61	2015-05-04 13:33:25.700
827	630510	53	85	2015-05-04 13:33:26.640
828	630510	55	89	2015-05-04 13:33:29.310
829	630510	45	72	2015-05-04 13:33:33.490
830	630510	34	55	2015-05-04 13:33:40.230
831	630510	31	50	2015-05-04 13:33:41.900
832	630510	31	50	2015-05-04 13:34:08.920
833	630510	16	26	2015-05-04 13:34:18.900
834	630510	10	16	2015-05-04 13:34:21.180
835	630510	27	43	2015-05-04 13:34:22.120
836	630510	43	69	2015-05-04 13:34:22.300
837	630510	6	10	2015-05-04 13:34:25.510
838	630510	31	50	2015-05-04 13:34:32.260

Figure 3-44: Spreadsheet showing the log file data along with the Hi-res data.

T1	Sensor				Picture				Log				High-res			
Picture #	Range	Speed	ETA	Time	Speed	Distance	Time	Diff	Speed	Distance	Time	Diff	Speed	Real Time	Comp Time	
1	4	275	44	4.2	14:13:11	44	262	12:12:28	0:00:00	44	275	14:13:12.00	0:00:00.00	44	13:12:28.53	14:13:12.14
2	5	280	48	3.9	14:13:39	48	250.8	12:12:55	0:00:27	48	280	14:13:38.76	0:00:26.76		13:12:55.15	
3	8	240	44	3.7	14:24:54	39	257.2	12:24:11	0:11:16	44	240	14:24:54.75	0:11:15.99	43	13:24:11.29	14:24:54.90
4	10	270	50	3.6	14:25:27	47	260.2	12:24:43	0:00:32	50	245	14:25:27.54	0:00:32.79	50	13:24:44.09	14:25:27.70
5	11	240	50	3.2	14:25:31	43	235.9	12:24:47	0:00:04	50	240	14:25:31.17	0:00:03.63		13:24:47.56	
6	12	280	38	5	14:25:54	40	259	12:25:10	0:00:23	38	280	14:25:53.86	0:00:22.69		13:25:10.25	
7	16	245	48	3.4	14:33:36	45	238.5	12:32:52	0:07:42	48	245	14:33:36.16	0:07:42.30	48	13:32:52.72	14:33:36.33
8	17	235	44	3.6	14:35:35	44	132.4	12:34:52	0:02:00	44	235	14:35:35.78	0:01:59.62		13:34:52.17	
9	19	275	35	5.3	14:40:20	31	256.4	12:39:36	0:04:44	35	275	14:40:19.88	0:04:44.10		13:39:36.27	
10	20	245	45	3.7	14:41:18	41	260	12:40:34	0:00:58	45	245	14:41:18.15	0:00:58.27		13:40:34.54	
11	21	240	45	3.6	14:41:26	44	244.3	12:40:42	0:00:08	45	250	14:41:26.31	0:00:08.16	45	13:40:42.85	14:41:26.46
12	23	255	42	4.1	14:43:07	42	249.5	12:42:24	0:01:42	42	255	14:43:08.13	0:01:41.82	43	13:42:24.48	14:43:08.09
13	24	270	40	4.6	14:43:24	38	258.4	12:42:41	0:00:17	41	245	14:43:24.92	0:00:16.79	40	13:42:24.48	14:43:08.09
14	25	245	33	5	14:44:30	31	249	12:43:47	0:01:06	33	245	14:44:31.05	0:01:06.13	34	13:43:47.59	14:44:31.20
15	27	240	55	2.9	14:53:43	53	253.7	12:52:59	0:09:12	55	240	14:53:43.32	0:09:12.27	52	13:52:59.86	14:53:43.47
16	29	275	45	4.1	14:53:57	43	270.6	12:53:13	0:00:14	45	275	14:53:56.95	0:00:13.63		13:53:13.34	
17	30	265	48	3.7	14:54:12	45	260.2	12:53:18	0:00:05	47	245	14:54:12.56	0:00:15.61	48	13:53:26.63	14:54:12.74
18	31	260	46	3.8	14:59:17	42	262.2	12:58:34	0:05:16	48	260	14:59:18.01	0:05:05.45	50	13:58:34.59	14:59:18.20
19	33	260	47	3.7	15:01:20	46	258.6	13:00:36	0:02:02	47	250	15:01:20.31	0:02:02.30	47	14:00:36.70	15:01:20.34
20	36*	245	55	3	15:01:42	46	261.6	13:00:58	0:00:22	55	245	15:01:42.72	0:00:22.41	55	14:00:59.28	15:01:42.89
21	37	265	46	3.9	15:02:06	47	266.3	13:01:23	0:00:25	46	255	15:02:07.19	0:00:24.47	47	14:01:23.77	15:02:07.38

Figure 3-45: Spreadsheet showing completed data reduction of speed data.

3.4 Chapter Summary

This chapter discussed the methodology used in collecting both approach volume and speed data. The design of the data collection method went through trials and errors to find the most effective and efficient way to compare the data retrieved from the Hi-res data file produced by the Advance Sensor with the ground truth data collected manually by the data collectors. It took the data collectors many hours to carry out the data collection and data reduction. The approach volume and approach speed data collection methods were explained in detail, including retrieving and reduction of the Hi-res data from the UDOT servers.

Approach volume counts were collected in the field, or by viewing video recordings of the studied approaches, using JAMAR counters. The effects of three factors and their combinations were studied. These factors were sensor location, number of lanes in the approach, and traffic volume level. Various sites with different combinations of sensor location and number of approach lanes were chosen for the study. Volume data were collected at three traffic volume levels at each study site during various times of the day. Using the approach volumes collected at the study sites using JAMAR counters as the ground truth data, the data were compared against the approach volume counts collected by the Advance sensor through the Hi-res data and were compiled into a spreadsheet for analysis.

Ground truth speed data collection was performed using a TruCam LiDAR speed gun, which uses laser technology to measure the speed of an approaching vehicle and also provides an image that contains a picture of the vehicle from which the speed is recorded. This picture also contains the distance from the speed gun to the nearest tenth of a foot, and the approach speed to the nearest mile per hour. The factors which were tested were the lane position of the approach vehicle and the offset distance of the lane relative to the speed gun being held by the data collector. The

summary data for each study site contained a data set of the speeds of the vehicles collected by the LiDAR gun and the speeds of the corresponding vehicles collected by the Advance sensor. Table 3-11 shows a portion of the data reduction summary table that shows speeds for the different lanes of an approach at a studied intersection. Only the vehicles that proved to be valid samples were included in this summary spreadsheet, meaning that the data reduction was performed successfully and without any reason to believe that the information retrieved from the LiDAR gun and the Advance sensor were referring to different vehicles.

Table 3-11: Data Reduction Summary Table

	Eastbound- try 1 and try 2											
	T1				T2				T3			
	Picture	Sensor	Log	High-res	Picture	Sensor	Log	High-res	Picture	Sensor	Log	High-res
1	50	46	46	46	41	42	43	43	50	48	49	49
2	50	46	47	47	45	47	47	47	45	41	41	41
3	38	42	42	42	42	38	38	38	44	48	46	46
4	40	40	43	43	47	43	44	44	42	41	41	41
5	42	36	36	36	45	47	47	47	45	40	40	40
6	47	44	45	45	41	39	38	38	45	42	42	42
7	48	45	46	46	51	48	46	46	50	46	46	46
8	48	48	48	47	48	42	42	42	42	45	45	45
9	45	38	38	38	46	48	48	48	43	41	41	41
10	47	41	41	41	48	50	50	50	38	40	40	40
11	47	45	45	45	44	42	42	42	41	41	41	41
12	34	36	36	36	42	43	40	40	49	45	46	46
13	48	48	48	48	55	49	49	49	43	45	46	46
14	40	40	40	40	43	47	47	47	37	40	41	41
15	41	40	40	40	43	40	39	39	40	43	43	42
16	39	43	44	45	48	52	52	52	45	42	42	42
17	48	48	48	48	46	45	45	45	45	55	55	55
18	28	25	26	26	50	48	48	48	39	41	40	40
19	44	42	42	42	46	47	45	45	39	39	37	37
20	43	42	42	42	46	44	44	44	48	45	44	44
21	47	46	47	46	45	42	42	42	47	39	38	38
22	51*	45	45	45	47	46	45	45	43	42	42	42
23	46	45	45	45	49	50	50	50	40	42	44	44
24	44	44	44	44	51	52	52	52	41	41	41	41
25	42	45	45	45	56	55	55	55	40	40	40	40
26	42	44	44	44	48	47	44	44	53	43	43	43
27	43	45	45	45	47	46	46	46	36	36	36	36
28	45	42	42	42	46	37	37	37	46	45	45	45
29	41	45	46	46	58	54	54	54	48	40	40	40
30	49	46	46	46	47	48	47	47	38	40	40	40
31	43	44	44	44	39	39	39	39	49	52	53	53
32	39	38	38	38	42	43	43	43	41	41	41	41
33	47	50	50	49	48	45	42	42	36	33	33	33
34	40	38	37	37	36	36	35	35	39	48	48	48

4 RESULTS

Following the data collection and reduction, both the approach volume and approach speed data went through statistical analyses to test either the accuracy or the difference between the ground truth data and the data collected by the Advance sensor. Ground truth approach volume data were collected manually using JAMAR counters and the ground truth speed data were collected by the LiDAR gun. The approach volume and speed data collected by the Advance sensor were extracted from the Hi-res data. The approach volume data were tested for accuracy at a 95% confidence level. The approach speed data were analyzed to see if the difference between the two datasets were statistically significant at a 95% confidence level. The 85th percentile speeds were compared for each study site and then the Bootstrapping method was used to create multiple 85th percentile speeds for each site to evaluate the significance in the difference in 85th percentile speeds between the two datasets at each site. The following sub-sections describe the analyses performed on approach volume accuracy, mean speed differences between the ground truth speed data and the speed obtained from the Hi-res data, and the difference in the 85th percentile speeds between the two datasets in terms of mean differences.

4.1 Approach Volume Accuracy

This section discusses the analysis used in evaluating the accuracy of the approach volumes collected by the Advance sensor. This section also explains the factors tested for their influence on the accuracy of approach volume.

4.1.1 Raw Data

The data for the approach volume accuracy were formatted into a spreadsheet with columns that separated the data by their factors: sensor position, volume level, and approach size in terms of the number of lanes. Table 4-1 shows a portion of the final, compiled data spreadsheet used to perform the statistical analysis on approach volume accuracy. The complete data set is contained in Appendix B: Raw Volume Data. The data columns included in the table were the ground truth volume data collected in the field, the Hi-res volume data collected by the Advance sensor, the volume per lane (that is, the ground truth volume divided by the number of approach lanes) and the percent accuracy, which is the quotient of the Hi-res approach volume divided by the ground truth volume, expressed in percentage. The percentage higher than 100% means the Advance sensor over-counted the approach volume while the percentage lower than 100% means the Advance sensor under-counted the approach volume.

4.1.2 Statistical Test Performed

The tests performed to determine the accuracy of approach volume were a comparison of descriptive statistics including the mean and standard deviation, and the Mixed-Model Analysis of Variance (ANOVA), using Statistical Analysis Software (SAS) to perform the ANOVA analysis. (SAS 2015) The Mixed Model ANOVA is a form of regression analysis which allows for there to be various groups among the datasets (Ramsey and Shafer 2002). In the case of the approach volume, three factors were analyzed including sensor position, number of approach lanes, and volume level. There were two sensor positions, three approach sizes for each position, and three volume levels for each approach size, totaling 18 factor combinations. Since these factors were preassigned, the Mixed Model ANOVA will analyze these factors as fixed effects. Furthermore, the various levels within each factor had their levels tested against each other to see if there was

any correlation within the factor and the analysis results were presented in a least squares mean table. For calculating the difference in least squares means, the Tukey-Kramer test was performed. This test uses a pairwise comparison which accounts for the multiple comparison effect that arises when the same sample is used to compare multiple factors. The Tukey-Kramer test identifies the two most divergent sample averages and, based on these values, applies a multiplier to the test results to correct the confidence levels which may have been affected by the multiple comparison effect created when using the same sample to compare various factors (Ramsey and Shafer 2002).

Table 4-1: The Sample Compiled Approach Volume Data

Intersection	Number of Lanes	Position Number	Volume Level	Direction	Ground Truth Volume	Hi-res Volume	Volume Per Lane	Percent Accuracy
1390N & Geneva Rd. Provo	1	1	Low	NB	100	116	100	116.0%
1390N & Geneva Rd. Provo	1	1	Mid	NB	285	295	285	103.5%
1390N & Geneva Rd. Provo	1	1	Mid	NB	338	344	338	101.8%
1390N & Geneva Rd. Provo	1	1	Mid	NB	241	255	241	105.8%
1390N & Geneva Rd. Provo	1	1	High	NB	473	468	473	98.9%
1390N & Geneva Rd. Provo	1	2	Low	SB	124	120	124	96.8%
1390N & Geneva Rd. Provo	1	2	Mid	SB	272	272	272	100.0%
1390N & Geneva Rd. Provo	1	2	High	SB	654	619	654	94.6%
1320 S & State St, Provo	2	1	Low	SB	224	214	112	95.5%
1320 S & State St, Provo	2	1	Low	NB	198	200	99	101.0%
1320 S & State St, Provo	2	1	Mid	SB	616	559	308	90.7%
1320 S & State St, Provo	2	1	Mid	NB	609	632	304.5	103.8%
1320 S & State St, Provo	2	1	High	SB	1310	1104	655	84.3%
1320 S & State St, Provo	2	1	High	NB	1042	926	521	88.9%

4.1.3 Analysis Results

The mean accuracies, standard deviations and 95% confidence intervals were first determined. Table 4-2 shows the number of samples which were collected for each factor combination of the factor levels. The first of the two numbers in each cell represent the number of study sites where approach volume data were collected and the second number after the slash (/) is the number of

total samples taken for the factor combination. Due to difficulty in predicting volume levels during the data collection phase, there were some instances where the samples that were collected did not meet the volume level classification originally set. Table 4-3 shows the mean accuracy of the factor combinations. As shown in the table, the lower the number of lanes and volume level, the higher the accuracy. This was anticipated due to the Advance sensor's inability to differentiate between the lanes where approach vehicles are traveling, that is, when two vehicles approach in different lanes at the same time, only one vehicle is registered. The chance of their undercount increases as the approach volume increases. What was observed during data collection was that heavy vehicles, such as semi-trucks, and vehicles towing trailers or other vehicles were sometimes recognized by the sensor as two separate vehicles and was double counted. This explains the overcounting which resulted from the mean and 95% confidence intervals. The accuracy of approach volume count ranges from approximately 76.3% to 104.2%, given the availability of data as shown in Table 4-3. While these accuracy values are good as an added value to the Advance sensor, the reader should be cautioned that the sample sizes of the factor combinations are not uniform. For example, the factor combination with one approach lane, mid-level volume, and with sensor position 2 shows an accuracy level of 100.0%. However, this is not a representative value of this factor combination because only one sample was taken at this site. There was only one site equipped with the Advance sensor that fits into this factor combination. The ANOVA test was later performed to compare the influences of each factor combination.

Table 4-4 shows the standard deviation of the accuracies determined for each factor combination. They range from approximately 4% to 22%; there can be a significant variation in accuracy levels among the different factor combinations. Standard deviations cannot be determined for the sites where only one data sample were taken; such combinations have an entry

N/A (Not Applicable) in Table 4-4. In Table 4-5, the 95% confidence intervals for the factor combinations are shown. These bounds show that at a 95% confidence level, the accuracy for each factor combination will be between those boundary values. As can be seen from the table, the lower the volume level and the lower the number of approach lanes, the center of the confidence interval was closer to 100%.

Table 4-2: Number of Samples (# of sites / # of total samples taken)

Number of Lanes	Position 1			Position 2		
	Low	Medium	High	Low	Medium	High
1	2 / 2	2 / 4	2 / 2	1 / 1	1 / 1	1 / 1
2	8 / 8	8 / 10	7 / 10	8 / 8	9 / 11	8 / 11
3	7 / 8	7 / 8	7 / 11	7 / 8	7 / 9	6 / 9

Table 4-3: Mean Accuracy for Factor Combinations

Number of Lanes	Position1			Position 2		
	Low	Medium	High	Low	Medium	High
1	104.2%	101.7%	92.9%	96.8%	100.0%	94.6%
2	98.0%	90.7%	90.5%	93.7%	90.3%	85.4%
3	88.5%	85.9%	76.3%	94.6%	86.9%	77.6%

Table 4-4: Standard Deviation of Accuracy

Number of Lanes	Position1			Position 2		
	Low	Medium	High	Low	Medium	High
1	8.33%	4.24%	8.48%	N/A	N/A	N/A
2	22.64%	11.44%	7.10%	8.65%	5.06%	12.25%
3	6.10%	8.01%	8.83%	10.50%	8.57%	9.68%

Table 4-5: 95 Percent Confidence Interval of the Mean

No. of Lanes	Position 1						Position 2					
	Low		Medium		High		Low		Medium		High	
	Lower	Upper	Lower	Upper	Lower	Upper	Lower	Upper	Lower	Upper	Lower	Upper
1	92.7%	115.8%	97.6%	105.9%	81.2%	104.7%	N/A	N/A	N/A	N/A	N/A	N/A
2	82.3%	113.7%	83.6%	97.7%	86.1%	94.9%	87.7%	99.7%	87.3%	93.3%	78.2%	92.7%
3	84.3%	92.7%	80.4%	91.5%	71.1%	81.5%	85.3%	103.7%	74.7%	94.1%	77.7%	87.6%

The output of the ANOVA, which compared the effects that the three variables had on accuracy at the 95% confidence level, is presented in the form of two-sided p-values in Table 4-6. The resulting F-value is indicative of the ratio between the variances of the two data sets, where a value closer to 1 means less variance between the two data sets (Ramsey and Shafer 2002). The p-value presents the probability of an F-value computed being larger than the critical values for the test. As can be seen in Table 4-6, the effects of the number of lanes and volume level are determined to be significant, with a p-value of 0.0117 and < 0.0001 , respectively. The sensor position shows a high p-value of 0.6530, which means that the effect of the sensor position on accuracy is not significant at a 95% confidence level.

Table 4-6: Results of Tests on Fixed Effects on Approach Volume

Effect	F-Value	Pr > F (p-value)
Number of Lanes	5.75	0.0117
Position Number	0.21	0.6530
Volume Level	15.39	< 0.0001

The Tukey-Kramer comparison test was then applied and the results are presented in adjusted p-values in Table 4-7. The Tukey-Kramer test was used to determine the effect of multiple comparisons. The adjusted p-values show which of the factors or effects are significant in comparing the accuracies of the volumes levels.

As explained in Section 2.1.1, the Advance sensor does not have the ability to differentiate between lanes as the vehicles approach. For this reason it is expected that the difference between two approaches with different number of lanes can be significant depending on the factor combination. For instance, the p-values for the one-lane and two-lane approach comparison is 0.1510, meaning the effect is not significant at a 95% confidence level, but the difference between one-lane and three-lane approaches are significant with a p-value of 0.0140. The comparison of two-lane and three-lane approaches shows a p-value of 0.1097, which is not significant at the 95% confidence levels and falls between the two p-values for the other two approach lane comparisons. This trend indicates that the higher number of lanes in the approach does adversely affect the accuracy in approach volume counts and that there is a significant difference in accuracy between one-lane and three-lane approaches.

Table 4-7: Results of the Tukey-Kramer Test

Effect	Volume Level	No. of Lanes	Position No.	Volume Level	No. of Lanes	Position No.	Estimate in the Output	Mean Standard Error	Adjusted p-value
No. of Lanes		1			2		0.0970	0.04947	0.1510
No. of Lanes		1			3		0.1592	0.05023	0.0140
No. of Lanes		2			3		0.0623	0.02909	0.1097
Position No.			1			2	0.0127	0.02767	0.6530
Volume Level	High			Low			-0.1138	0.02073	< 0.0001
Volume Level	High			Mid			-0.0637	0.01957	0.0062
Volume Level	Low			Mid			0.0501	0.02089	0.0537

Comparison of sensor position 1 and sensor position 2 results in a p-value of 0.6530, which indicates that the sensor position does not affect the accuracy of the approach volume counts at a 95 % confidence level.

Comparison of the volume levels provides a similar result to the number of lanes. As volume level increases, it is increasingly difficult for the sensor to differentiate the vehicles by lane. For instance, when the accuracies of the low and medium approach volumes are compared, the p-value resulted in 0.0537 indicating the difference is not significant. When high is compared to medium and low approach volumes, the p-values are 0.0062 and <0.0001 , respectively, which means their effect on accuracy is significant.

Overall, the Tukey-Kramer test shows that the accuracy of the Advance sensor in approach volume count is affected by the number of approach lanes and volume levels. The sensor position is not significant in affecting the accuracy of the approach volume counts. Based on the results of the two statistical tests, it can be said that the Advance sensor can perform approach volume counts at a mean accuracy level somewhere between 76.3% and 104.2% depending on the factor combination within the data range available for the study. The accuracy of approach volume counts tends to degrade as the number of approach lanes and the approach volume increase.

4.2 Mean Approach Speed Comparison

This section discusses the analysis used in testing the difference between the means of the ground truth data, the data collected by the Advance sensor and the process and tests used to compare the means.

4.2.1 Cosine Effect

Before performing the statistical analysis of the speed data, possible errors that could result from the use of the LiDAR speed gun and from the method of the data collection needed to be evaluated. The cosine effect test was discussed in section 3.3.1 of this thesis. Potential errors caused by parallax were analyzed prior to the data collection as part of the preparation for a full-scale data collection. After validating the insignificance of the cosine effect on speed measurements, the full-scale data collection took place.

4.2.2 Raw Data

The data from the speed study were compiled into two spreadsheets for performing two statistical tests: a Mixed Model ANOVA and a paired two-tailed t-test. Each spreadsheet contained the data points collected from the various study sites. These spreadsheets are included in Appendix C: Raw Approach Speed Data. A sample of the approach speed data collected for the eastbound approach of the 9000 S 700 W intersection in Sandy, UT is shown in Table 4-8.

The first spreadsheet contains a combined table of all of the speed data, separated into columns, which denote each lane position in relation to the LiDAR gun speed and the Advance sensor speed. The purpose of running a statistical analysis on the number of lanes and the lane position of the speed data was to test the effects that these factors would have on speed accuracy. The Advance sensor, as previously explained, does not have the ability to differentiate between lanes. The ANOVA would show if there was any significant effect by lane position on the speed data between the ground truth speed data and the speed data collected by the Advance sensor. The second spreadsheet separates the data by the study site location into different sheets for a comparison of individual sites.

4.2.3 Statistical Tests Performed

A Mixed Model ANOVA was applied to the speed data in the first spreadsheet. The dependent variable was percent accuracy of speed and the independent variable included in the analysis was the positioning of the LiDAR speed gun in relation to the number of lanes and lane offset. The Mixed Models ANOVA was used to account for the multiple observations from each study site. The purpose for using this approach was to determine if there was evidence of any influence, by the factors, on the accuracy of sensor speeds. The factors entered, as previously stated in section 3.1.3, were the number of lanes and the lane's position relative to the location of the LiDAR speed gun. Since there were a total of three possible approach lanes from the study sites where the Advance sensor would detect a vehicle, as well as three possible offset distances the LiDAR speed gun could be from any lane, the data were sorted in the various treatments (one through six) depending on the combination of lane number and the number of lanes the speed gun was offset from, as shown in Table 4-9.

The test performed on the second spreadsheet for the mean speed accuracy was a paired two-tailed t-test on speed data using the data analysis feature of Excel. A paired two-tailed t-test was used here because one vehicle's speed was collected by two methods. The paired t-test would provide a comparison of the means of the two samples by testing if the means of the differences were equal to zero (Roess et al. 2009). The outcome of the paired t-test provided a t-statistic, which tells how many standard errors the estimate is away from the hypothesized value (being zero if assuming equality). The t-critical value, and the p-value, would show the significance of the difference between mean speeds as well as the probability of obtaining a t-statistic as extreme or more extreme than the t-critical (Ramsey and Schafer. 2002). The t-statistic is the estimate of error

in the sample and the p-value shows the likeliness of having an estimate of error as large as the error resulting from the sample.

Table 4-8: Sample Approach Speed Data

Lane	Sample No.	Gun Speed, mph	Hi-res Speed, mph	Speed Accuracy	Difference, mph
T1	1	39	37	94.87%	2
T1	2	53	46	86.79%	7
T1	3	52	49	94.23%	3
T1	4	47	49	104.26%	-2
T1	5	40	42	105.00%	-2
T1	6	48	50	104.17%	-2
T1	7	49	49	100.00%	0
T1	8	47	48	102.13%	-1
T1	9	42	43	102.38%	-1
T1	10	45	43	95.56%	2
T1	11	44	45	102.27%	-1
T1	12	45	46	102.22%	-1
T1	13	48	48	100.00%	0
T1	14	49	48	97.96%	1
T1	15	46	43	93.48%	3
T1	16	45	46	102.22%	-1
T1	17	46	44	95.65%	2
T1	18	47	49	104.26%	-2

Table 4-9: Assigned Treatments

Effect	Treatment
Treatment 1	1 Lane offset 1
Treatment 2	2 Lanes offset 1
Treatment 3	2 Lanes offset 2
Treatment 4	3 Lanes offset 1
Treatment 5	3 Lanes offset 2
Treatment 6	3 Lanes offset 3

4.2.4 Results of Statistical Analyses

A Mixed-Model ANOVA was performed on the treatments to evaluate the effects of the treatments on the mean approach speed and the results are shown in Table 4-10. The resulting p-value was 0.4919 and was greater than 0.05, which indicates that there was no significant effect on the difference in speeds collected by the LiDAR gun and the Advance sensor by the lane position and number of lanes, meaning that the accuracy of speed data collected by the sensor is not affected by the location of the approaching vehicles in relation to the sensor.

Table 4-10: Results of Mixed-Model ANOVA on Mean Approach Speed

Effect	F-Value	Pr>F (p-value)
Treatment	0.92	0.4919

The various treatments which were tested in the ANOVA to compare the effect of lane number and LiDAR gun position are shown in Table 4-11. Treatments were defined by their lane number and offset position, along with their least squares mean. The “Estimate” shown in the table refers to a multiplier which would provide the predicted difference that would exist within each group and the standard error is the standard deviation of the sample mean divided by the square root of the sample size. A low standard of error means that there is not much variation in the data. The overall estimate, or proportion of the sample that was estimated was very close to 1.00, which shows positive results, and the standard error is low, within the range of 0.1207 and 0.1861. This implied that the various treatments, (i.e., combinations of the number of lanes and lane position,) do not significantly affect the difference between the mean approach speeds collected by the LiDAR speed gun and the Advance sensors.

Table 4-11: Least Squares Means Result for Approach Speed

Least Squares Means			
Effect	Treatment	Estimate	Standard Error
Treatment 1	1 Lane offset 1	1.0013	0.01861
Treatment 2	2 Lanes offset 1	0.9941	0.01343
Treatment 3	2 Lanes offset 2	1.0091	0.01284
Treatment 4	3 Lanes offset 1	0.9827	0.01234
Treatment 5	3 Lanes offset 2	0.9755	0.01207
Treatment 6	3 Lanes offset 3	0.9859	0.01295

The results of paired t-test performed on the second spreadsheet are shown in Table 4-12. Some of the study sites resulted in significant differences between the mean speeds of the speeds collected by the LiDAR gun and the speeds reported in the Hi-res data. Intersections 2, 5, 7, 8, 9, 11, and 14 all show p-values greater than 0.05, indicating that the differences between the mean speeds were not significant and that there was not sufficient evidence to disprove the claim that the means are equal. At the other sites whose p-values were below the p-value of 0.05, there was sufficient evidence to classify the differences as significant. Overall, it can be seen that at some locations, the difference in mean speeds was greater than other intersections. While the differences between the two speed groups were significant at some intersections, the difference was only within a few miles per hour, which resulted in the data being statistically significant, but not practically significant enough considering the application of this technology would round speeds to the nearest 5 mph. A look at the results in Appendix D: Results of Paired t-Test for Means shows that most of the samples had a small difference in speed. For instance, the first study site in Table 4-12 has the largest difference in speed, being 2.20 mph. The p-value is 1.70E-08, which means that this difference is very statistically significant. However, a difference of 2.20 mph may not be large enough to claim that the difference is significant for practical applications considering the

error margin of the LiDAR speed gun. Thus the claim is acceptable that although statistically significant, these differences may not be significant for practical applications.

4.3 85th Percentile Approach Speed Comparison

This section discusses the analysis used in testing the difference between the 85th percentile speeds calculated of the ground truth data and the data collected by the Advance sensor for each study site where approach speed data were collected. The process and tests used to compare the 85th percentile speeds are also explained in this section.

4.3.1 Raw Data

The speed data were grouped by individual sample sites, similar to the procedure performed for the two-tailed, paired t-test of mean speeds by the two methods. Each of the 14 approaches was assigned a number and the speeds by the LiDAR speed gun and the Hi-res data from the Advance sensor were used to perform statistical analyses on 85th percentile speeds. The speed data of each approach was tested individually to compare the differences between the ground truth and Hi-res 85th percentile speeds. The SPMs website by UDOT posts an 85th percentile speed along with the average speed and the posted speed limit. Because each site gives only one 85th percentile speed, the Bootstrapping method was used to generate a large number of 85th percentile speeds from each dataset and determined the differences between the 85th percentile speeds by the LiDAR gun and the Advance sensors at each approach. UDOT uses the typical sample size calculation in Equation 2 to calculate the number of vehicle speeds needed for the sample size. As a standard and as a result of the equation, UDOT uses approximately 100 vehicle samples when collecting speed data to calculate an 85th percentile speed (UDOT Traffic &

Table 4-12: Paired Two-Sample for Means t-Test

No.	Intersection	Approach	No. of Samples	t Stat	t Critical	P(T<=t) two-tail	Gun Speed Mean, mph	Sensor Speed Mean, mph	Difference, mph
1	9000 S 700 W, Sandy	EB	129	6.02	1.98	1.70E-08	46.09	43.89	2.20
2	1320 S State St, Provo	SB	125	0.93	1.98	0.35661	48.58	48.14	0.44
3	400 E 800 N, Orem	EB	118	3.58	1.98	0.00051	44.60	43.39	1.21
4	Geneva Rd Univ Pkwy, Orem	WB	89	2.51	1.99	0.01385	44.82	43.78	1.04
5	3500 S 2200 W, WV	EB	83	1.60	1.99	0.11247	37.51	36.70	0.81
6	400 E 800 N, Orem	WB	64	-2.52	2.00	0.01426	44.91	46.20	-1.29
7	1320 S State St, Provo	NB	54	-1.67	2.01	0.10008	45.87	46.43	-0.56
8	9000 S 700 W, Sandy	WB	51	-1.10	2.01	0.27827	43.45	44.03	-0.58
9	3500 S 2200 W, WV	WB	45	0.25	2.02	0.80214	38.58	38.42	0.16
10	800 N Geneva Rd, Orem	NB	44	2.87	2.02	0.00633	45.61	44.41	1.20
11	Univ Ave Univ Pkwy, Provo	SB	36	-1.08	2.03	0.28905	39.36	39.78	-0.42
12	3300 N Univ Ave, Provo	NB	32	4.19	2.04	0.00022	46.31	44.19	2.12
13	Geneva Rd Univ Pkwy, Orem	SB	30	2.09	2.05	0.04541	41.57	40.70	0.87
14	Geneva Rd Univ Pkwy, Orem	NB	18	0.36	2.11	0.72510	37.67	37.50	0.17

Safety 2015). Collecting many speed samples reaching 100 at each study site was difficult in this study, due to the complexity of speed data collection and reduction. For this reason, under recommendation by UDOT and Wavetronix, only the sites with 50 or more speed samples were used in this portion of the analysis. Note that UDOT uses a z-score of 1.96, which is for a 95% confidence level two-tail test, and tolerance of 1.0 mph. Increasing the tolerance to 2.0 mph would significantly decrease the number of samples needed. Eight of the 14 study sites were found to have at least 50 speed data points or more per approach.

$$N = (s \times Z)^2 / E^2 = s^2 \times 3.84$$

Equation 2

Where:

N = sample size

s = sample standard deviation (mph)

Z = z-score of confidence level

E = tolerance (mph)

4.3.2 Statistical Test Performed

The first step of statistical analyses on 85th percentile speed was to calculate the 85th percentile speeds for both the speeds collected by the LiDAR gun and the Advance sensor for each of the eight study sites. The difference of the 85th percentile speeds of the raw datasets was determined as a preliminary observation. Then, in order to perform statistical analysis, the distribution of 85th percentile speeds was created by the Bootstrapping method with replacement. The approaches were analyzed individually because each 85th percentile speed was calculated at each individual approach studied. The Bootstrapping method allows for a data point to be selected, recorded, and

then returned to the pool of potential data points. A new data point is then selected from the full data set. A sample size of 50 speeds was used in this study and 85th percentile speeds computed for each dataset and the process was repeated 1,000 times, that is 1,000 85th percentile speeds were computed for each dataset. Using a statistical computer program, R (R Core Team 2015), the Bootstrapping method was performed by approach that had more than 50 speed samples. This test was performed by the statisticians who worked as summer interns at Wavetronix during the summer of 2015.

4.3.3 Results of Statistical Analysis

Each of the eight approaches that had 50 or more samples that were analyzed using the Bootstrapping method was assigned a number for analysis purpose and Table 4-13 shows the approach number, intersection name, and approach direction. Table 4-14 shows the results of the preliminary comparison of the 85th percentile speed of the eight approaches analyzed. The range of difference between the 85th percentile speeds by the LiDAR gun and the Advance sensor was -1.6 mph and 1.5 mph, allowing for an approximate ± 1.5 mph difference for the given approaches. While there was only one data point from each intersection, this preliminary analysis showed the differences were relatively low, which was close to the ± 1 mph error margin of the LiDAR speed gun (Laser Technology, Inc. 2009).

The second statistical analysis was performed using the Bootstrapping method. The results of the Bootstrapping analysis provided a distribution of 85th percentile speeds for each approach for both the speeds by the LiDAR gun and by the Advance sensor. Figure 4-1, Figure 4-2, and Figure 4-3 show the results of this analysis for approach 1. The red color represents the distribution of 85th percentile speeds created from LiDAR gun speeds, the blue color represents the distribution of 85th percentile speeds created from the speeds by the Advance sensor, and

Table 4-13: Numbering of Approaches Used in 85th Percentile Analysis

Approach Number	Intersection	Approach
Approach 1	1320 S State St, Provo	NB
Approach 2	1320 S State St, Provo	SB
Approach 3	3500 S 2200 W, West Valley	EB
Approach 4	400 E 800 N, Orem	EB
Approach 5	400 E 800 N, Orem	WB
Approach 6	9000 S 700 W, Sandy	EB
Approach 7	9000 S 700 W, Sandy	WB
Approach 8	Geneva Rd Univ Pkwy, Orem	WB

Table 4-14: 85th Percentile Speeds and Differences

Approach Number	Hi-res Speed (mph)	Gun Speed (mph)	Hi-res Speed – Gun Speed, (mph)
Approach 1	50.0	50.0	0.0
Approach 2	53.4	54.4	-1.0
Approach 3	42.7	43.7	-1.0
Approach 4	47.5	49.0	-1.5
Approach 5	50.5	49.0	1.5
Approach 6	49.0	49.8	-0.8
Approach 7	49.0	48.0	1.0
Approach 8	48.0	49.6	-1.6

the purple color represents an overlapping area between the two 85th percentile speed distributions. The resulting figures show the 85th percentile for these two sample speed distributions and the distribution of the 85th percentile speed differences. These three figures for each of the eight approaches analyzed are presented in Appendix E: Results of Bootstrapping Method on 85th percentile speeds. Two examples are presented in this section: the best case and the worst case out of the eight approaches studied.

The approach which had the best results from the Bootstrapping method was Approach 1 (i.e., the NB approach at 1320 S State St, Provo). The distribution created by the Bootstrapping method of the ground truth speeds and the speeds by the Advance sensor can be seen in Figure 4-1. The blue, representing the speeds from the Advance sensor, and the red color, representing the speeds

from the LiDAR gun, are only shown in small areas along the edge of the distribution. The majority of the graph is in purple, representing an overlap of the ground truth speeds and the speeds by the Advance sensor. The 85th percentile speeds for the 1,000 resampled speed datasets created by the Bootstrapping method are shown in the distribution in Figure 4-2. The distribution chart shows the 85th percentile speed at approximately 50 mph. The overall distribution is mostly purple, meaning that the majority of the 85th percentile speeds are overlapping for each resampled dataset with only a range of approximately ± 5 mph in difference. The bar in the center shows that the mean 85th percentile speeds for both speed data sets are approximately equal for the resampled data; that is 50 mph using 1,000 samples. Figure 4-3 shows the distribution of the difference between the 85th percentile speeds of the ground truth data and the speeds by the Hi-res speed data. The difference between the ground truth speeds and the speeds reported by the Advance sensor was 0 mph as the mode with a range from -2.0 mph to 4.0 mph.

The approach that had the largest differences between the ground truth speeds and the speeds by the Advance sensors was Approach 5 (i.e., WB approach at 400 E 800 N, Orem). Figure 4-4 shows the speed distributions created by the Bootstrapping method. While there was still a large amount of purple, denoting the high number of overlapping speed values, the 85th percentile speeds were different by approximately 2 mph. Figure 4-5 shows the distribution for the 85th percentile speeds created by the Bootstrapping method. This distribution shows a larger difference between the 85th percentile speeds of the ground truth data and the Hi-res data. Overall the ground truth speeds show slower speeds than the speeds in the Hi-res data. The thin, vertical line showing the mean 85th percentile speeds show that the mean LiDAR gun speed is approximately 48 mph and the mean Hi-res speed is approximately 51 mph. Figure 4-6 shows the difference in the 85th percentile speeds between the two data sets. The mode of the difference between the LiDAR speed

gun and Hi-res 85th percentile speeds is approximately 2 mph, with a range from -2 mph to 5 mph. This wide range is a representation of the difficulty in collecting data using the Advance sensor.

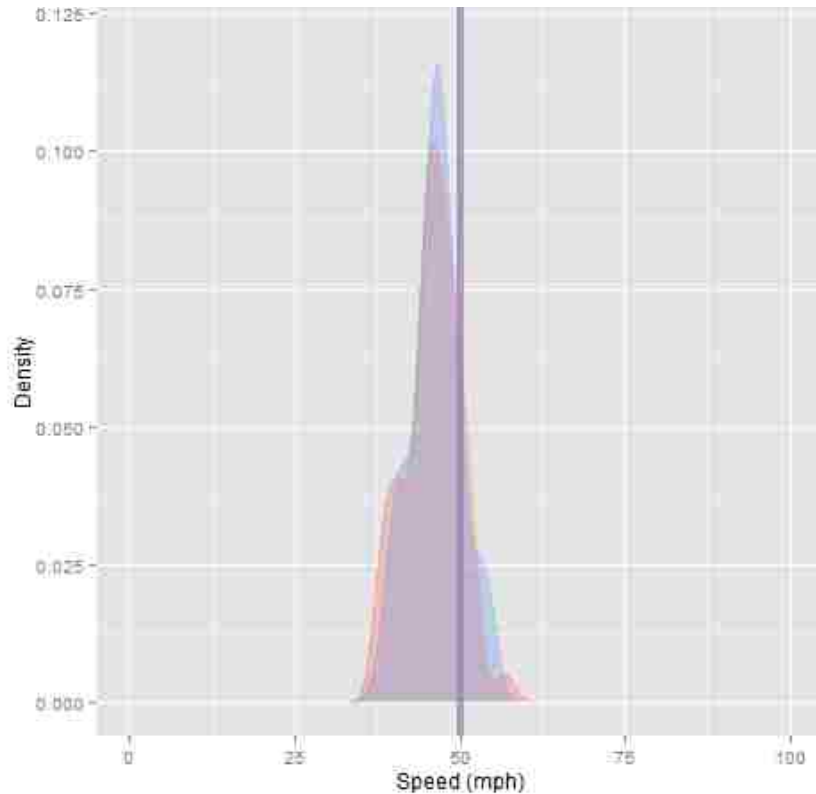


Figure 4-1: Speed distributions created by Bootstrapping for approach 1.

Although these were only two samples, the test showed a difficulty in constantly gathering speed data correctly by the Advance sensor. Installation of the Advance sensor requires skilled technicians. The Bootstrapping method was performed using only one 85th percentile data sample per site. Further investigation into this topic may result in better and more revealing results of the effectiveness of the sensor's 85th percentile calculation.

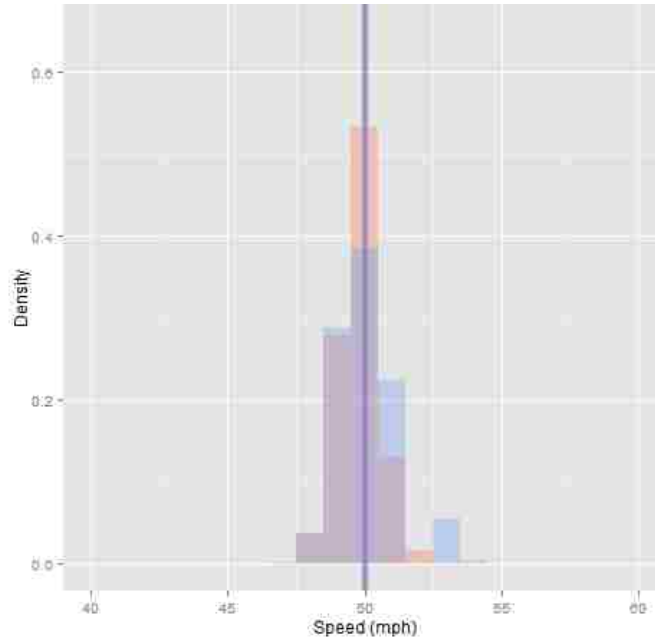


Figure 4-2: 85th percentile speed distributions created by Bootstrapping for approach 1.

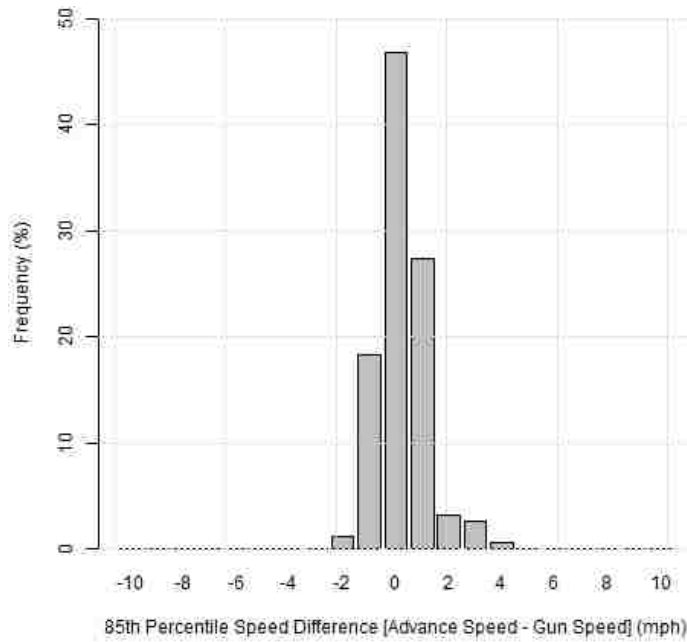


Figure 4-3: Expected 85th percentile speed difference distribution created by Bootstrapping for approach 1.

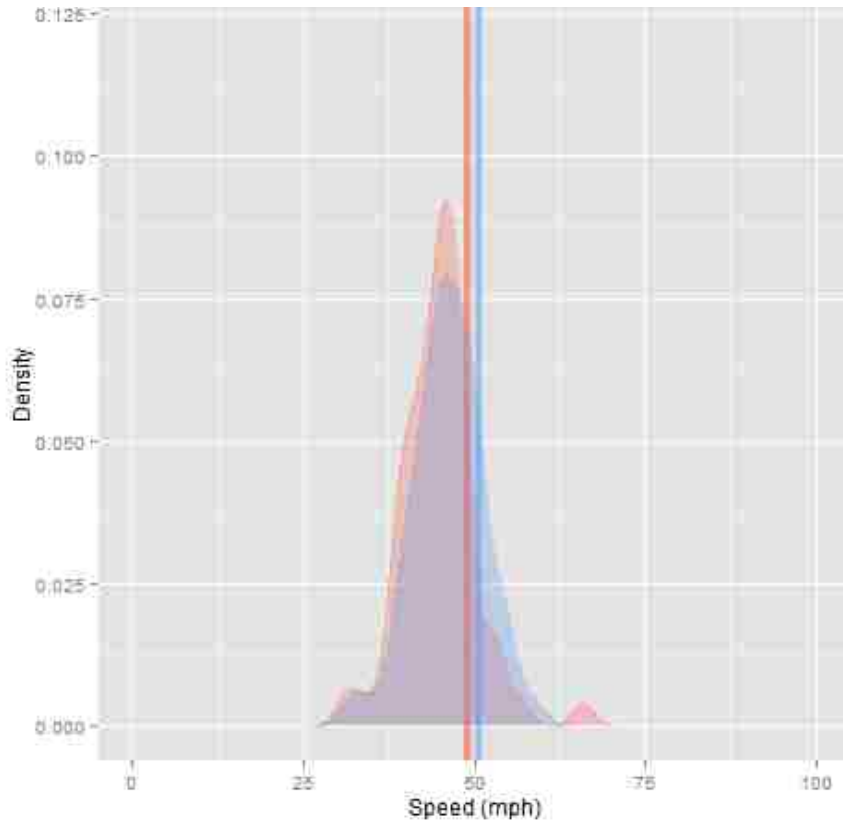


Figure 4-4: Speed distributions for approach 5.

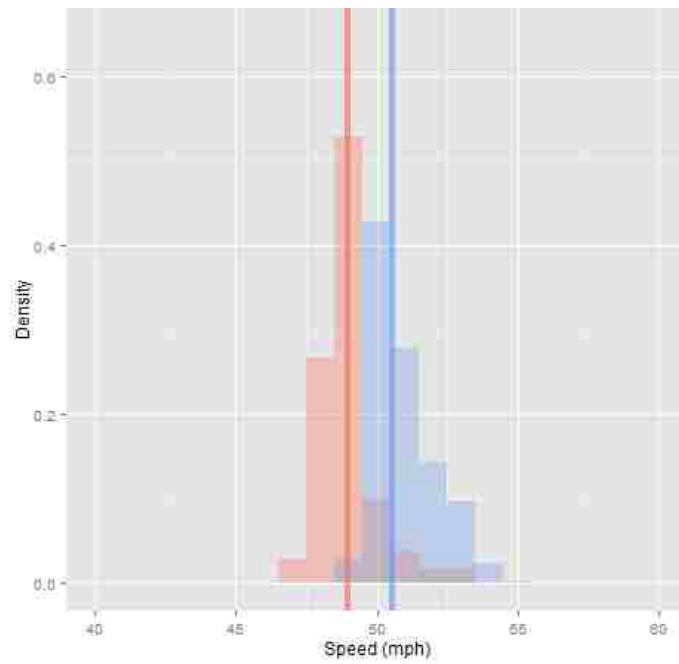


Figure 4-5: 85th percentile speed distributions for approach 5.

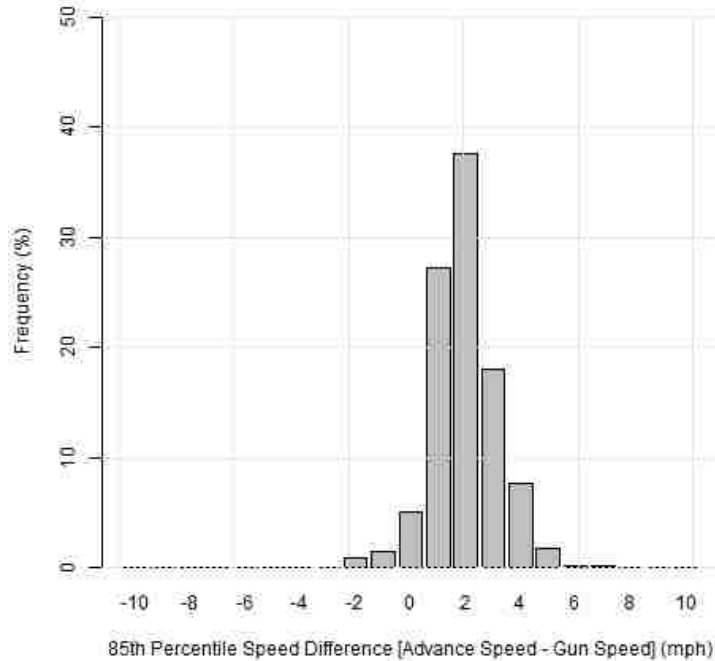


Figure 4-6: Expected 85th percentile speed difference distribution for approach 5.

4.4 Chapter Summary

The accuracy of approach volumes was first analyzed by comparing the mean and standard deviation of the accuracy values. It was observed that the accuracy values resulted in percentages from 76% to 104% when all sites were analyzed, with an accuracy of at least 85% for all one and two-lane approaches at the studied intersections. The approach volumes were then analyzed for the influences of the factors, including sensor position, number of approach lanes, and volume level using the Mixed Model ANOVA. The results from the Mixed Model ANOVA showed that the sensor position was not significant in affecting the accuracy of the volume counts at a 95 % confidence level. The number of lanes and volume levels were found to be significant in affecting the accuracy of approach volume at a 95 % confidence level with p-values of 0.0117 and <0.0001, respectively. The comparison of the various levels of these effects, or factors, showed that there

was a significant difference between one lane and three lane approaches, with a p-value of 0.0140, and between low and high volumes, with a p-value of <0.0001 . Overall, the volume counts were found to be more accurate for sites with the lower number of approach lanes and lower approach volumes. The Advance sensor, whose primary function is not to count approach volume, performed at an acceptable accuracy level to application by traffic engineers. The Mixed Model ANOVA test shows that the difference between the number of lanes and the lane position of the vehicle, from which the speed was being recorded, was not significant, with a p-value of 0.4919.

Performing a two-tailed paired t-test for each site allowed for the mean speeds to be compared. For the few sites with a high p-value (greater than 0.05), the test showed that the speeds by the LiDAR gun and the Advance sensors had mean speeds which were close, or not significantly different. Though some of the sites showed that the difference in the mean speeds was statistically significant at a 95% confidence level, the difference was not practically significant and the difference in the LiDAR gun speed and Hi-res speed, was only 1 or 2 mph. Hence it can be said that the Advance sensor can collect fairly accurate speed data.

Evaluation of 85th percentile speeds required two methods. First, the differences in 85th percentile speeds of each dataset were determined and the difference was found to be approximately ± 1.5 mph. Considering that UDOT rounds their 85th percentile speed to 5 mph increments, and the 85th percentile speeds computed by speed data continuously collected by the Advance sensor, the 85th percentile speeds provided by the SPMs can be used for practical engineering applications. The second statistical analysis performed on speeds was the Bootstrapping method. This method allowed for a creation of speed samples from the data already collected. Each site was tested individually and some of the sites showed a small difference between the 85th percentile speed calculated from ground truth data and Hi-res data. The mean

difference was ± 2 mph from the mean. Other sites showed a larger spread in the difference of up to ± 4 mph. This test was only performed on one data sample per site taken by the BYU team. The analysis shows that further investigation on the 85th percentile speed would provide a more comprehensive result as to the sensor's effectiveness in determining the 85th percentile speed. Based on the results of the Bootstrapping method and the descriptive analysis, it can be reported that there is a potential in the sensor's ability to calculate 85th percentile speeds at accuracy levels acceptable by traffic engineers.

5 APPLICATIONS

The Wavetronix SmartSensor Advance's approach volume counting feature can be an alternative to other onsite counts performed by cities, states, and consulting firms, such as manual counts and tube counts. The Advance sensor also provides approach speed data. These performance data are available to the public through UDOT's SPMs website. The SPMs site allows data to be collected at various locations, during the course of a longer period of time, and they are collected dynamically throughout the year. The SPMs website is beneficial because it provides the users access to data samples which are representative of the traffic conditions on the road. Currently volume counts and speed data are collected using short period data collection in the field and such data may not be a good representation of actual roadway conditions because of daily traffic fluctuations and irregular traffic patterns that may arise during data collection. The biggest gain from the approach volume and speed data collection features of the Advance sensor would be the possible reduction in UDOT's expenditure on approach volume and speed data collection currently done by sending technicians to the field. This chapter presents the applications of the results of both the approach volume and approach speed studies.

5.1 Approach Volume

This study found that based on the results from the approach volume analysis, the Advance sensor could provide at least 85% accuracy, meaning a 15% undercounting in approach volume counts for intersections with one or two approach lanes and with low and medium volume levels.

The approach volume accuracy is approximately 75%, meaning a 25% undercounting for intersections with high volumes and with three approach lanes. Table 5-1, Table 5-2, Table 5-3 and Table 5-4 provide a summary of descriptive statistics for approach volume counts. Note that the sites with only a one-lane approach have a significantly smaller sample size of 3 to 5. These results do not result in strong evidence supporting the confidence interval for the one lane approaches, but the two and three-lane approaches do have the sufficient sample sizes, ranging from 8 to 11 to allow the results to be applied to other intersections that use the Advance sensor. Once the Advance sensors are installed at more locations, statistical inferences for the one-lane approaches can be analyzed. Since the sensor position was found not to be significant in affecting the accuracy of the Advance sensor's approach volume counts, this factor was removed from the descriptive statistics and the two sensor position's data were combined. Table 5-1 shows the number of combined samples. Table 5-2 shows the combined mean accuracies for the different factor combinations with accuracies ranging from 77.8% to 105.7%. Table 5-3 shows the standard deviations of combined volume count data for the same factor combinations shown in Table 5-2. Table 5-4 shows the upper and lower bounds of the combined accuracies at the 95% confidence level. These values can be posted in the SPMs website to let the user know the accuracy of approach volume counts they are dealing with.

For instance, when the approach volume count collected by the Advance sensor is 650 vehicles for the hour in question at an intersection with two approach lanes and the volume level is medium, the mean accuracy is 90.5% from Table 5-2, which means a 9.5% undercounting. Hence the volume reported by the SPMs needs to be divided by 0.905, resulting in 718 vehicles. Or, the 95% confidence boundaries can be given: lower bound of 691 ($650 \div 0.941 = 691$) and the upper bound of 748 ($650 \div 0.869 = 748$).

Table 5-1: Combined Sample Size

Number of Lanes	Low	Medium	High
1	3	5	3
2	16	21	21
3	15	13	19

Table 5-2: Combined Mean Accuracy

Number of Lanes	Low	Medium	High
1	105.7%	101.4%	93.5%
2	95.8%	90.5%	87.8%
3	90.3%	85.4%	77.8%

Table 5-3: Combined Standard Deviation of Accuracy

Number of Lanes	Low	Medium	High
1	9.69%	3.75%	6.07%
2	16.71%	8.47%	10.22%
3	9.15%	8.87%	8.21%

Table 5-4: Combined 95% Confidence Interval of the Mean

No. of Lanes	Low		Medium		High	
	Upper	Lower	Upper	Lower	Upper	Lower
1	116.6%	98.1%	104.7%	98.1%	100.4%	86.6%
2	104.0%	86.9%	94.1%	86.9%	92.2%	83.5%
3	95.0%	80.5%	90.2%	80.5%	81.5%	74.1%

UDOT may present these values on their SPMs website as multiplication factors. Table 5-5 and Table 5-6 show the mean and 95% confidence interval percentages converted into factors that can be multiplied by the approach volume collected by the Advance sensor shown on the SPMs website.

Table 5-5: Mean Multiplication Factors

Number of Lanes	Low	Medium	High
1	0.946	0.986	1.070
2	1.044	1.105	1.139
3	1.107	1.171	1.285

Table 5-6: 95% Confidence Interval Multiplication Factors

No. of Lanes	Low		Medium		High	
	Upper	Lower	Upper	Lower	Upper	Lower
1	0.858	1.019	0.955	1.019	0.996	1.155
2	0.962	1.151	1.063	1.151	1.085	1.198
3	1.053	1.242	1.109	1.242	1.227	1.350

5.2 Approach Speed

Through Advance sensor's approach speed measurement feature, speed data can be collected continuously without having to send data collectors to the field. The sensor may not always measure approach speeds with 100% accuracy; however, the difference between the ground truth speeds and the speeds recorded in the Hi-res data file by the Advance sensors would be ± 1.0 mph to ± 2.0 mph. Considering that the error range of the LiDAR speed gun is ± 1.0 mph, the speeds reported in the Hi-res data file, which are eventually reported in the SPMs website, are within acceptable error ranges for practical traffic engineering applications.

An important benefit of this feature is that large speed data samples are analyzed to calculate the average 85th percentile speed for the day at each site. The analysis on 85th percentile speeds performed in this study is not yet a conclusive study. More research and data collection are recommended in order to compare the accuracy of 85th percentile speeds. In this study only one 85th percentile speed was available per intersection. To make the results valid, several speed data sets need to be collected to find the distribution of 85th percentile speeds. Nevertheless, the results

of the analysis from the samples taken at the study sites in this study were promising with an error range of -1.6 mph to 1.5 mph (approximately ± 1.5 mph) between the ground truth speed data and the speeds recorded in the Hi-res data. Hence, practically no adjustment factors are needed for speed data. When determining 85th percentile speeds, UDOT usually takes a sample of 100 vehicles at each approach. The Advance sensor on the other hand would collect countless number of speed data, continuously at each site where the sensor is available. Further research is recommended to analyze specifically the 85th percentile speed function of the Advance sensor so that it may be referred to with more confidence in real world applications.

5.3 Chapter Summary

The findings from the approach volume study may be applied to traffic engineering studies. The multiplication factors determined by the results from this study can be used to adjust the data collected by the Advance sensor into calibrated means and 95% confidence intervals.

The approach speed study showed that there was a difference between the speeds recorded in the Hi-res data file by the Advance sensors and the LiDAR gun of approximately ± 1.0 mph to ± 2.0 mph. These differences are not practically significant considering that the speeds are often rounded to the nearest 5 mph; thus the mean speed measured by the Advance sensor can be used for traffic engineering studies without any adjustment.

As for the 85th percentile speeds, it was found that there was a difference of approximately ± 1.5 mph in the 85th percentile speeds between the speeds collected by the LiDAR gun and the Advance sensor. While not yet conclusive, these results can be used to approximate the 85th percentile speeds, considering that the 85th percentile speeds are often rounded to the nearest 5mph in traffic engineering applications.

6 CONCLUSIONS AND RECOMMENDATIONS

The purpose of this study was to evaluate the accuracy of approach volumes and approach speeds collected by the Wavetronix SmartSensor Advance sensors. These sensors have been purchased and installed at many signalized intersection across the state of Utah by UDOT. The primary function of these sensors is dilemma zone reduction, but UDOT would like to have added value in their investment by testing the accuracy of the approach volume and approach speed measurement features of the sensor. By testing the accuracy of these features, the data that are collected by the sensors can be used to provide valuable approach volume counts and speeds to be applied by traffic engineers around the state. The approach volume and speeds collected by the Advance sensor as reported in the Hi-res data were compared against ground truth data that were collected in the field. This chapter summarizes the findings from the study and recommends a further research for calibrating the accuracy of 85th percentile speeds.

6.1 Summary of Findings

The findings from the results of this study show that the Advance sensor provides a insightful view of dynamic approach volumes and approach speeds existing at signalized intersections and offers their data at a level of accuracy sufficient for typical traffic engineering applications. The application of the findings of this study can increase the amount of data used in such applications. This section briefly summarizes the findings of the approach volume and speed studies.

6.1.1 Approach Volume

This study of the Wavetronix SmartSensor Advance version 3.2.0 sensor provided insight into the complexity of calibrating data provided by automated data collection using a microwave sensor. The study found that the Advance sensor was able to collect approach volume at an accuracy level that is acceptable to engineers for practical traffic engineering applications. The application of this tool is recommended at one-lane or two-lane approaches where the accuracy of approach volume counts ranges from 85.4% to 105.7%, which can be acceptable for designing roads and timing signals at intersections. In other words, approach volumes by the Advance sensor ranges from 14.6% undercount to 5.7% overcount at the study sites used in this study. The results of the analysis on approach volume accuracies are found in Table 5-2. For three-lane roads with a high approach volume, the approach volume accuracy began to deteriorate down to 77.8%, meaning a 22.2% undercount for approaches with three or more lanes with high approach volumes. Given the variation of daily traffic, these accuracy ranges still provide useful and insightful data as to the condition of the roadway. As with any data that are collected in the field, engineers must exercise their judgment when using the data collected by the Advance sensor.

6.1.2 Approach Speed

The approach speed data collection function of the Advance sensor uses its continuous vehicle tracking feature to measure the speed of the approaching vehicle. The LiDAR gun used in data collection has an error margin of ± 1 mph. The analysis showed a difference in mean accuracy of approximately 2 mph between the ground truth speed data by the LiDAR gun and the speed data collected by the Advance sensor. While the difference in mean accuracies was found to be statistically significant at a 95 % confidence level, it can be considered practically acceptable for use in traffic engineering applications considering the error margin of ± 1 mph of the LiDAR gun.

As for determining 85th percentile speeds, the sensor showed only ± 1.5 mph difference between the ground truth speed data by the LiDAR gun and the speeds measured by the Advance sensor. This preliminary analysis showed promising results but the analysis was inconclusive due to data limitations.

6.2 Conclusion

While the Advance sensor is not perfect for providing approach volume counts and approach speeds, the statistical analyses performed in this study show that the Advance sensor is performing at an accuracy level sufficient for typical traffic engineering applications when taking into account the variability of traffic conditions on a daily and seasonal basis. The system's ability to store past data also enables this system to be a useful feature of UDOT's SPMs system. The time and resources saved by using the microwave sensor outweigh the costs associated with the installation of microwave sensors. To ensure that the sensors provide accurate data, it is important to monitor the installation and maintenance of these devices with periodic quality assurance and quality control (QA/QC) checkups. By doing so, potential errors that may occur due to other factors than the ones studied in this research can be minimized. It is important to note that all data collection utilized in this study were performed after both Wavetronix and UDOT engineers had performed a QA/QC by inspecting the installation and programming of the sensors. The accuracy of approach volumes and speeds reported in this thesis is based upon this premise.

The results of this study show that the approach volume collected by the Advance sensor as presented in UDOT's SPMs website can be calibrated with a multiplication factor to adjust the reported volumes into mean volumes and 95% confidence interval ranges of volumes. The results of the approach speed study show that the difference between mean speeds collected by the LiDAR gun and the Advance sensor was statistically significant, but not considered practically significant

given that the speeds are generally rounded to the nearest 5mph by traffic engineers for typical traffic engineering applications. The 85th percentile speed study showed similar results in the differences between the two methods. In conclusion it can be said that the Advance sensor does provide valuable information on approach volume and speed, which are dynamically reported continuously. As for approach volumes, the calibration factors presented in section 5.1 can be used to adjust them, and for approach speeds, both mean speeds and 85th percentile speeds reported in UDOT's SPMs website were found to be a couple of miles per hour off the true speed.

6.3 Recommendations

Further research is recommended for testing the accuracy of the 85th percentile speeds, as they are more often used in roadway and signal timing design than the mean speeds. Another recommendation is to test the variability in the sensing capabilities of the Advance sensor to different vehicle sizes ranging from large trucks, including semi-trucks, to smaller vehicles, such as motorcycles and bicyclists.

LIST OF ACRONYMS

ANOVA – Analysis of Variance

BYU – Brigham Young University

CCTV – Closed Circuit Television

DWR – Digital Wave Radar

EB – Eastbound

ETA – Estimated Time of Arrival

kph – kilometers per hour

LiDAR – Light Detector and Ranging

mph – miles per hour

NB – Northbound

QA/QC – Quality Assurance / Quality Control

SB – Southbound

SPMs – Signal Performance Metrics

SQL – Structured Query Language

SSM – SmartSensor Manager

SUV – Sport Utility Vehicle

UDOT – Utah Department of Transportation

vphpl – vehicles per hour per lane

WB – Westbound

REFERENCES

- Chang, D. K. (2015). Evaluation of the Accuracy of Traffic Volume Counts Collected by Microwave Sensors. Brigham Young University.
- JAMAR Technologies, Inc. (2015). Petra for Windows, Version 3.3.1.
- Laser Technology, In., (2015a). “How Lasers Work.” <<http://www.lasertech.com/How-Lasers-Work.aspx>> (July 2015).
- Laser Technology, Inc. (2015b). “TruCAM Laser Speed Gun with Video.” <<http://www.lasertech.com/TruCAM-Laser-Speed-Gun.aspx>> (July 2015).
- Laser Technology, Inc. (2009). “TruCAM User’s Manual, 2nd Edition.” Laser Technology, Inc., United States of America.
- Marsh Products. (2000). “The Basics of Loop Vehicle Detection.” <<http://www.marshproducts.com/pdf/Inductive%20Loop%20Write%20up.pdf>> (July 2015)
- Microsoft. (2015). “Windows Movie Maker.” < <http://windows.microsoft.com/en-us/windows/movie-maker>>
- Officer.com. (2015). “TruCAM - 2009 Innovation Awards Winner: Traffic Enforcement.” <<http://www.officer.com/product/10053208/laser-technology-inc-trucam-2009-innovation-awards-winner-traffic-enforcement>>
- R Core Team. (2015). “R: A Language and Environment for Statistical Computing.” R Foundation for Statistical Computing. Vienna, Austria. <<https://www.R-project.org>> (January 2016).
- Ramsey, F. L. and Schafer, D. W. (2002). The Statistical Sleuth 2nd Edition. CENGAGE Learning. United States of America.

Roess, R.P., Prassas E. S., and McShane, W. R. (2009). “Statistical Applications in TrafficEngineering.” *Traffic Engineering 4th edition*, Pearson, New Delhi, India, 139.

SAS. (2015). SAS Statistical Software Version 9.2.

Saito, M., Chang, D. K., and Shultz, G. G. (2015). “Calibration of Automatic Performance Measures – Speed and Volume Data: Volume 1, Evaluation of the Accuracy of Traffic Volume Counts collected by Microwave Sensors.” Report UT-15.14, Utah Department of Transportation, Research Division, Salt Lake City, UT.

Sturdevant, J. R., Overman, T., Raamot, E., Deer, R., Miller, D., Bullock, D. M., Day, C. M., Brennan Jr., T. M., Li, H., Hainen, A. and Remias, S. M. (2012). “Indiana Traffic Signal Hi Resolution Data Logger Enumerations.” *Joint Transportation Research Program DataPapers, Purdue e-Pubs*, Purdue University, IN.

TechSmith. (2014). “SnagIt”. < <https://www.techsmith.com/snagit.html>>

UDOT. (2015). “Signal Performance Metrics.” <<http://udottraffic.utah.gov/signalperformance/metrics/>> (Feb. 25 2015).

UDOT Traffic & Safety. (2015). “Minimum Data Collection Requirements for Traffic Studies.”

Wavetronix. (2015a). “SmartSensor Advance.” Wavetronix. <<http://www.wavetronix.com/en/products/smartsensor/advance/features>> (July 2015).

Wavetronix. (2015b). “SmartSensor Advance.” Wavetronix,<<http://www.wavetronix.com/en/products/smartsensor/advance/specs>> (July 2015).

Wavetronix. (2015c). “SmartSensor Advance.” Wavetronix, <<http://www.wavetronix.com/en/products/smartsensor/advance/safearrival>> (July 2015).

APPENDIX A: SPEED GUN CALIBRATION DATA

Table A-1: Speed Data from Calibration Test

Clip No.	Lane#	Distance	Lidar Speed	Video Speed	(Lidar V) - (Video V)	Absolute Difference
9124	2	331	55	56	1	1
9125	1	331	48	49	1	1
9126	1	395	59	57	-2	2
9127	1	291	59	60	1	1
9128	1	324	55	56	1	1
9129	2	282	46	48	2	2
9130	2	312	56	55	-1	1
9131	2	346	52	56	4	4
9132	1	324	51	51	0	0
9133	2	343	54	59	5	5
9134	2	367	54	56	2	2
9135	1	331	48	50	2	2
9136	2	323	53	55	2	2
9137	2	346	48	50	2	2
9138	2	317	50	50	0	0
9139	1	272	38	39	1	1
9140	1	407	47	48	1	1
9141	2	316	45	49	4	4
9142	1	371	44	47	3	3
9143	2	316	48	52	4	4
9144	2	365	47	50	3	3
9145	2	335	48	50	2	2
9146	2	356	32	36	4	4
9147	1	289	49	47	-2	2
9148	1	300	51	48	-3	3
9149	1	353	51	53	2	2
9150	1	322	48	47	-1	1
9151	1	290	51	49	-2	2
9152	2	347	48	52	4	4
9153	NA	NA	NA			
9154	2	275	46	49	3	3
9155	2	280	50	52	2	2
9156	1	333	48	49	1	1
9157	1	315	48	46	-2	2
9158	2	317	50	52	2	2
9159	1	316	44	41	-3	3
9160	2	331	50	50	0	0

Table A-1: (Continued)

9161	2	286	53	54	1	1
9162	1	301	49	46	-3	3
9163	2	310	40	40	0	0
9164	2	324	43	46	3	3
9165	NA	NA	NA			
9166	2	339	47	50	3	3
9167	2	322	48	49	1	1
9168	2	321	40	40	0	0
9169	2	234	41	45	4	4
9170	2	387	52	59	7	7
9171	1	350	44	43	-1	1
9172	1	320	49	46	-3	3
9173	2	275	48	50	2	2
9174	2	320	46	48	2	2
9175	2	320	51	52	1	1
9176	1	340	45	47	2	2
9177	2	340	49	51	2	2
9178	1	345	55	58	3	3
9179	2	334	50	52	2	2
9180	2	312	44	45	1	1
9181	1	295	42	40	-2	2
9182	2	336	44	45	1	1
9183	1	331	53	53	0	0
9184	1	331	52	50	-2	2
9185	2	308	49	49	0	0
9186	1	300	48	46	-2	2
9187	2	344	53	56	3	3
9188	1	351	51	53	2	2
9189	NA	NA	NA			
9190	NA	NA	NA			
9191	2	237	46	49	3	3
9192	2	285	44	43	-1	1
9193	2	308	47	47	0	0
9194	2	306	45	46	1	1
9195	1	318	51	49	-2	2
9196	1	329	57	57	0	0
9197	2	334	54	53	-1	1
9198	2	304	37	39	2	2

APPENDIX B: RAW VOLUME DATA

Table A-1: Approach Volume for Sensor Position 1

Sensor Position	Lanes 1					Lanes 2					Lanes 3							
	Direction	Volume	Vehicles	Hours	Accuracy	Time	Direction	Volume	Vehicles	Hours	Accuracy	Time	Direction	Volume	Vehicles	Hours	Accuracy	Time
Low	12908 & Geneva Rd. Provo																	
	NB	100	100	116	116.0%	06:23:10 PM	NB	214	112	214	95.9%	10:10:55 PM	EB	479	166	466	99.0%	5:55:52 AM
	SB	142	142	148	104.2%	10:23:10 PM	SB	198	90	208	45.90% A	4:57:07 AM	SB	91	259	95.9%	5:55:52 AM	
	12908 & Geneva Rd. Provo																	
	NB	100	100	116	116.0%	06:23:10 PM	NB	340	170	296	81.2%	5:46:02 AM	EB	178	125	201	79.7%	05:10:11 PM
	SB	142	142	148	104.2%	10:23:10 PM	SB	89	45	132	148.7%	11:40:10 AM	WB	212	71	180	81.9%	5:10:11 PM
	12908 & Geneva Rd. Provo																	
	NB	100	100	116	116.0%	06:23:10 PM	NB	215	118	212	90.7%	5:46:10 AM	EB	171	121	202	97.0%	4:52:52 AM
	SB	142	142	148	104.2%	10:23:10 PM	SB	167	88	170	101.8%	7:55:15 PM	WB	257	79	207	87.7%	11:08:39 PM
	12908 & Geneva Rd. Provo																	
	NB	100	100	116	116.0%	06:23:10 PM	NB	162	81	117	72.2%	10:25:02 PM	WB	287	96	266	85.7%	10:48:42 PM
	SB	142	142	148	104.2%	10:23:10 PM	SB	157	79	147	93.0%	5:29:17 AM	WB	423	141	360	85.1%	10:18:15 AM
12908 & Geneva Rd. Provo																		
NB	100	100	116	116.0%	06:23:10 PM	NB	609	304.5	602	101.8%	12:12:08 PM	EB	180	291	783	80.9%	9:11:41 AM	
SB	142	142	148	104.2%	10:23:10 PM	SB	410	205	298	96.7%	1:35:09 PM	WB	591	197	554	91.7%	7:27:46 PM	
12908 & Geneva Rd. Provo																		
NB	100	100	116	116.0%	06:23:10 PM	NB	369	184.5	368	99.6%	10:01:46 PM	WB	619	211	571	92.1%	8:01:01 AM	
SB	142	142	148	104.2%	10:23:10 PM	SB	425	212.5	177	82.7%	10:10:11 AM	WB	653	314	824	92.2%	4:10:24 PM	
12908 & Geneva Rd. Provo																		
NB	100	100	116	116.0%	06:23:10 PM	NB	362	181	352	97.2%	5:42:50 PM	EB	554	185	511	92.8%	6:58:52 PM	
SB	142	142	148	104.2%	10:23:10 PM	SB	662	331	592	89.6%	5:27:00 PM	WB	786	266	699	80.1%	9:59:48 PM	
12908 & Geneva Rd. Provo																		
NB	100	100	116	116.0%	06:23:10 PM	NB	609	304.5	602	101.8%	7:57:14 PM	WB	772	257	603	85.9%	7:50:28 AM	
SB	142	142	148	104.2%	10:23:10 PM	SB	411	205.5	353	77.8%	10:56:11 AM	WB	772	257	603	85.9%	7:50:28 AM	
12908 & Geneva Rd. Provo																		
NB	100	100	116	116.0%	06:23:10 PM	NB	641	320.5	625	97.5%	3:40:15 AM	WB	1088	361	841	77.3%	7:45:57 AM	
SB	142	142	148	104.2%	10:23:10 PM	SB	465	232.5	504	108.6%	8:13:25 AM	WB	1088	361	841	77.3%	7:45:57 AM	
12908 & Geneva Rd. Provo																		
NB	100	100	116	116.0%	06:23:10 PM	NB	1042	521	930	88.9%	7:56:33 AM	EB	1177	429	996	73.6%	7:57:23 AM	
SB	142	142	148	104.2%	10:23:10 PM	SB	1310	655	1104	84.9%	4:34:50 PM	WB	1180	387	966	86.2%	10:10:45 AM	
12908 & Geneva Rd. Provo																		
NB	100	100	116	116.0%	06:23:10 PM	NB	1013	506.5	999	96.6%	10:59:46 AM	EB	1403	468	1204	83.9%	7:40:30 AM	
SB	142	142	148	104.2%	10:23:10 PM	SB	764	382	701	91.0%	6:36:03 AM	WB	1128	375	956	83.1%	5:03:16 PM	
12908 & Geneva Rd. Provo																		
NB	100	100	116	116.0%	06:23:10 PM	NB	1459	729.5	1302	89.2%	5:06:20 PM	EB	1698	609	1644	69.7%	4:52:29 PM	
SB	142	142	148	104.2%	10:23:10 PM	SB	808	404	792	98.2%	3:06:50 PM	WB	1139	380	826	72.7%	11:56:23 AM	
12908 & Geneva Rd. Provo																		
NB	100	100	116	116.0%	06:23:10 PM	NB	908	454	874	96.2%	8:57:51 PM	WB	1152	407	1011	88.1%	7:49:34 AM	
SB	142	142	148	104.2%	10:23:10 PM	SB	706	353	577	81.6%	8:57:51 PM	WB	1152	407	1011	88.1%	7:49:34 AM	
12908 & Geneva Rd. Provo																		
NB	100	100	116	116.0%	06:23:10 PM	NB	912	456	816	97.0%	4:57:51 PM	WB	1064	351	799	73.9%	10:06:26 AM	
SB	142	142	148	104.2%	10:23:10 PM	SB	641	320.5	625	97.5%	3:40:15 AM	WB	2018	673	1209	59.9%	10:06:26 AM	
12908 & Geneva Rd. Provo																		
NB	100	100	116	116.0%	06:23:10 PM	NB	641	320.5	625	97.5%	3:40:15 AM	WB	1088	361	841	77.3%	7:45:57 AM	
SB	142	142	148	104.2%	10:23:10 PM	SB	465	232.5	504	108.6%	8:13:25 AM	WB	1088	361	841	77.3%	7:45:57 AM	
12908 & Geneva Rd. Provo																		
NB	100	100	116	116.0%	06:23:10 PM	NB	641	320.5	625	97.5%	3:40:15 AM	WB	1088	361	841	77.3%	7:45:57 AM	
SB	142	142	148	104.2%	10:23:10 PM	SB	465	232.5	504	108.6%	8:13:25 AM	WB	1088	361	841	77.3%	7:45:57 AM	
12908 & Geneva Rd. Provo																		
NB	100	100	116	116.0%	06:23:10 PM	NB	641	320.5	625	97.5%	3:40:15 AM	WB	1088	361	841	77.3%	7:45:57 AM	
SB	142	142	148	104.2%	10:23:10 PM	SB	465	232.5	504	108.6%	8:13:25 AM	WB	1088	361	841	77.3%	7:45:57 AM	
12908 & Geneva Rd. Provo																		
NB	100	100	116	116.0%	06:23:10 PM	NB	641	320.5	625	97.5%	3:40:15 AM	WB	1088	361	841	77.3%	7:45:57 AM	
SB	142	142	148	104.2%	10:23:10 PM	SB	465	232.5	504	108.6%	8:13:25 AM	WB	1088	361	841	77.3%	7:45:57 AM	
12908 & Geneva Rd. Provo																		
NB	100	100	116	116.0%	06:23:10 PM	NB	641	320.5	625	97.5%	3:40:15 AM	WB	1088	361	841	77.3%	7:45:57 AM	
SB	142	142	148	104.2%	10:23:10 PM	SB	465	232.5	504	108.6%	8:13:25 AM	WB	1088	361	841	77.3%	7:45:57 AM	
12908 & Geneva Rd. Provo																		
NB	100	100	116	116.0%	06:23:10 PM	NB	641	320.5	625	97.5%	3:40:15 AM	WB	1088	361	841	77.3%	7:45:57 AM	
SB	142	142	148	104.2%	10:23:10 PM	SB	465	232.5	504	108.6%	8:13:25 AM	WB	1088	361	841	77.3%	7:45:57 AM	
12908 & Geneva Rd. Provo																		
NB	100	100	116	116.0%	06:23:10 PM	NB	641	320.5	625	97.5%	3:40:15 AM	WB	1088	361	841	77.3%	7:45:57 AM	
SB	142	142	148	104.2%	10:23:10 PM	SB	465	232.5	504	108.6%	8:13:25 AM	WB	1088	361	841	77.3%	7:45:57 AM	
12908 & Geneva Rd. Provo																		
NB	100	100	116	116.0%	06:23:10 PM	NB	641	320.5	625	97.5%	3:40:15 AM	WB	1088	361	841	77.3%	7:45:57 AM	
SB	142	142	148	104.2%	10:23:10 PM	SB	465	232.5	504	108.6%	8:13:25 AM	WB	1088	361	841	77.3%	7:45:57 AM	
12908 & Geneva Rd. Provo																		
NB	100	100	116	116.0%	06:23:10 PM	NB	641	320.5	625	97.5%	3:40:15 AM	WB	1088	361	841	77.3%	7:45:57 AM	
SB	142	142	148	104.2%	10:23:10 PM	SB	465	232.5	504	108.6%	8:13:25 AM	WB	1088	361	841	77.3%	7:45:57 AM	
12908 & Geneva Rd. Provo																		
NB	100	100	116	116.0%	06:23:10 PM	NB	641	320.5	625	97.5%	3:40:15 AM	WB	1088	361	841	77.3%	7:45:57 AM	
SB	142	142	148	104.2%	10:23:10 PM	SB	465	232.5	504	108.6%	8:13:25 AM	WB	1088	361	841	77.3%	7:45:57 AM	
12908 & Geneva Rd. Provo																		
NB	100	100	116	116.0%	06:23:10 PM	NB	641	320.5	625	97.5%	3:40:15 AM	WB	1088	361	841	77.3%	7:45:57 AM	
SB	142	142	148	104.2%	10:23:10 PM	SB	465	232.5	504	108.6%	8:13:25 AM	WB	1088	361	841	77.3%	7:45:57 AM	
12908 & Geneva Rd. Provo																		
NB	100	100	116	116.0%	06:23:10 PM	NB	641	320.5	625	97.5%	3:40:15 AM	WB	1088	361	841	77.3%	7:45:57 AM	
SB	142	142	148	104.2%	10:23:10 PM	SB	465	232.5	504	108.6%	8:13:25 AM	WB	1088	361	841	77.3%	7:45:57 AM	
12908 & Geneva Rd. Provo																		
NB	100	100	116	116.0%	06:23:10 PM	NB	641	320.5	625	97.5%	3:40:15 AM	WB	1088	361	841	77.3%	7:45:57 AM	
SB	142	142	148	104.2%	10:23:10 PM	SB	465	232.5	504	108.6%	8:13:25 AM	WB	1088	361	841	77.3%	7:45:57 AM	
12908 & Geneva Rd. Provo																		
NB	100	100	116	116.0%	06:23:10 PM	NB	641	320.5	625	97.5%	3:40:15 AM	WB	1088	361	841	77.3%	7:45:57 AM	
SB	142	142	148	104.2%	10:23:10 PM	SB	465	232.5	504	108.6%	8:13:25 AM	WB	1088	361	841	77.3%	7:45:57 AM	
12908 & Geneva Rd. Provo																		
NB	100	100	116	116.0%	06:23:10 PM	NB	641	320.5	625	97.5%	3:40:15 AM	WB	1088	361	841	77.3%	7:45:57 AM	
SB	142	142	148	104.2%	10:23:10 PM	SB	465	232.5	504	108.6%	8:13:25 AM	WB	1088	361	841	77.3%	7:45:57 AM	
12908 & Geneva Rd. Provo																		
NB	100	100	116	116.0%	06:23:10 PM	NB	641	320.5	625	97.5%	3:40:15 AM	WB	1088	361	841	77.3%	7:45:57 AM	
SB	142	142	148	104.2%	10:23:10 PM	SB	465	232.5	504	108.6%	8:13:25 AM	WB	1088	361	841	77.3%	7:45:57 AM	
12908 & Geneva Rd. Provo																		
NB	100																	

Table A-2: Approach Volume for Sensor Position 2

Location	Direction	Volume	Vehicle	Flow	Accuracy	Time	Date	Location	Direction	Volume	Vehicle	Flow	Accuracy	Time	Date
Mid	E1001 & Gower Rd, Penn	SB	274	128	47%	1:00:00 PM	March 19, 2015	Mid	E1001 & Gower Rd, Penn	SB	278	131	47%	1:00:00 PM	March 19, 2015
		WB	274	128	47%	1:00:00 PM	March 19, 2015			WB	278	131	47%	1:00:00 PM	March 19, 2015
		SB	274	128	47%	1:00:00 PM	March 19, 2015			SB	278	131	47%	1:00:00 PM	March 19, 2015
		WB	274	128	47%	1:00:00 PM	March 19, 2015			WB	278	131	47%	1:00:00 PM	March 19, 2015
		SB	274	128	47%	1:00:00 PM	March 19, 2015			SB	278	131	47%	1:00:00 PM	March 19, 2015
Mid	E1001 & Gower Rd, Penn	SB	274	128	47%	1:00:00 PM	March 19, 2015	Mid	E1001 & Gower Rd, Penn	SB	278	131	47%	1:00:00 PM	March 19, 2015
		WB	274	128	47%	1:00:00 PM	March 19, 2015			WB	278	131	47%	1:00:00 PM	March 19, 2015
		SB	274	128	47%	1:00:00 PM	March 19, 2015			SB	278	131	47%	1:00:00 PM	March 19, 2015
		WB	274	128	47%	1:00:00 PM	March 19, 2015			WB	278	131	47%	1:00:00 PM	March 19, 2015
		SB	274	128	47%	1:00:00 PM	March 19, 2015			SB	278	131	47%	1:00:00 PM	March 19, 2015
High	E1001 & Gower Rd, Penn	SB	274	128	47%	1:00:00 PM	March 19, 2015	High	E1001 & Gower Rd, Penn	SB	278	131	47%	1:00:00 PM	March 19, 2015
		WB	274	128	47%	1:00:00 PM	March 19, 2015			WB	278	131	47%	1:00:00 PM	March 19, 2015
		SB	274	128	47%	1:00:00 PM	March 19, 2015			SB	278	131	47%	1:00:00 PM	March 19, 2015
		WB	274	128	47%	1:00:00 PM	March 19, 2015			WB	278	131	47%	1:00:00 PM	March 19, 2015
		SB	274	128	47%	1:00:00 PM	March 19, 2015			SB	278	131	47%	1:00:00 PM	March 19, 2015

APPENDIX C: RAW APPROACH SPEED DATA

Table C-1: EB at 9000S and 700W, Sandy

Lane	Sample No.	Gun Speed	Hi-res Speed	Speed Accuracy	difference
T1	1	39	37	94.87%	2
T1	2	53	46	86.79%	7
T1	3	52	49	94.23%	3
T1	4	47	49	104.26%	-2
T1	5	40	42	105.00%	-2
T1	6	48	50	104.17%	-2
T1	7	49	49	100.00%	0
T1	8	47	48	102.13%	-1
T1	9	42	43	102.38%	-1
T1	10	45	43	95.56%	2
T1	11	44	45	102.27%	-1
T1	12	45	46	102.22%	-1
T1	13	48	48	100.00%	0
T1	14	49	48	97.96%	1
T1	15	46	43	93.48%	3
T1	16	45	46	102.22%	-1
T1	17	46	44	95.65%	2
T1	18	47	49	104.26%	-2
T1	19	45	47	104.44%	-2
T1	20	50	49	98.00%	1
T1	21	46	48	104.35%	-2
T1	22	41	36	87.80%	5
T1	23	49	53	108.16%	-4
T1	24	44	47	106.82%	-3
T1	25	44	35	79.55%	9
T1	26	44	42	95.45%	2
T1	27	43	37	86.05%	6
T1	28	46	44	95.65%	2
T1	29	40	39	97.50%	1
T1	30	47	46	97.87%	1
T1	31	41	37	90.24%	4
T1	32	48	47	97.92%	1
T1	33	50	49	98.00%	1
T1	34	46	43	93.48%	3
T1	35	48	49	102.08%	-1
T1	36	50	48	96.00%	2

Table C-1: (Continued)

T1	37	52	50	96.15%	2
T1	38	52	47	90.38%	5
T1	39	48	48	100.00%	0
T1	40	46	46	100.00%	0
T1	41	39	44	112.82%	-5
T1	42	44	46	104.55%	-2
T1	43	44	42	95.45%	2
T1	44	47	51	108.51%	-4
T2	45	45	43	95.56%	2
T2	46	42	40	95.24%	2
T2	47	49	49	100.00%	0
T2	48	35	37	105.71%	-2
T2	49	40	37	92.50%	3
T2	50	47	47	100.00%	0
T2	51	47	46	97.87%	1
T2	52	43	38	88.37%	5
T2	53	50	48	96.00%	2
T2	54	40	37	92.50%	3
T2	55	48	36	75.00%	12
T2	56	47	42	89.36%	5
T2	57	48	44	91.67%	4
T2	58	47	44	93.62%	3
T2	59	41	42	102.44%	-1
T2	60	43	49	113.95%	-6
T2	61	48	44	91.67%	4
T2	62	44	41	93.18%	3
T2	63	47	42	89.36%	5
T2	64	49	48	97.96%	1
T2	65	44	43	97.73%	1
T2	66	44	25	56.82%	19
T2	67	44	45	102.27%	-1
T2	68	61	54	88.52%	7
T2	69	41	42	102.44%	-1
T2	70	56	54	96.43%	2
T2	71	46	45	97.83%	1
T2	72	51	49	96.08%	2
T2	73	48	45	93.75%	3
T2	74	54	54	100.00%	0
T2	75	53	47	88.68%	6

Table C-1: (Continued)

T2	76	48	48	100.00%	0
T2	77	46	44	95.65%	2
T2	78	42	38	90.48%	4
T2	79	64	58	90.63%	6
T2	80	40	39	97.50%	1
T2	81	49	49	100.00%	0
T2	82	48	47	97.92%	1
T2	83	37	21	56.76%	16
T2	84	44	44	100.00%	0
T2	85	41	44	107.32%	-3
T2	86	40	41	102.50%	-1
T2	87	44	45	102.27%	-1
T3	88	39	39	100.00%	0
T3	89	40	40	100.00%	0
T3	90	43	44	102.33%	-1
T3	91	42	45	107.14%	-3
T3	92	53	45	84.91%	8
T3	93	40	38	95.00%	2
T3	94	49	43	87.76%	6
T3	95	44	37	84.09%	7
T3	96	47	49	104.26%	-2
T3	97	48	47	97.92%	1
T3	98	42	40	95.24%	2
T3	99	48	45	93.75%	3
T3	100	46	38	82.61%	8
T3	101	49	48	97.96%	1
T3	102	44	44	100.00%	0
T3	103	40	34	85.00%	6
T3	104	43	44	102.33%	-1
T3	105	46	46	100.00%	0
T3	106	45	37	82.22%	8
T3	107	55	48	87.27%	7
T3	108	44	31	70.45%	13
T3	109	50	46	92.00%	4
T3	110	53	46	86.79%	7
T3	111	47	49	104.26%	-2
T3	112	46	41	89.13%	5
T3	113	47	45	95.74%	2
T3	114	47	31	65.96%	16

Table C-1: (Continued)

T3	115	43	42	97.67%	1
T3	116	48	46	95.83%	2
T3	117	41	42	102.44%	-1
T3	118	47	45	95.74%	2
T3	119	45	42	93.33%	3
T3	120	60	46	76.67%	14
T3	121	51	46	90.20%	5
T3	122	48	47	97.92%	1
T3	123	42	45	107.14%	-3
T3	124	47	41	87.23%	6
T3	125	43	36	83.72%	7
T3	126	48	45	93.75%	3
T3	127	44	43	97.73%	1
T3	128	44	38	86.36%	6
T3	129	47	48	102.13%	-1
	Mean	46.09	43.89		2.20
	St. Dev.	4.54	5.40		4.15

Table C-2: SB at 1320 S and State St., Provo

Lane	Sample No.	Gun Speed	Hi-res Speed	Speed Accuracy	difference
T1	1	50	48	104.17%	2
T1	2	45	46	97.83%	-1
T1	3	49	51	96.08%	-2
T1	4	50	50	100.00%	0
T1	5	43	46	93.48%	-3
T1	6	50	49	102.04%	1
T1	7	55	56	98.21%	-1
T1	8	58	53	109.43%	5
T1	9	56	49	114.29%	7
T1	10	59	57	103.51%	2
T1	11	49	48	102.08%	1
T1	12	42	54	77.78%	-12
T1	13	50	48	104.17%	2
T1	14	49	46	106.52%	3
T1	15	39	40	97.50%	-1
T1	16	55	53	103.77%	2
T1	17	37	42	88.10%	-5
T1	18	61	60	101.67%	1
T1	19	56	56	100.00%	0
T1	20	42	40	105.00%	2
T1	21	51	48	106.25%	3
T1	22	50	52	96.15%	-2
T1	23	47	55	85.45%	-8
T1	24	45	47	95.74%	-2
T1	25	57	50	114.00%	7
T1	26	45	47	95.74%	-2
T1	27	47	50	94.00%	-3
T1	28	55	60	91.67%	-5
T1	29	51	52	98.08%	-1
T1	30	39	39	100.00%	0
T1	31	52	51	101.96%	1
T1	32	55	55	100.00%	0
T1	33	45	46	97.83%	-1
T1	34	51	51	100.00%	0
T1	35	53	50	106.00%	3
T1	36	47	19	247.37%	28

Table C-2: (Continued)

T1	37	50	40	125.00%	10
T1	38	47	50	94.00%	-3
T1	39	49	48	102.08%	1
T1	40	49	47	104.26%	2
T1	41	41	43	95.35%	-2
T1	42	54	45	120.00%	9
T1	43	51	45	113.33%	6
T1	44	44	42	104.76%	2
T1	45	46	49	93.88%	-3
T1	46	51	50	102.00%	1
T1	47	38	42	90.48%	-4
T1	48	49	47	104.26%	2
T1	49	51	40	127.50%	11
T1	50	54	51	105.88%	3
T1	51	49	49	100.00%	0
T1	52	38	41	92.68%	-3
T1	53	57	55	103.64%	2
T1	54	58	58	100.00%	0
T1	55	58	51	113.73%	7
T1	56	56	51	109.80%	5
T1	57	51	46	110.87%	5
T1	58	52	51	101.96%	1
T2	59	45	55	81.82%	-10
T2	60	48	46	104.35%	2
T2	61	50	50	100.00%	0
T2	62	48	48	100.00%	0
T2	63	49	48	102.08%	1
T2	64	54	54	100.00%	0
T2	65	47	43	109.30%	4
T2	66	47	46	102.17%	1
T2	67	51	47	108.51%	4
T2	68	45	54	83.33%	-9
T2	69	46	45	102.22%	1
T2	70	48	43	111.63%	5
T2	71	49	48	102.08%	1
T2	72	33	37	89.19%	-4
T2	73	52	54	96.30%	-2
T2	74	55	53	103.77%	2
T2	75	53	49	108.16%	4

Table C-2: (Continued)

T2	76	47	49	95.92%	-2
T2	77	55	56	98.21%	-1
T2	78	46	46	100.00%	0
T2	79	49	41	119.51%	8
T2	80	42	42	100.00%	0
T2	81	54	48	112.50%	6
T2	82	50	48	104.17%	2
T2	83	41	49	83.67%	-8
T2	84	46	47	97.87%	-1
T2	85	49	49	100.00%	0
T2	86	43	42	102.38%	1
T2	87	50	42	119.05%	8
T2	88	49	46	106.52%	3
T2	89	42	50	84.00%	-8
T2	90	46	41	112.20%	5
T2	91	46	48	95.83%	-2
T2	92	56	53	105.66%	3
T2	93	47	48	97.92%	-1
T2	94	44	44	100.00%	0
T2	95	49	49	100.00%	0
T2	96	46	48	95.83%	-2
T2	97	44	44	100.00%	0
T2	98	53	47	112.77%	6
T2	99	52	50	104.00%	2
T2	100	47	61	77.05%	-14
T2	101	47	46	102.17%	1
T2	102	45	53	84.91%	-8
T2	103	37	41	90.24%	-4
T2	104	33	51	64.71%	-18
T2	105	44	45	97.78%	-1
T2	106	40	40	100.00%	0
T2	107	53	56	94.64%	-3
T2	108	40	50	80.00%	-10
T2	109	45	46	97.83%	-1
T2	110	52	54	96.30%	-2
T2	111	43	43	100.00%	0
T2	112	52	50	104.00%	2
T2	113	51	50	102.00%	1
T2	114	52	46	113.04%	6

Table C-2: (Continued)

T2	115	46	50	92.00%	-4
T2	116	43	43	100.00%	0
T2	117	47	47	100.00%	0
T2	118	41	43	95.35%	-2
T2	119	48	47	102.13%	1
T2	120	53	47	112.77%	6
T2	121	44	47	93.62%	-3
T2	122	58	51	113.73%	7
T2	123	53	53	100.00%	0
T2	124	64	55	116.36%	9
T2	125	50	51	98.04%	-1
	Mean	48.58	48.14		0.43
	St. Dev.	5.63	5.46		5.22

Table C-3: EB at 400 East and 800 North, Orem

Lane	Sample No.	Gun Speed	Hi-res Speed	Speed Accuracy	difference
T3	1	50	49	98.00%	1
T3	2	45	41	91.11%	4
T3	3	44	46	104.55%	-2
T3	4	42	41	97.62%	1
T3	5	45	40	88.89%	5
T3	6	45	42	93.33%	3
T3	7	50	46	92.00%	4
T3	8	42	45	107.14%	-3
T3	9	43	41	95.35%	2
T3	10	38	40	105.26%	-2
T3	11	41	41	100.00%	0
T3	12	49	46	93.88%	3
T3	13	43	46	106.98%	-3
T3	14	37	41	110.81%	-4
T3	15	40	42	105.00%	-2
T3	16	45	42	93.33%	3
T3	17	45	55	122.22%	-10
T3	18	39	40	102.56%	-1
T3	19	39	37	94.87%	2
T3	20	48	44	91.67%	4
T3	21	47	38	80.85%	9
T3	22	43	42	97.67%	1
T3	23	40	44	110.00%	-4
T3	24	41	41	100.00%	0
T3	25	40	40	100.00%	0
T3	26	53	43	81.13%	10
T3	27	36	36	100.00%	0
T3	28	46	45	97.83%	1
T3	29	48	40	83.33%	8
T3	30	38	40	105.26%	-2
T3	31	49	53	108.16%	-4
T3	32	41	41	100.00%	0
T3	33	36	33	91.67%	3
T3	34	39	48	123.08%	-9
T3	35	51	48	94.12%	3
T3	36	40	41	102.50%	-1

Table C-3: (Continued)

T3	37	41	42	102.44%	-1
T3	38	46	35	76.09%	11
T3	39	49	47	95.92%	2
T2	40	41	43	104.88%	-2
T2	41	45	47	104.44%	-2
T2	42	42	38	90.48%	4
T2	43	47	44	93.62%	3
T2	44	45	47	104.44%	-2
T2	45	41	38	92.68%	3
T2	46	51	46	90.20%	5
T2	47	48	42	87.50%	6
T2	48	46	48	104.35%	-2
T2	49	48	50	104.17%	-2
T2	50	44	42	95.45%	2
T2	51	42	40	95.24%	2
T2	52	55	49	89.09%	6
T2	53	43	47	109.30%	-4
T2	54	43	39	90.70%	4
T2	55	48	52	108.33%	-4
T2	56	46	45	97.83%	1
T2	57	50	48	96.00%	2
T2	58	46	45	97.83%	1
T2	59	46	44	95.65%	2
T2	60	45	42	93.33%	3
T2	61	47	45	95.74%	2
T2	62	49	50	102.04%	-1
T2	63	51	52	101.96%	-1
T2	64	56	55	98.21%	1
T2	65	48	44	91.67%	4
T2	66	47	46	97.87%	1
T2	67	46	37	80.43%	9
T2	68	58	54	93.10%	4
T2	69	47	47	100.00%	0
T2	70	39	39	100.00%	0
T2	71	42	43	102.38%	-1
T2	72	48	42	87.50%	6
T2	73	36	35	97.22%	1
T2	74	50	47	94.00%	3
T2	75	58	45	77.59%	13

Table C-3: (Continued)

T2	76	42	42	100.00%	0
T2	77	51	48	94.12%	3
T2	78	41	43	104.88%	-2
T2	79	49	47	95.92%	2
T2	80	41	38	92.68%	3
T1	81	50	46	92.00%	4
T1	82	50	47	94.00%	3
T1	83	38	42	110.53%	-4
T1	84	40	43	107.50%	-3
T1	85	42	36	85.71%	6
T1	86	47	45	95.74%	2
T1	87	48	46	95.83%	2
T1	88	48	47	97.92%	1
T1	89	45	38	84.44%	7
T1	90	47	41	87.23%	6
T1	91	47	45	95.74%	2
T1	92	34	36	105.88%	-2
T1	93	48	48	100.00%	0
T1	94	40	40	100.00%	0
T1	95	41	40	97.56%	1
T1	96	39	45	115.38%	-6
T1	97	48	48	100.00%	0
T1	98	28	26	92.86%	2
T1	99	44	42	95.45%	2
T1	100	43	42	97.67%	1
T1	101	47	46	97.87%	1
T1	102	51	45	88.24%	6
T1	103	46	45	97.83%	1
T1	104	44	44	100.00%	0
T1	105	42	45	107.14%	-3
T1	106	42	44	104.76%	-2
T1	107	43	45	104.65%	-2
T1	108	45	42	93.33%	3
T1	109	41	46	112.20%	-5
T1	110	49	46	93.88%	3
T1	111	43	44	102.33%	-1
T1	112	39	38	97.44%	1
T1	113	47	49	104.26%	-2
T1	114	40	37	92.50%	3

Table C-3: (Continued)

T1	115	42	40	95.24%	2
T1	116	47	45	95.74%	2
T1	117	41	41	100.00%	0
T1	118	45	38	84.44%	7
	Mean	44.60	43.39		1.21
	St. Dev.	4.84	4.59		3.68

Table C-4: WB at Geneva Rd and University Parkway, Orem

Lane	Sample No.	Gun Speed	Hi-res Speed	Speed Accuracy	difference
T1	1	42	40	95.24%	2
T1	2	47	55	117.02%	-8
T1	3	45	49	108.89%	-4
T1	4	40	36	90.00%	4
T1	5	50	50	100.00%	0
T1	6	43	43	100.00%	0
T1	7	42	43	102.38%	-1
T1	8	46	41	89.13%	5
T1	9	46	42	91.30%	4
T1	10	38	44	115.79%	-6
T1	11	48	42	87.50%	6
T1	12	46	45	97.83%	1
T1	13	45	48	106.67%	-3
T1	14	40	40	100.00%	0
T1	15	51	50	98.04%	1
T1	16	36	31	86.11%	5
T2	17	41	43	104.88%	-2
T2	18	45	47	104.44%	-2
T2	19	42	38	90.48%	4
T2	20	47	44	93.62%	3
T2	21	45	47	104.44%	-2
T2	22	41	38	92.68%	3
T2	23	51	46	90.20%	5
T2	24	48	42	87.50%	6
T2	25	46	48	104.35%	-2
T2	26	48	50	104.17%	-2
T2	27	44	42	95.45%	2
T2	28	42	40	95.24%	2
T2	29	55	49	89.09%	6
T2	30	43	47	109.30%	-4
T2	31	43	39	90.70%	4
T2	32	48	52	108.33%	-4
T2	33	46	45	97.83%	1
T2	34	50	48	96.00%	2
T2	35	46	45	97.83%	1
T2	36	46	44	95.65%	2

Table C-4: (Continued)

T2	37	45	42	93.33%	3
T2	38	47	45	95.74%	2
T2	39	49	50	102.04%	-1
T2	40	51	52	101.96%	-1
T2	41	56	55	98.21%	1
T2	42	48	44	91.67%	4
T2	43	47	46	97.87%	1
T2	44	46	37	80.43%	9
T2	45	58	54	93.10%	4
T2	46	47	47	100.00%	0
T2	47	39	39	100.00%	0
T2	48	42	43	102.38%	-1
T2	49	48	42	87.50%	6
T2	50	36	35	97.22%	1
T2	51	50	47	94.00%	3
T2	52	58	45	77.59%	13
T2	53	42	42	100.00%	0
T3	54	50	49	98.00%	1
T3	55	45	41	91.11%	4
T3	56	44	46	104.55%	-2
T3	57	42	41	97.62%	1
T3	58	45	40	88.89%	5
T3	59	45	42	93.33%	3
T3	60	50	46	92.00%	4
T3	61	42	45	107.14%	-3
T3	62	43	41	95.35%	2
T3	63	38	40	105.26%	-2
T3	64	41	41	100.00%	0
T3	65	49	46	93.88%	3
T3	66	43	46	106.98%	-3
T3	67	37	41	110.81%	-4
T3	68	40	42	105.00%	-2
T3	69	45	42	93.33%	3
T3	70	45	55	122.22%	-10
T3	71	39	40	102.56%	-1
T3	72	39	37	94.87%	2
T3	73	48	44	91.67%	4
T3	74	47	38	80.85%	9
T3	75	43	42	97.67%	1

Table C-4: (Continued)

T3	76	40	44	110.00%	-4
T3	77	41	41	100.00%	0
T3	78	40	40	100.00%	0
T3	79	53	43	81.13%	10
T3	80	36	36	100.00%	0
T3	81	46	45	97.83%	1
T3	82	48	40	83.33%	8
T3	83	38	40	105.26%	-2
T3	84	49	53	108.16%	-4
T3	85	41	41	100.00%	0
T3	86	36	33	91.67%	3
T3	87	39	48	123.08%	-9
T3	88	51	48	94.12%	3
T3	89	40	41	102.50%	-1
	Mean	44.82	43.78		1.04
	St. Dev.	4.83	4.85		3.93

Table C-5: EB at 3500 South and 2200 West, West Valley City

Lane	Sample No.	Gun Speed	Hi-res Speed	Speed Accuracy	difference
T1	1	39	38	97.44%	1
T1	2	43	42	97.67%	1
T1	3	40	39	97.50%	1
T1	4	40	39	97.50%	1
T1	5	38	36	94.74%	2
T1	6	43	37	86.05%	6
T1	7	45	39	86.67%	6
T1	8	35	34	97.14%	1
T1	9	42	39	92.86%	3
T1	10	49	47	95.92%	2
T1	11	43	43	100.00%	0
T1	12	37	37	100.00%	0
T1	13	42	42	100.00%	0
T1	14	38	45	118.42%	-7
T1	15	44	47	106.82%	-3
T1	16	44	18	40.91%	26
T1	17	35	33	94.29%	2
T1	18	43	39	90.70%	4
T1	19	40	47	117.50%	-7
T1	20	48	46	95.83%	2
T1	21	40	40	100.00%	0
T1	22	45	43	95.56%	2
T1	23	45	42	93.33%	3
T2	24	41	42	102.44%	-1
T2	25	35	37	105.71%	-2
T2	26	33	29	87.88%	4
T2	27	37	29	78.38%	8
T2	28	36	36	100.00%	0
T2	29	43	44	102.33%	-1
T2	30	39	36	92.31%	3
T2	31	34	35	102.94%	-1
T2	32	42	42	100.00%	0
T2	33	43	42	97.67%	1
T2	34	38	36	94.74%	2
T2	35	45	39	86.67%	6
T2	36	36	54	150.00%	-18

Table C-5: (Continued)

T2	37	35	35	100.00%	0
T2	38	33	27	81.82%	6
T2	39	42	39	92.86%	3
T2	40	38	38	100.00%	0
T2	41	39	38	97.44%	1
T2	42	33	31	93.94%	2
T2	43	33	37	112.12%	-4
T2	44	41	41	100.00%	0
T2	45	46	44	95.65%	2
T2	46	30	31	103.33%	-1
T2	47	33	28	84.85%	5
T2	48	35	34	97.14%	1
T2	49	35	34	97.14%	1
T2	50	44	42	95.45%	2
T2	51	43	40	93.02%	3
T2	52	31	29	93.55%	2
T2	53	54	52	96.30%	2
T2	54	43	42	97.67%	1
T2	55	37	45	121.62%	-8
T2	56	44	42	95.45%	2
T2	57	39	42	107.69%	-3
T2	58	40	41	102.50%	-1
T2	59	46	47	102.17%	-1
T3	60	34	32	94.12%	2
T3	61	26	28	107.69%	-2
T3	62	28	28	100.00%	0
T3	63	29	34	117.24%	-5
T3	64	29	26	89.66%	3
T3	65	31	24	77.42%	7
T3	66	27	29	107.41%	-2
T3	67	35	31	88.57%	4
T3	68	28	33	117.86%	-5
T3	69	33	28	84.85%	5
T3	70	28	26	92.86%	2
T3	71	33	33	100.00%	0
T3	72	36	35	97.22%	1
T3	73	31	31	100.00%	0
T3	74	33	31	93.94%	2
T3	75	33	32	96.97%	1

Table C-5: (Continued)

T3	76	32	34	106.25%	-2
T3	77	32	30	93.75%	2
T3	78	33	35	106.06%	-2
T3	79	34	37	108.82%	-3
T3	80	37	36	97.30%	1
T3	81	30	30	100.00%	0
T3	82	37	40	108.11%	-3
T3	83	30	31	103.33%	-1
	Mean	37.51	36.70		0.81
	St. Dev.	5.79	6.58		4.58

Table C-6: WB at 400 East and 800 North, Orem

Lane	Sample No.	Gun Speed	Hi-res Speed	Speed Accuracy	difference
T1	1	44	44	100.00%	0
T1	2	39	43	110.26%	-4
T1	3	47	50	106.38%	-3
T1	4	45	48	106.67%	-3
T1	5	44	45	102.27%	-1
T1	6	42	43	102.38%	-1
T1	7	38	40	105.26%	-2
T1	8	31	34	109.68%	-3
T1	9	53	52	98.11%	1
T1	10	45	48	106.67%	-3
T1	11	42	50	119.05%	-8
T1	12	46	47	102.17%	-1
T1	13	46	55	119.57%	-9
T1	14	47	47	100.00%	0
T1	15	42	41	97.62%	1
T1	16	48	51	106.25%	-3
T1	17	46	46	100.00%	0
T1	18	40	46	115.00%	-6
T1	19	41	40	97.56%	1
T2	20	45	45	100.00%	0
T2	21	44	45	102.27%	-1
T2	22	48	49	102.08%	-1
T2	23	42	41	97.62%	1
T2	24	45	49	108.89%	-4
T2	25	50	50	100.00%	0
T2	26	54	51	94.44%	3
T2	27	47	50	106.38%	-3
T2	28	46	47	102.17%	-1
T2	29	52	54	103.85%	-2
T2	30	40	44	110.00%	-4
T2	31	42	49	116.67%	-7
T2	32	47	46	97.87%	1
T2	33	44	41	93.18%	3
T2	34	36	38	105.56%	-2
T2	35	47	46	97.87%	1
T2	36	57	59	103.51%	-2

Table C-6: (Continued)

T2	37	39	43	110.26%	-4
T2	38	46	44	95.65%	2
T2	39	44	41	93.18%	3
T2	40	48	49	102.08%	-1
T2	41	47	49	104.26%	-2
T2	42	48	50	104.17%	-2
T2	43	45	49	108.89%	-4
T2	44	46	45	97.83%	1
T2	45	53	53	100.00%	0
T2	46	49	55	112.24%	-6
T3	47	48	47	97.92%	1
T3	48	43	43	100.00%	0
T3	49	49	53	108.16%	-4
T3	50	49	47	95.92%	2
T3	51	49	50	102.04%	-1
T3	52	42	43	102.38%	-1
T3	53	39	46	117.95%	-7
T3	54	45	43	95.56%	2
T3	55	39	40	102.56%	-1
T3	56	33	32	96.97%	1
T3	57	44	44	100.00%	0
T3	58	41	38	92.68%	3
T3	59	47	46	97.87%	1
T3	60	44	45	102.27%	-1
T3	61	39	55	141.03%	-16
T3	62	41	40	97.56%	1
T3	63	39	45	115.38%	-6
T3	64	66	48	72.73%	18
	Mean	44.91	46.20		-1.30
	St. Dev.	5.43	5.06		4.12

Table C-7: NB at 1320 South and State St, Provo

Lane	Sample No.	Gun Speed	Hi-res Speed	Speed Accuracy	difference
T1	1	41	40	102.50%	1
T1	2	45	47	95.74%	-2
T1	3	47	46	102.17%	1
T1	4	45	49	91.84%	-4
T1	5	42	45	93.33%	-3
T1	6	51	51	100.00%	0
T1	7	50	48	104.17%	2
T1	8	47	48	97.92%	-1
T1	9	46	40	115.00%	6
T1	10	48	46	104.35%	2
T1	11	45	46	97.83%	-1
T1	12	44	44	100.00%	0
T1	13	47	44	106.82%	3
T1	14	42	42	100.00%	0
T1	15	50	49	102.04%	1
T1	16	39	42	92.86%	-3
T1	17	48	47	102.13%	1
T1	18	47	55	85.45%	-8
T1	19	46	46	100.00%	0
T1	20	51	47	108.51%	4
T1	21	52	54	96.30%	-2
T1	22	50	49	102.04%	1
T1	23	52	54	96.30%	-2
T2	24	49	49	100.00%	0
T2	25	46	46	100.00%	0
T2	26	45	47	95.74%	-2
T2	27	49	50	98.00%	-1
T2	28	47	47	100.00%	0
T2	29	40	45	88.89%	-5
T2	30	41	41	100.00%	0
T2	31	39	45	86.67%	-6
T2	32	45	47	95.74%	-2
T2	33	44	44	100.00%	0
T2	34	48	47	102.13%	1
T2	35	45	48	93.75%	-3
T2	36	38	40	95.00%	-2

Table C-7: (Continued)

T2	37	45	46	97.83%	-1
T2	38	48	48	100.00%	0
T2	39	46	47	97.87%	-1
T2	40	47	46	102.17%	1
T2	41	52	53	98.11%	-1
T2	42	45	46	97.83%	-1
T2	43	50	53	94.34%	-3
T2	44	57	51	111.76%	6
T2	45	44	45	97.78%	-1
T2	46	38	40	95.00%	-2
T2	47	49	50	98.00%	-1
T2	48	41	41	100.00%	0
T2	49	48	48	100.00%	0
T2	50	49	50	98.00%	-1
T2	51	38	38	100.00%	0
T2	52	44	44	100.00%	0
T2	53	40	42	95.24%	-2
T2	54	45	44	102.27%	1
	Mean	45.87	46.43		-0.56
	St. Dev.	4.12	3.86		2.44

Table C-8: WB at 9000 South and 700 West, Sandy

Lane	Sample No.	Gun Speed	Hi-res Speed	Speed Accuracy	difference
T1	1	42	40	95.24%	2
T1	2	47	55	117.02%	-8
T1	3	45	49	108.89%	-4
T1	4	40	36	90.00%	4
T1	5	50	50	100.00%	0
T1	6	43	43	100.00%	0
T1	7	42	43	102.38%	-1
T1	8	46	41	89.13%	5
T1	9	46	42	91.30%	4
T1	10	38	44	115.79%	-6
T1	11	48	42	87.50%	6
T1	12	46	45	97.83%	1
T1	13	45	48	106.67%	-3
T1	14	40	40	100.00%	0
T1	15	51	50	98.04%	1
T1	16	36	31	86.11%	5
T2	17	48	46	104.35%	2
T2	18	50	45	111.11%	5
T2	19	39	39	100.00%	0
T2	20	43	45	95.56%	-2
T2	21	39	35	111.43%	4
T2	22	40	39	102.56%	1
T2	23	49	48	102.08%	1
T2	24	43	43	100.00%	0
T2	25	49	47	104.26%	2
T2	26	44	43	102.33%	1
T2	27	46	49	93.88%	-3
T2	28	40	40	100.00%	0
T2	29	44	42	104.76%	2
T2	30	41	41	100.00%	0
T2	31	43	43	100.00%	0
T2	32	39	45	86.67%	-6
T2	33	44	46	95.65%	-2
T2	34	43	42	102.38%	1
T2	35	43	42	102.38%	1
T2	36	50	52	96.15%	-2

Table C-8: (Continued)

T2	37	43	48	89.58%	-5
T3	38	45	45	100.00%	0
T3	39	39	38	102.63%	1
T3	40	39	45	86.67%	-6
T3	41	44	39	112.82%	5
T3	42	45	44	102.27%	1
T3	43	47	55	85.45%	-8
T3	44	41	39	105.13%	2
T3	45	37	42	88.10%	-5
T3	46	50	48	104.17%	2
T3	47	41	46	89.13%	-5
T3	48	48	55	87.27%	-7
T3	49	39	39	100.00%	0
T3	50	41	49	83.67%	-8
T3	51	35	43	81.40%	-8
	Mean	43.45	44.04		-0.59
	St. Dev.	4.02	4.97		3.83

Table C-9: WB at 3500 South and 2200 West, West Valley City

Lane	Sample No.	Gun Speed	Hi-res Speed	Speed Accuracy	difference
T1	1	38	33	86.84%	5
T1	2	43	42	97.67%	1
T1	3	35	36	102.86%	-1
T1	4	50	49	98.00%	1
T1	5	42	42	100.00%	0
T1	6	40	38	95.00%	2
T1	7	33	38	115.15%	-5
T1	8	40	38	95.00%	2
T1	9	39	40	102.56%	-1
T2	10	43	39	90.70%	4
T2	11	40	40	100.00%	0
T2	12	47	35	74.47%	12
T2	13	36	34	94.44%	2
T2	14	48	47	97.92%	1
T2	15	42	43	102.38%	-1
T2	16	41	40	97.56%	1
T2	17	38	42	110.53%	-4
T2	18	42	36	85.71%	6
T2	19	40	42	105.00%	-2
T2	20	35	37	105.71%	-2
T2	21	38	37	97.37%	1
T2	22	38	34	89.47%	4
T2	23	42	42	100.00%	0
T2	24	40	39	97.50%	1
T2	25	35	37	105.71%	-2
T2	26	36	35	97.22%	1
T3	27	26	27	103.85%	-1
T3	28	31	35	112.90%	-4
T3	29	34	33	97.06%	1
T3	30	42	42	100.00%	0
T3	31	45	45	100.00%	0
T3	32	41	49	119.51%	-8
T3	33	35	45	128.57%	-10
T3	34	31	32	103.23%	-1
T3	35	32	35	109.38%	-3
T3	36	34	42	123.53%	-8

Table C-9: (Continued)

T3	37	44	44	100.00%	0
T3	38	34	32	94.12%	2
T3	39	44	42	95.45%	2
T3	40	45	34	75.56%	11
T3	41	40	38	95.00%	2
T3	42	38	36	94.74%	2
T3	43	27	23	85.19%	4
T3	44	35	40	114.29%	-5
T3	45	37	40	108.11%	-3
	Mean	38.58	38.42		0.16
	St. Dev.	5.18	5.20		4.14

Table C-10: NB at 800 North and Geneva Rd, Orem

Lane	Sample No.	Gun Speed	Hi-res Speed	Speed Accuracy	difference
T1	1	46	45	97.83%	1
T1	2	53	49	92.45%	4
T1	3	58	45	77.59%	13
T1	4	46	45	97.83%	1
T1	5	50	47	94.00%	3
T1	6	50	49	98.00%	1
T1	7	50	48	96.00%	2
T1	8	49	48	97.96%	1
T1	9	45	46	102.22%	-1
T1	10	54	50	92.59%	4
T1	11	39	38	97.44%	1
T1	12	52	52	100.00%	0
T1	13	44	43	97.73%	1
T1	14	50	48	96.00%	2
T1	15	47	46	97.87%	1
T1	16	54	52	96.30%	2
T1	17	54	52	96.30%	2
T1	18	53	55	103.77%	-2
T1	19	53	51	96.23%	2
T1	20	47	49	104.26%	-2
T2	21	59	51	86.44%	8
T2	22	35	33	94.29%	2
T2	23	45	42	93.33%	3
T2	24	34	36	105.88%	-2
T2	25	45	43	95.56%	2
T2	26	50	49	98.00%	1
T2	27	46	45	97.83%	1
T2	28	39	41	105.13%	-2
T2	29	38	37	97.37%	1
T2	30	38	40	105.26%	-2
T2	31	36	36	100.00%	0
T2	32	39	40	102.56%	-1
T2	33	40	37	92.50%	3
T2	34	44	45	102.27%	-1
T2	35	40	40	100.00%	0
T2	36	46	44	95.65%	2

Table C-10: (Continued)

T2	37	45	44	97.78%	1
T2	38	40	41	102.50%	-1
T2	39	39	39	100.00%	0
T2	40	48	44	91.67%	4
T2	41	43	41	95.35%	2
T2	42	40	44	110.00%	-4
T2	43	47	48	102.13%	-1
T2	44	37	36	97.30%	1
	Mean	45.61	44.41		1.20
	St. Dev.	6.31	5.24		2.78

Table C-11: SB at University Avenue and University Parkway, Provo

Lane	Sample No.	Gun Speed	Hi-res Speed	Speed Accuracy	difference
T1	1	38	41	92.68%	-3
T1	2	42	40	105.00%	2
T1	3	43	41	104.88%	2
T1	4	34	38	89.47%	-4
T1	5	42	41	102.44%	1
T1	6	41	45	91.11%	-4
T1	7	41	41	100.00%	0
T1	8	42	43	97.67%	-1
T1	9	42	39	107.69%	3
T1	10	43	41	104.88%	2
T1	11	43	44	97.73%	-1
T1	12	48	42	114.29%	6
T1	13	41	39	105.13%	2
T1	14	33	32	103.13%	1
T1	15	33	33	100.00%	0
T1	16	40	39	102.56%	1
T2	17	36	36	100.00%	0
T2	18	43	42	102.38%	1
T2	19	37	37	100.00%	0
T2	20	44	44	100.00%	0
T2	21	38	39	97.44%	-1
T2	22	37	37	100.00%	0
T2	23	36	42	85.71%	-6
T2	24	42	42	100.00%	0
T2	25	42	42	100.00%	0
T2	26	36	38	94.74%	-2
T2	27	39	39	100.00%	0
T2	28	34	34	100.00%	0
T2	29	40	42	95.24%	-2
T2	30	29	31	93.55%	-2
T2	31	40	40	100.00%	0
T2	32	41	40	102.50%	1
T2	33	38	40	95.00%	-2
T2	34	41	43	95.35%	-2
T2	35	40	42	95.24%	-2
T2	36	38	43	88.37%	-5

Table C-11: (Continued)

	Mean	39.36	39.78		-0.42
	St. Dev.	3.80	3.35		2.32

Table C-12: NB at 3300 North and University Parkway, Provo

Lane	Sample No.	Gun Speed	Hi-res Speed	Speed Accuracy	difference
T1	1	52	50	104.00%	2
T1	2	52	48	108.33%	4
T1	3	47	40	117.50%	7
T1	4	46	43	106.98%	3
T1	5	48	45	106.67%	3
T1	6	39	38	102.63%	1
T1	7	48	45	106.67%	3
T1	8	52	50	104.00%	2
T1	9	49	46	106.52%	3
T1	10	48	48	100.00%	0
T1	11	40	36	111.11%	4
T1	12	54	50	108.00%	4
T1	13	50	45	111.11%	5
T1	14	49	48	102.08%	1
T1	15	49	50	98.00%	-1
T1	16	49	50	98.00%	-1
T2	17	29	34	85.29%	-5
T2	18	39	36	108.33%	3
T2	19	42	39	107.69%	3
T2	20	49	49	100.00%	0
T2	21	42	41	102.44%	1
T2	22	35	35	100.00%	0
T2	23	46	45	102.22%	1
T2	24	55	49	112.24%	6
T2	25	47	45	104.44%	2
T2	26	48	38	126.32%	10
T2	27	46	43	106.98%	3
T2	28	43	44	97.73%	-1
T2	29	55	51	107.84%	4
T2	30	47	50	94.00%	-3
T2	31	40	39	102.56%	1
T2	32	47	44	106.82%	3
	Mean	46.31	44.19		2.13
	St. Dev.	5.77	5.17		2.87

Table C-13: SB at Geneva Rd and University Parkway, Orem

Lane	Sample No.	Gun Speed	Hi-res Speed	Speed Accuracy	difference
T1	1	43	41	95.35%	2
T1	2	51	47	92.16%	4
T1	3	40	38	95.00%	2
T1	4	41	41	100.00%	0
T1	5	35	38	108.57%	-3
T1	6	53	49	92.45%	4
T1	7	41	39	95.12%	2
T1	8	52	53	101.92%	-1
T1	9	33	27	81.82%	6
T1	10	35	36	102.86%	-1
T1	11	38	40	105.26%	-2
T1	12	45	42	93.33%	3
T1	13	48	45	93.75%	3
T1	14	40	40	100.00%	0
T1	15	42	41	97.62%	1
T1	16	37	35	94.59%	2
T1	17	36	37	102.78%	-1
T1	18	41	37	90.24%	4
T2	19	43	40	93.02%	3
T2	20	49	49	100.00%	0
T2	21	41	43	104.88%	-2
T2	22	37	40	108.11%	-3
T2	23	36	37	102.78%	-1
T2	24	41	43	104.88%	-2
T2	25	38	36	94.74%	2
T2	26	41	40	97.56%	1
T2	27	40	40	100.00%	0
T2	28	48	46	95.83%	2
T2	29	35	35	100.00%	0
T2	30	47	46	97.87%	1
	Mean	41.57	40.70		0.87
	St. Dev.	5.42	5.17		2.27

Table C-14: NB at Geneva Rd and University Parkway, Orem

Lane	Sample No.	Gun Speed	Hi-res Speed	Speed Accuracy	difference
T1	1	37	34	108.82%	3
T1	2	46	46	100.00%	0
T1	3	36	37	97.30%	-1
T1	4	41	41	100.00%	0
T1	5	40	41	97.56%	-1
T1	6	35	33	106.06%	2
T1	7	40	43	93.02%	-3
T1	8	35	38	92.11%	-3
T1	9	43	42	102.38%	1
T1	10	31	30	103.33%	1
T1	11	39	40	97.50%	-1
T1	12	37	33	112.12%	4
T1	13	31	28	110.71%	3
T1	14	35	35	100.00%	0
T1	15	34	34	100.00%	0
T1	16	29	30	96.67%	-1
T1	17	42	44	95.45%	-2
T1	18	47	46	102.17%	1
	Mean	37.67	37.50		0.17
	St. Dev.	5.03	5.65		1.98

APPENDIX D: RESULTS OF PAIRED T-TEST FOR MEANS

Table D-1: EB at 9000 South and 700 West, Sandy, Results of Paired t-Test

	<i>Variable 1</i>	<i>Variable 2</i>
Mean	46.093	43.891
Variance	20.569	29.207
Observations	129	129
Pearson Correlation	0.663713082	
Hypothesized Mean Difference	0	
df	128	
t Stat	6.022141401	
P(T<=t) one-tail	8.50635E-09	
t Critical one-tail	1.656845226	
P(T<=t) two-tail	1.70127E-08	
t Critical two-tail	1.97867085	

Table D-2: SB at 1320 South and State St, Provo, Results of Paired t-Test

	<i>Variable 1</i>	<i>Variable 2</i>
Mean	48.576	48.144
Variance	31.649	29.850
Observations	125	125
Pearson Correlation	0.557188399	
Hypothesized Mean Difference	0	
Df	124	
t Stat	0.925287254	
P(T<=t) one-tail	0.178306876	
t Critical one-tail	1.65723497	
P(T<=t) two-tail	0.356613753	
t Critical two-tail	1.979280117	

Table D-3: EB at 400 East and 800 North, Orem, Results of Paired t-Test

	<i>Variable 1</i>	<i>Variable 2</i>
Mean	44.602	43.390
Variance	23.404	21.060
Observations	118	118
Pearson Correlation	0.696162375	
Hypothesized Mean Difference	0	
df	117	
t Stat	3.575831019	
P(T<=t) one-tail	0.000254332	
t Critical one-tail	1.657981659	
P(T<=t) two-tail	0.000508664	
t Critical two-tail	1.980447599	

Table D-4: WB at Geneva Rd and University Pkwy, Orem, Results of Paired t-Test

	<i>Variable 1</i>	<i>Variable 2</i>
Mean	44.820	43.775
Variance	23.285	23.540
Observations	89	89
Pearson Correlation	0.67097757	
Hypothesized Mean Difference	0	
Df	88	
t Stat	2.511471345	
P(T<=t) one-tail	0.006924152	
t Critical one-tail	1.662354029	
P(T<=t) two-tail	0.013848303	
t Critical two-tail	1.987289865	

Table D-5: EB at 3500 South and 2200 West, West Valley City, Results of Paired t-Test

	<i>Variable 1</i>	<i>Variable 2</i>
Mean	37.506	36.699
Variance	33.497	43.359
Observations	83	83
Pearson Correlation	0.732675019	
Hypothesized Mean Difference	0	
df	82	
t Stat	1.604392685	
P(T<=t) one-tail	0.056236194	
t Critical one-tail	1.663649184	
P(T<=t) two-tail	0.112472388	
t Critical two-tail	1.989318557	

Table D-6: WB at 400 East and 800 North, Orem, Results of Paired t-Test

	<i>Variable 1</i>	<i>Variable 2</i>
Mean	44.906	46.203
Variance	29.515	25.593
Observations	64	64
Pearson Correlation	0.694323366	
Hypothesized Mean Difference	0	
df	63	
t Stat	-2.52059486	
P(T<=t) one-tail	0.007130259	
t Critical one-tail	1.669402222	
P(T<=t) two-tail	0.014260519	
t Critical two-tail	1.998340543	

Table D-7: NB at 1320 South and State St, Provo, Results of Paired t-Test

	<i>Variable 1</i>	<i>Variable 2</i>
Mean	45.870	46.426
Variance	16.945	14.891
Observations	54	54
Pearson Correlation	0.814811739	
Hypothesized Mean Difference	0	
df	53	
t Stat	-1.67369905	
P(T<=t) one-tail	0.05004122	
t Critical one-tail	1.674116237	
P(T<=t) two-tail	0.10008244	
t Critical two-tail	2.005745995	

Table D-8: WB at 9000 South and 700 West, Sandy, Results of Paired t-Test

	<i>Variable 1</i>	<i>Variable 2</i>
Mean	43.451	44.039
Variance	16.173	24.718
Observations	51	51
Pearson Correlation	0.655294622	
Hypothesized Mean Difference	0	
df	50	
t Stat	-1.09614687	
P(T<=t) one-tail	0.139133083	
t Critical one-tail	1.675905025	
P(T<=t) two-tail	0.278266166	
t Critical two-tail	2.008559112	

Table D-9: WB at 3500 South and 2200 West, West Valley City, Results of Paired t-Test

	<i>Variable 1</i>	<i>Variable 2</i>
Mean	38.578	38.422
Variance	26.795	27.068
Observations	45	45
Pearson Correlation	0.681896822	
Hypothesized Mean Difference	0	
df	44	
t Stat	0.252091411	
P(T<=t) one-tail	0.401072132	
t Critical one-tail	1.680229977	
P(T<=t) two-tail	0.802144265	
t Critical two-tail	2.015367574	

Table D-10: NB at 800 North and Geneva Rd, Orem, Results of Paired t-Test

	<i>Variable 1</i>	<i>Variable 2</i>
Mean	45.614	44.409
Variance	39.824	27.410
Observations	44	44
Pearson Correlation	0.900240501	
Hypothesized Mean Difference	0	
df	43	
t Stat	2.87050247	
P(T<=t) one-tail	0.003167012	
t Critical one-tail	1.681070703	
P(T<=t) two-tail	0.006334025	
t Critical two-tail	2.016692199	

Table D-11: SB at University Ave and University Pkwy, Provo, Results of Paired t-Test

	<i>Variable 1</i>	<i>Variable 2</i>
Mean	39.361	39.778
Variance	14.409	11.206
Observations	36	36
Pearson Correlation	0.795708419	
Hypothesized Mean Difference	0	
df	35	
t Stat	-1.07654094	
P(T<=t) one-tail	0.144525093	
t Critical one-tail	1.689572458	
P(T<=t) two-tail	0.289050186	
t Critical two-tail	2.030107928	

Table D-12: NB at 3300 North and University Ave, Provo, Results of Paired t-Test

	<i>Variable 1</i>	<i>Variable 2</i>
Mean	46.313	44.188
Variance	33.319	26.738
Observations	32	32
Pearson Correlation	0.86799004	
Hypothesized Mean Difference	0	
df	31	
t Stat	4.187157703	
P(T<=t) one-tail	0.000108285	
t Critical one-tail	1.695518783	
P(T<=t) two-tail	0.00021657	
t Critical two-tail	2.039513446	

Table D-13: SB at Geneva Rd and University Pkwy, Orem, Results of Paired t-Test

	<i>Variable 1</i>	<i>Variable 2</i>
Mean	41.567	40.700
Variance	29.426	26.700
Observations	30	30
Pearson Correlation	0.90924461	
Hypothesized Mean Difference	0	
df	29	
t Stat	2.090930246	
P(T<=t) one-tail	0.022703792	
t Critical one-tail	1.699127027	
P(T<=t) two-tail	0.045407584	
t Critical two-tail	2.045229642	

Table D-14: NB at Geneva Rd and University Pkwy, Orem

	<i>Variable 1</i>	<i>Variable 2</i>
Mean	37.667	37.500
Variance	25.294	31.912
Observations	18	18
Pearson Correlation	0.937916342	
Hypothesized Mean Difference	0	
df	17	
t Stat	0.357518599	
P(T<=t) one-tail	0.362551807	
t Critical one-tail	1.739606726	
P(T<=t) two-tail	0.725103614	
t Critical two-tail	2.109815578	

**APPENDIX E: RESULTS OF BOOTSTRAPPING METHOD ON 85TH PERCENTILE
SPEEDS**

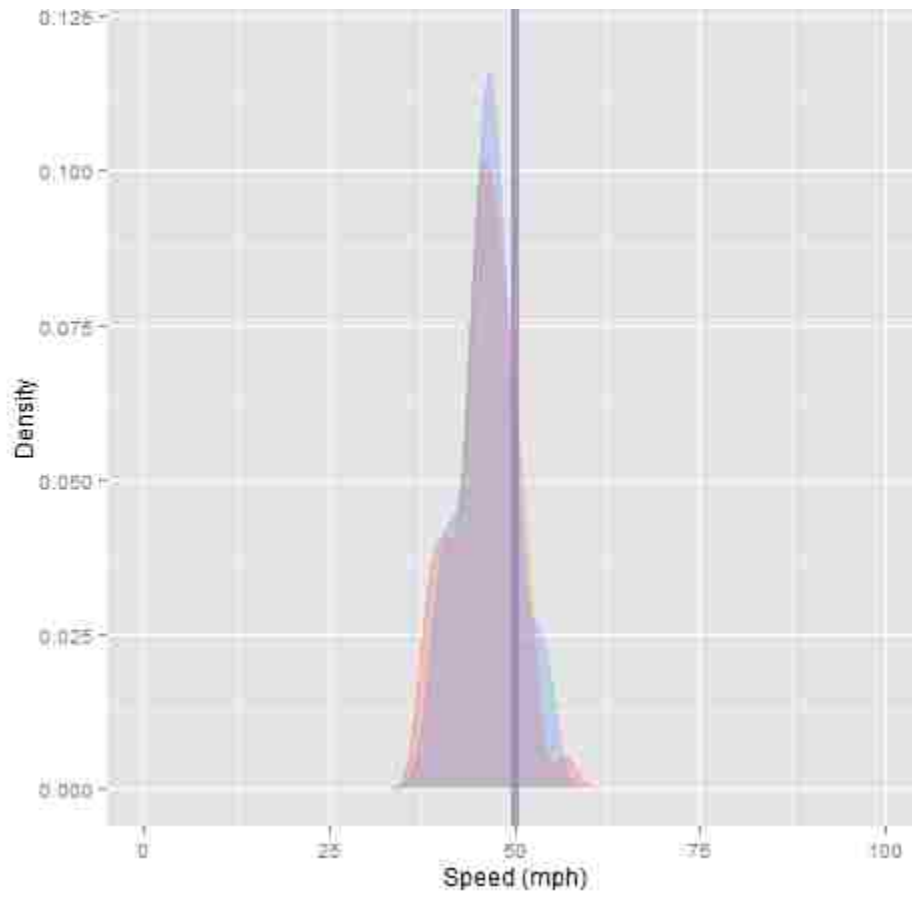


Figure E-1(a). Speed Distribution for Approach 1, NB at 1320 South and State St, Provo.

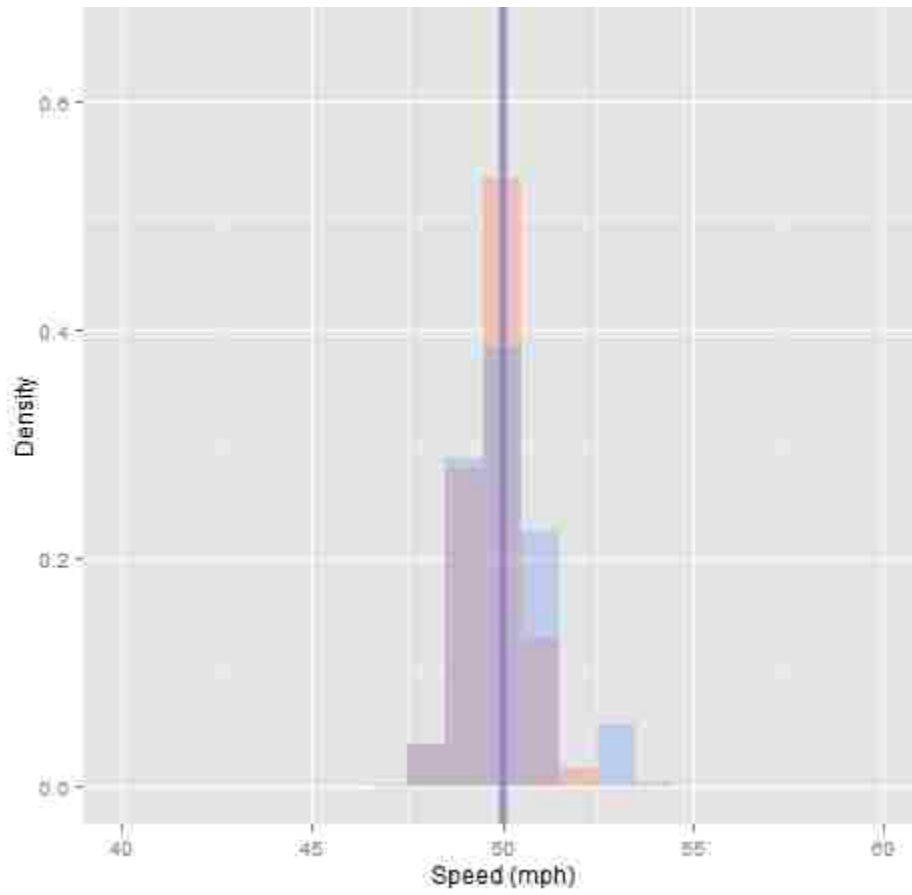


Figure E-1(b). 85th Percentile Speed Distribution for Approach 1, NB at 1320 South and State St, Provo.

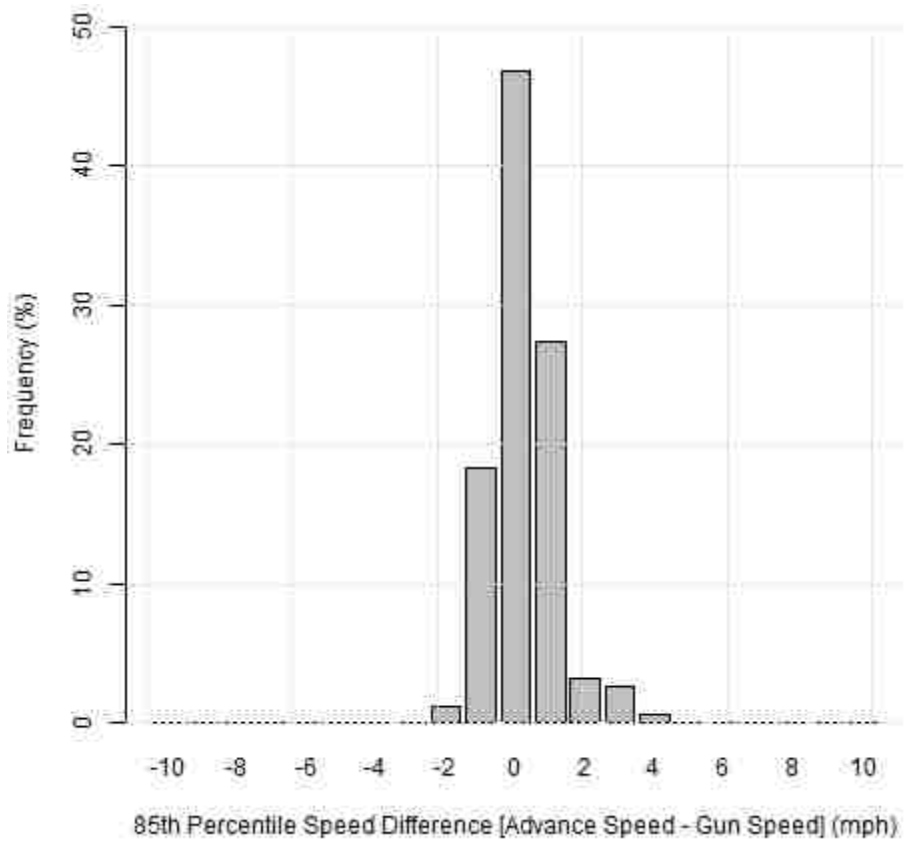


Figure E-1(c). Expected 85% Difference Distribution for Approach 1, NB at 1320 South and State St, Provo.

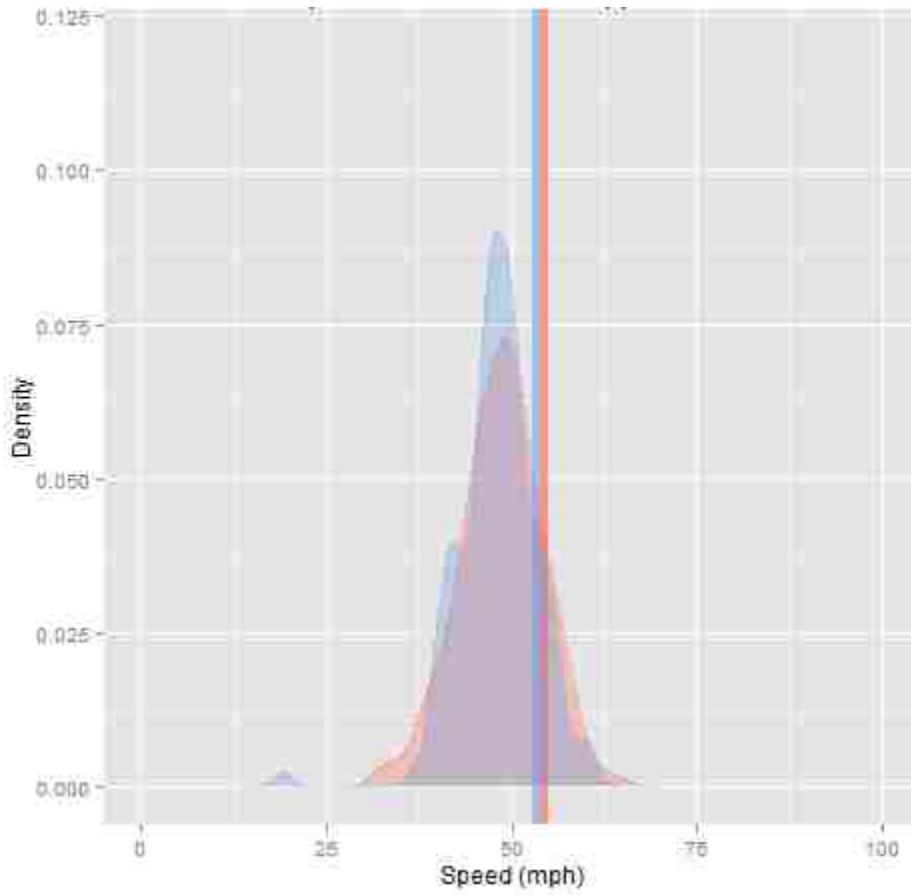


Figure E-2(a). Speed Distribution for Approach 2, SB at 1320 South and State St, Provo.

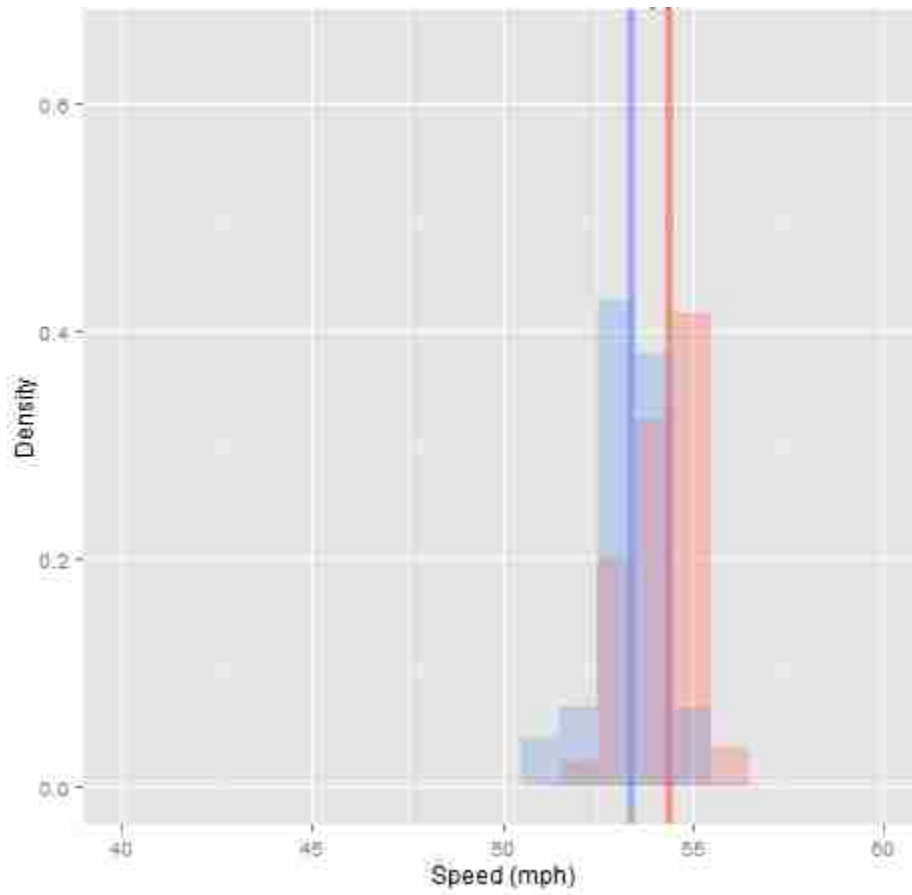


Figure E-2(b). 85th Percentile Speed Distribution for Approach 2, SB at 1320 South and State St, Provo.

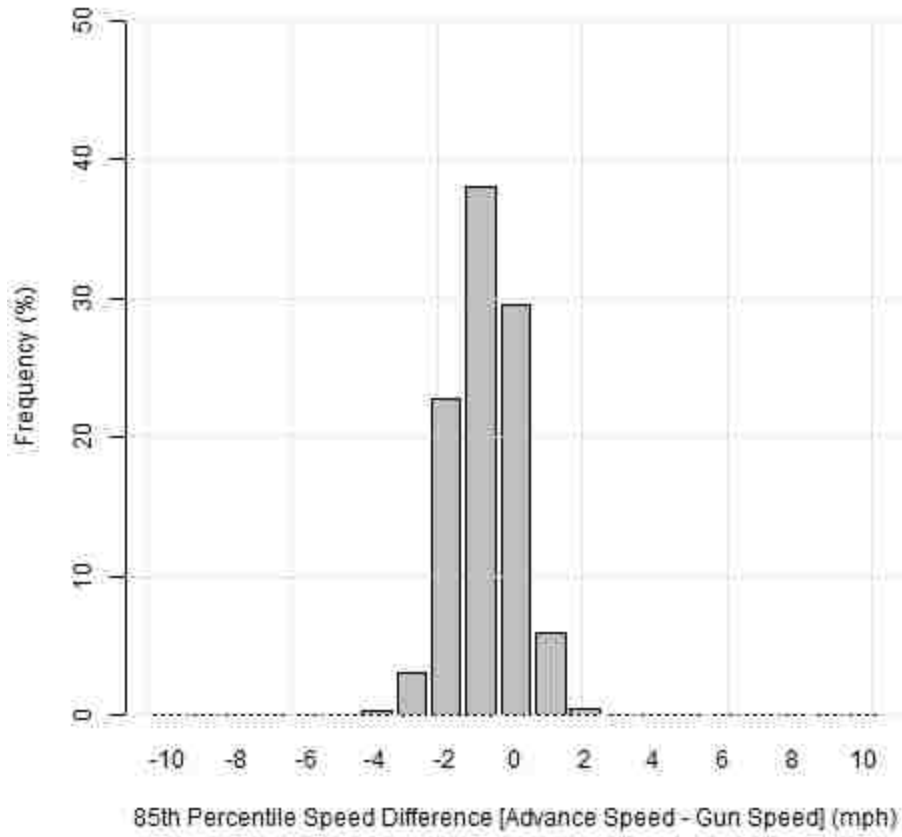


Figure E-2(c). Expected 85% Difference Distribution for Approach 2, SB at 1320 South and State St, Provo.

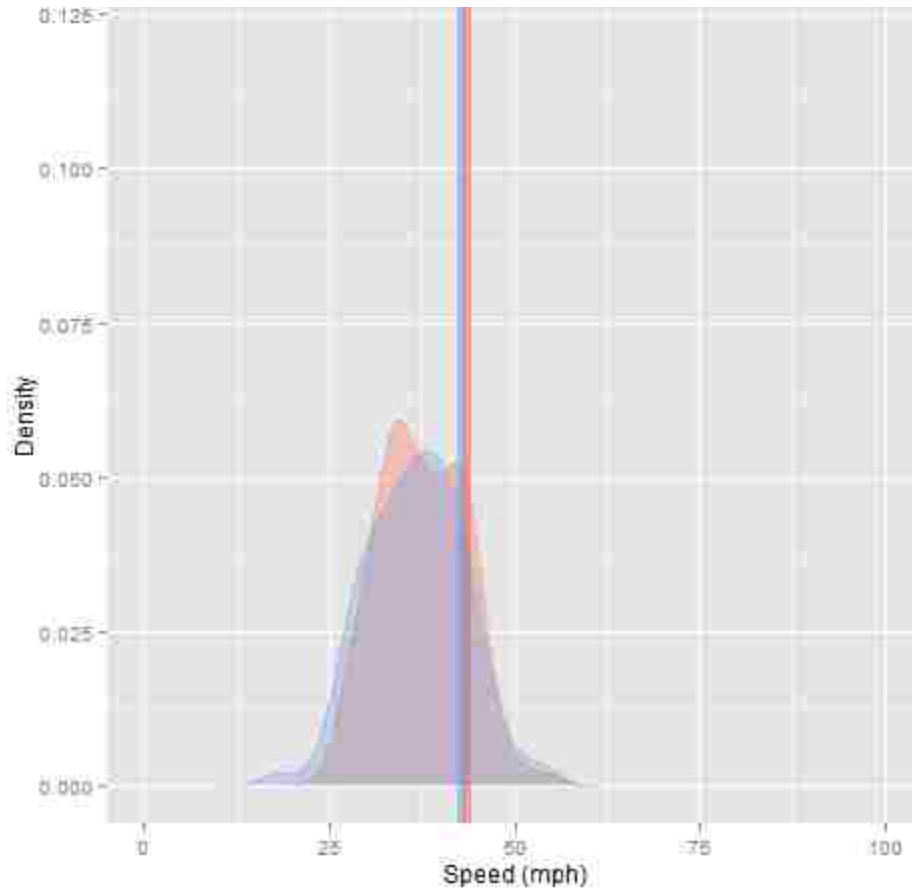


Figure E-3(a). Speed Distribution for Approach 3, EB at 3500 South and 2200 West, West Valley City.

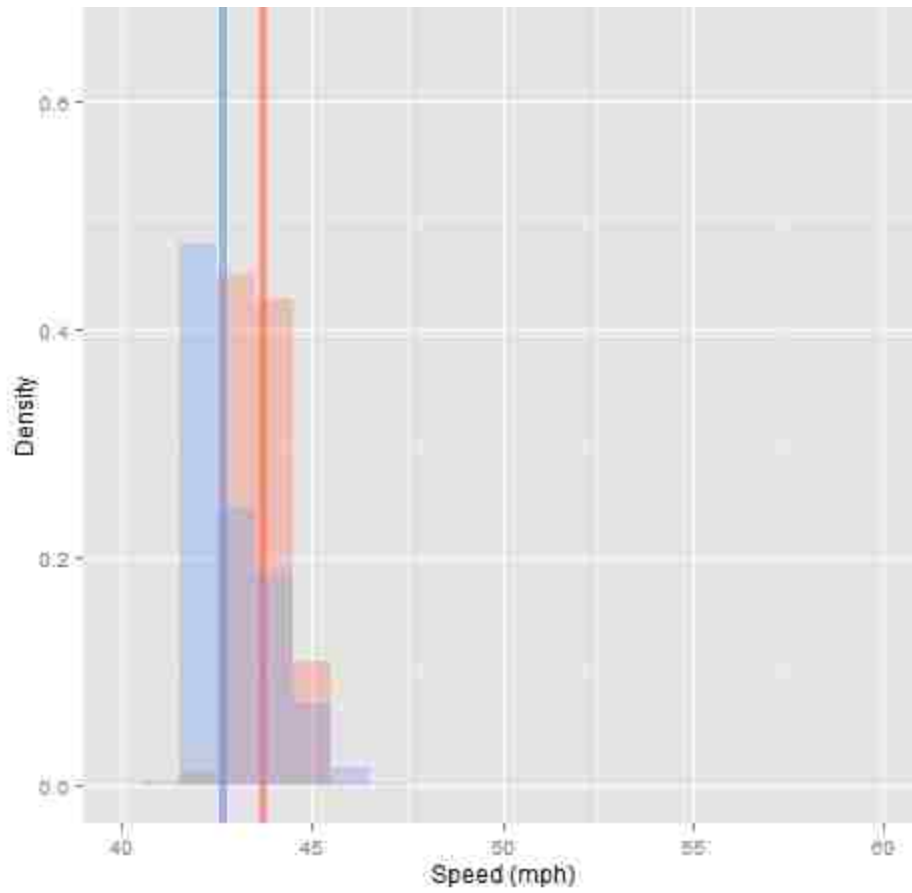


Figure E-3(b). 85th Percentile Speed Distribution for Approach 3, EB at 3500 South and 2200 West, West Valley City.

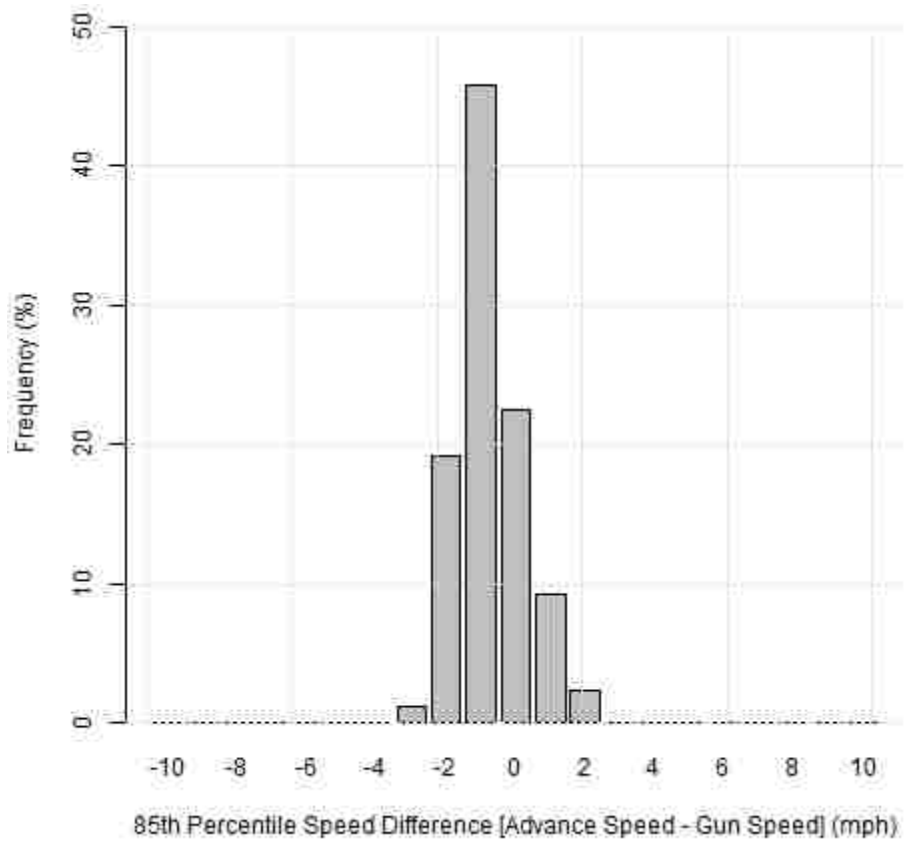


Figure E-3(c). Expected 85% Difference Distribution for Approach 3, EB at 3500 South and 2200 West, West Valley City.

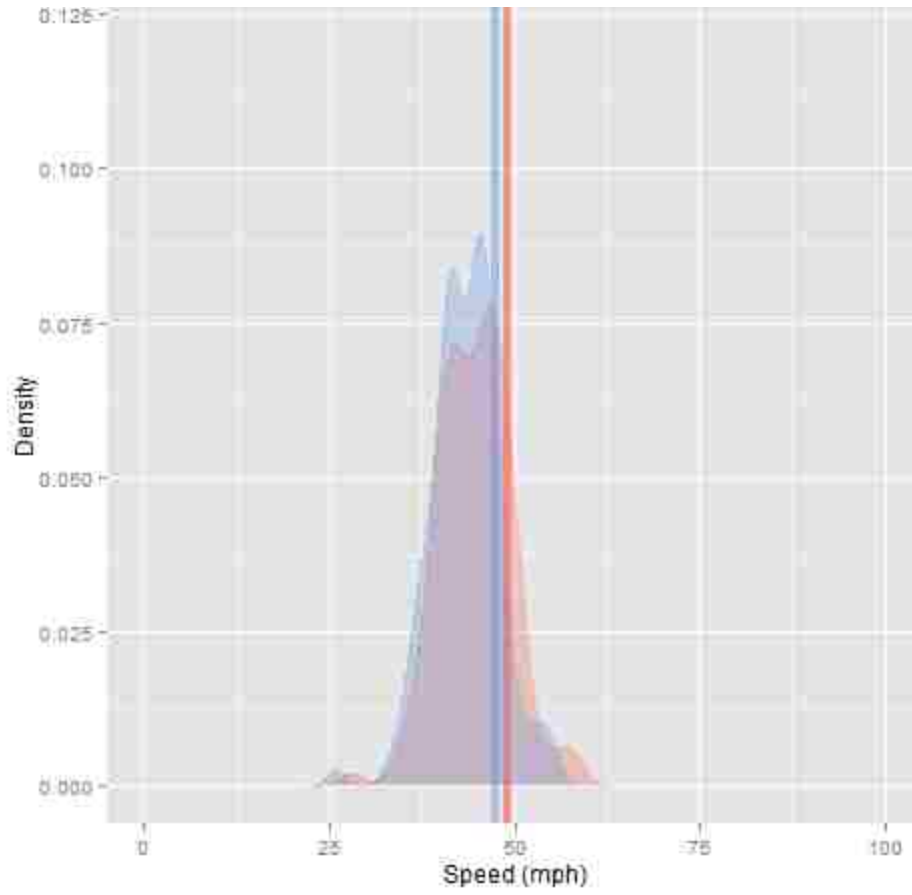


Figure E-4(a). Speed Distribution for Approach 4, EB at 400 East and 800 North, Orem.

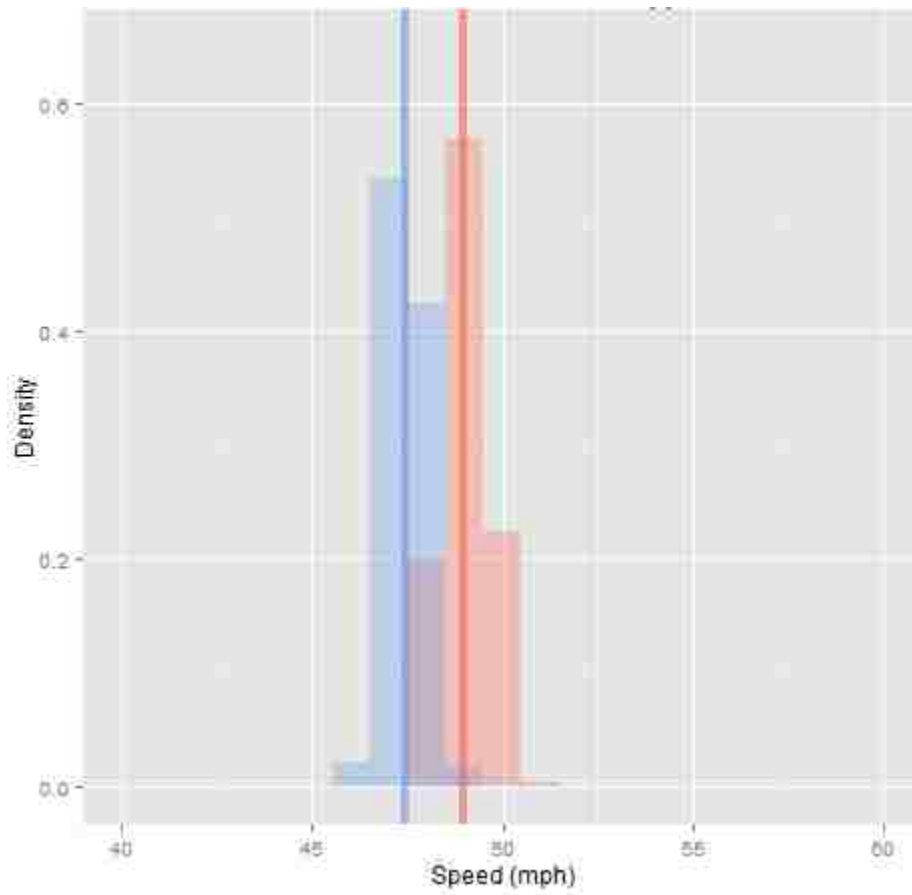


Figure E-4(b). 85th Percentile Speed Distribution for Approach 4, EB at 400 East and 800 North, Orem.

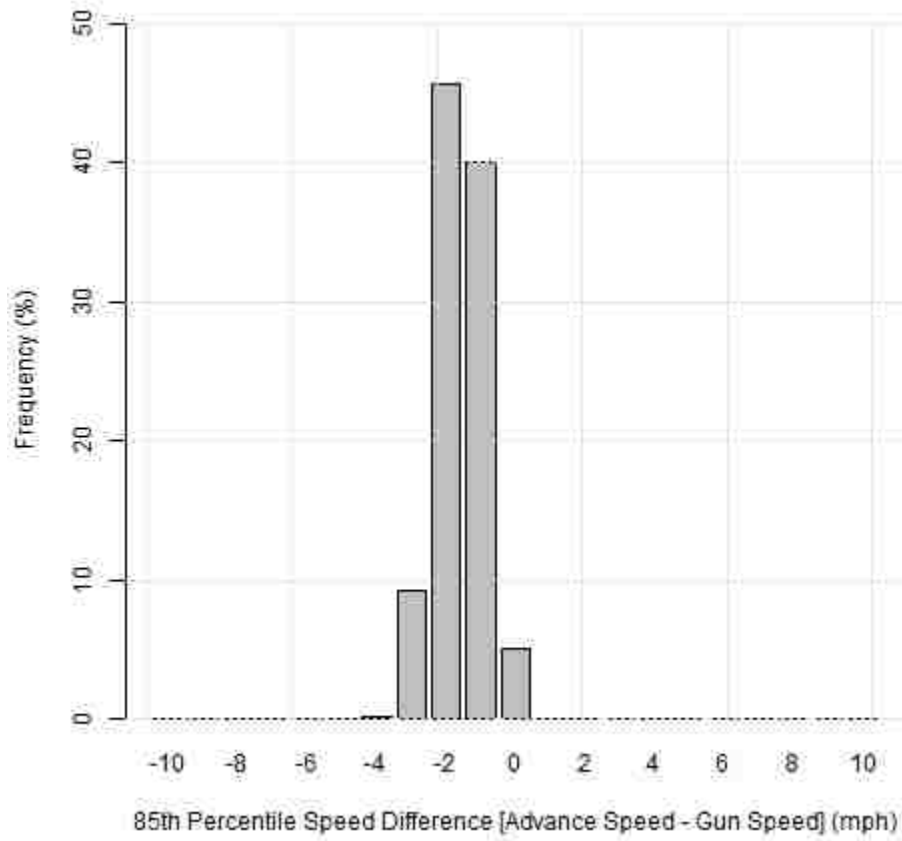


Figure E-4(c). Expected 85% Difference Distribution for Approach 4, EB at 400 East and 800 North, Orem.

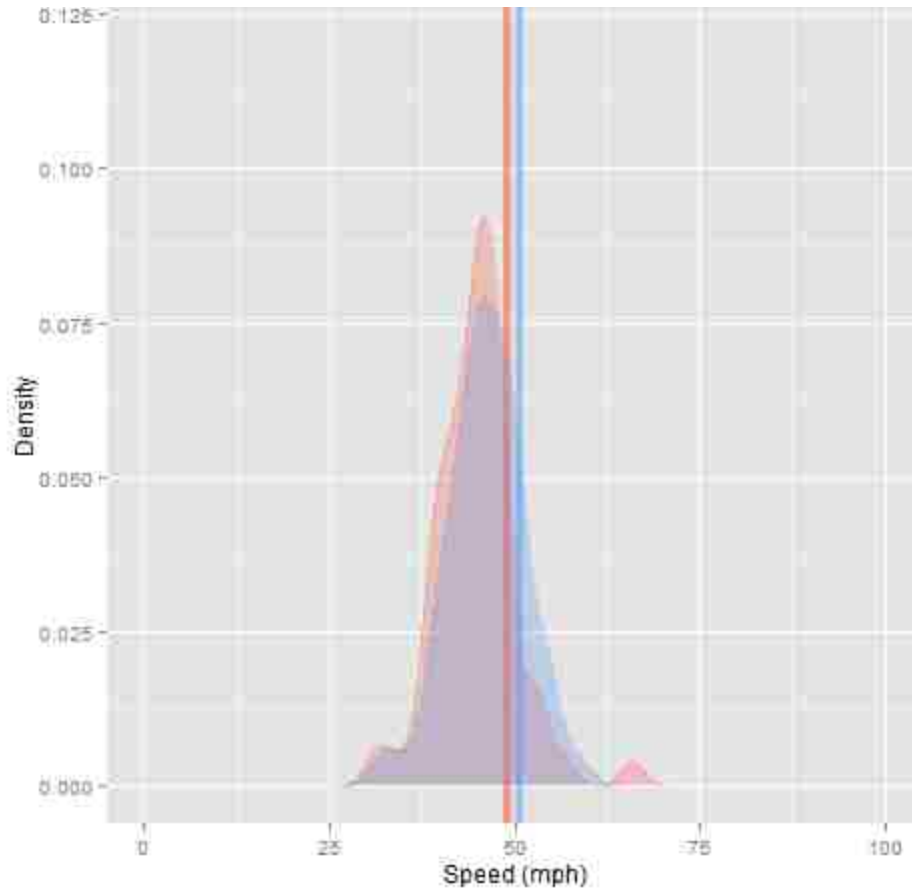


Figure E-5(a). Speed Distribution for Approach 5, WB at 400 East and 800 North, Orem.

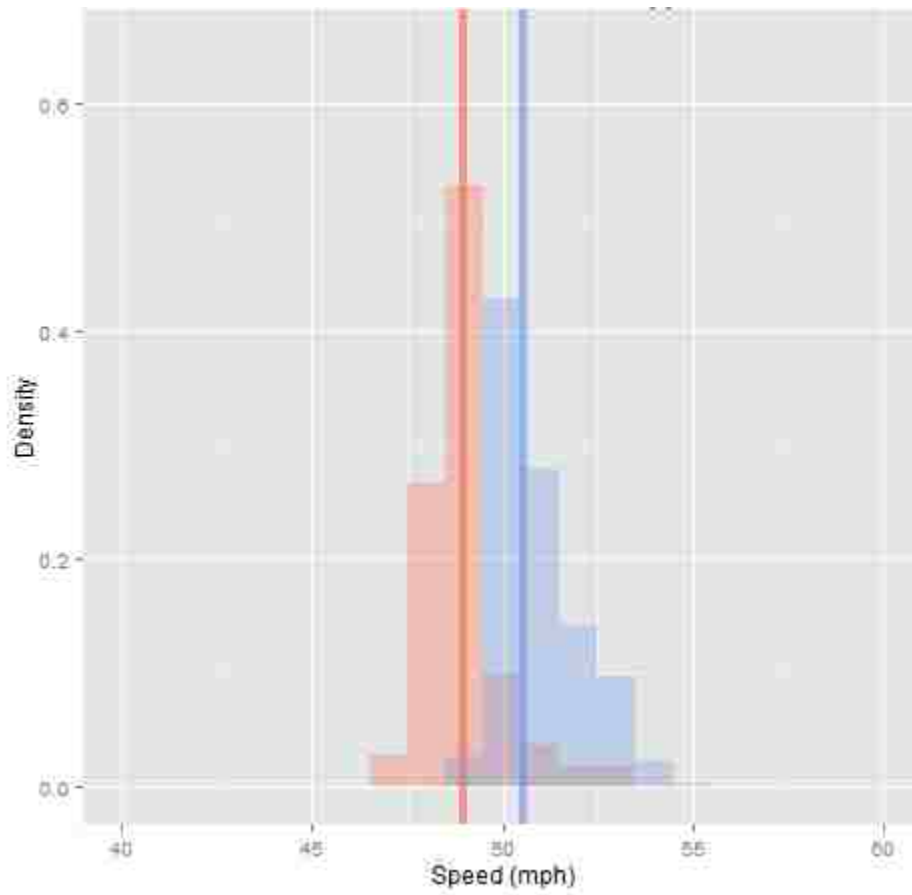


Figure E-5(b). 85th Percentile Speed Distribution for Approach 5, WB at 400 East and 800 North, Orem.

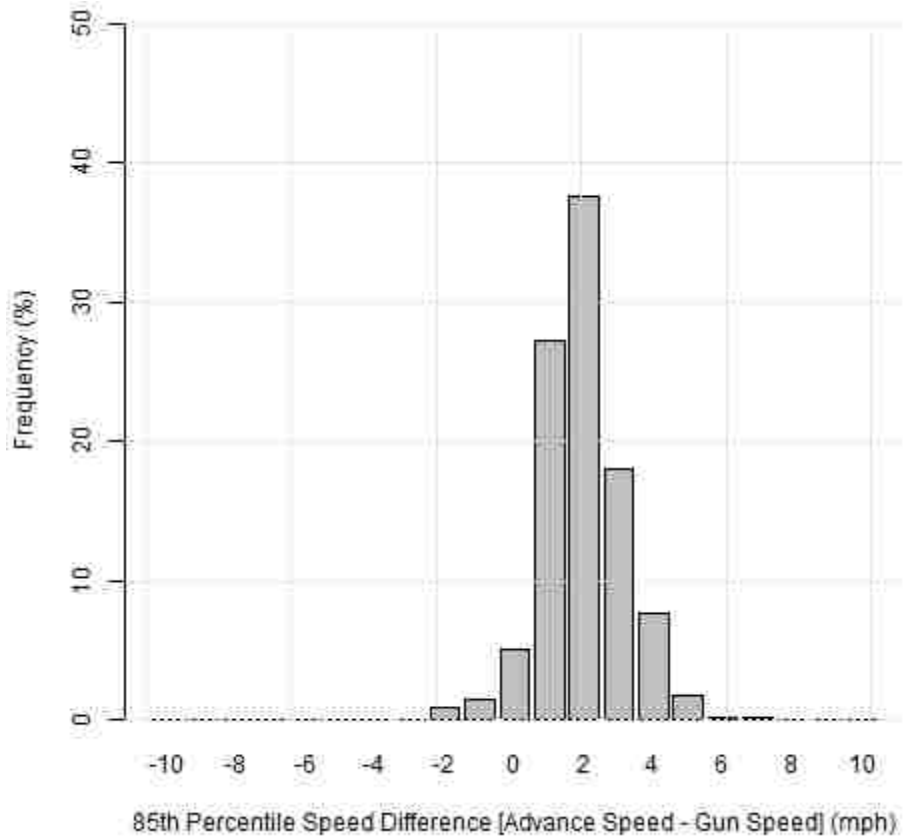


Figure E-5(c). Expected 85% Difference Distribution for Approach 5, WB at 400 East and 800 North, Orem.

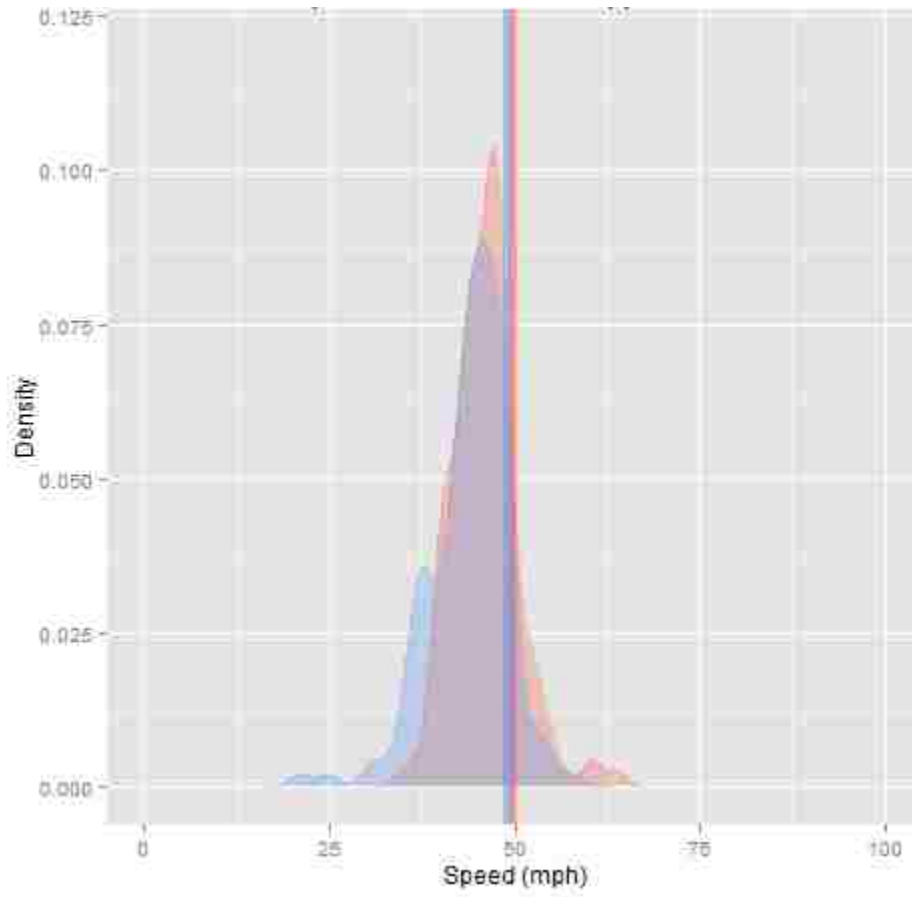


Figure E-6(a). Speed Distribution for Approach 6, EB at 9000 South and 700 West, Sandy.

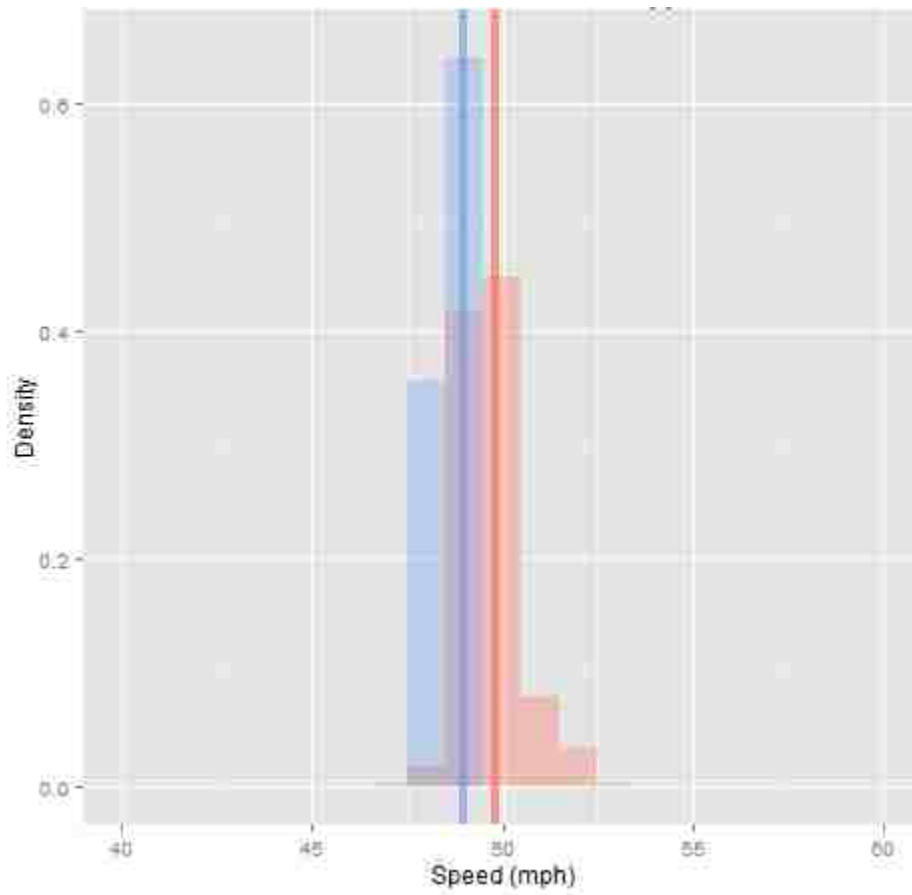


Figure E-6(b). 85th Percentile Speed Distribution for Approach 6, EB at 9000 South and 700 West, Sandy.

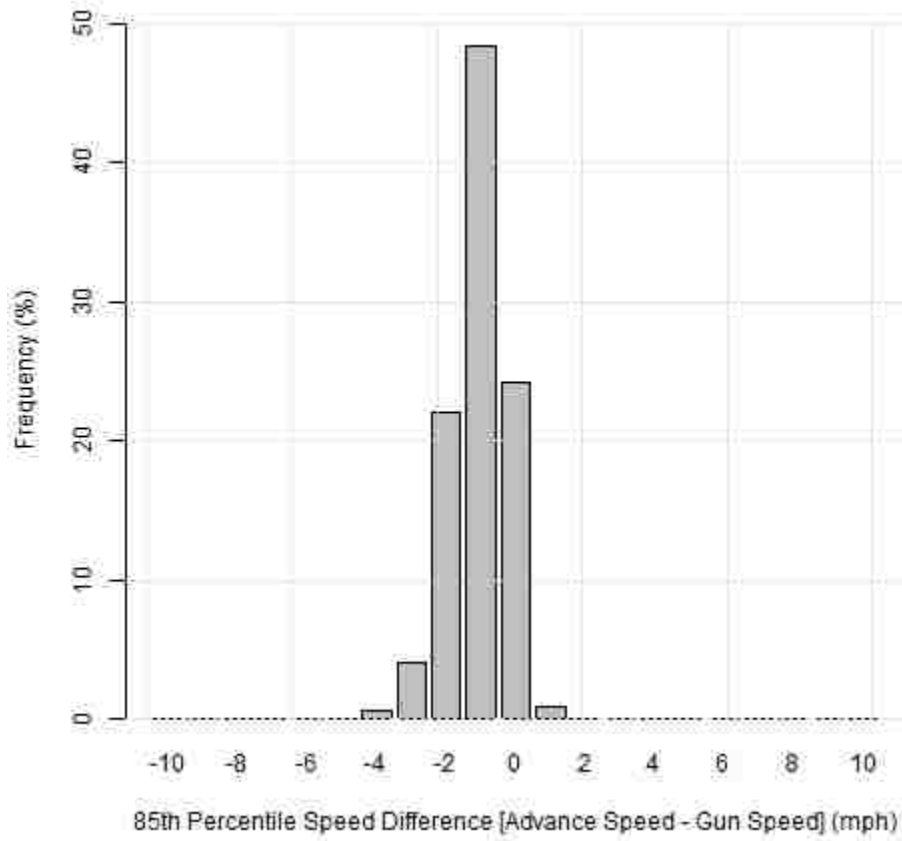


Figure E-6(c). Expected 85% Difference Distribution for Approach 6, EB at 9000 South and 700 West, Sandy.

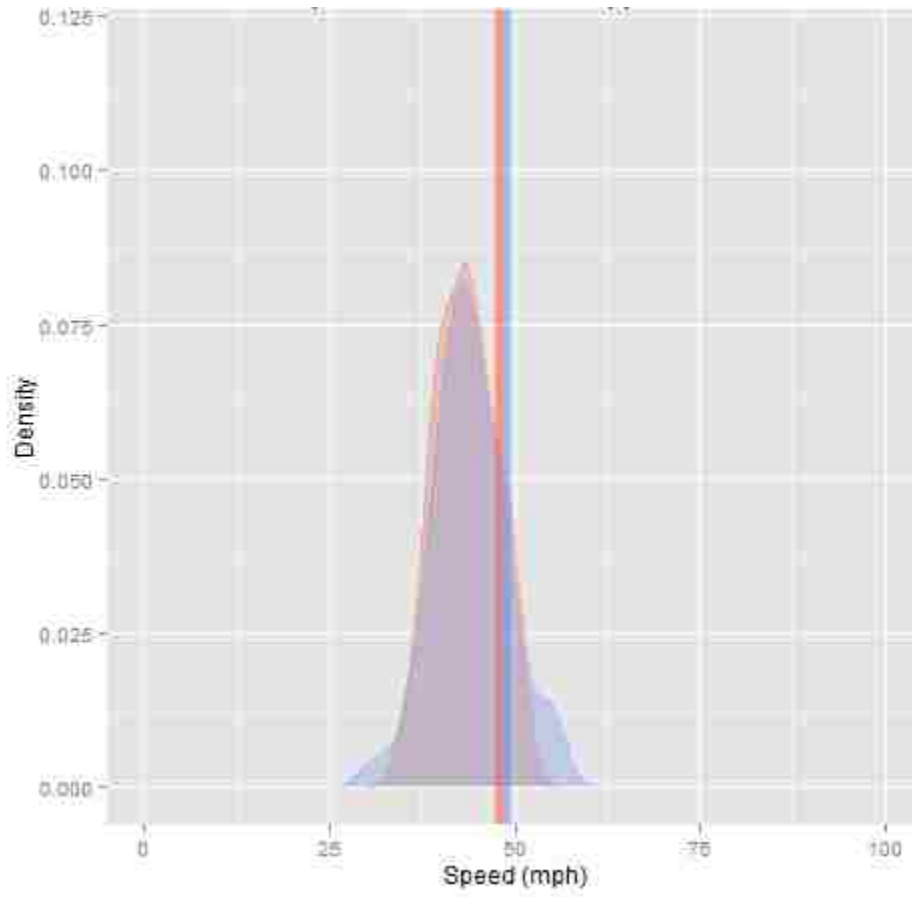


Figure E-7(a). Speed Distribution for Approach 7, WB at 9000 South and 700 West, Sandy.

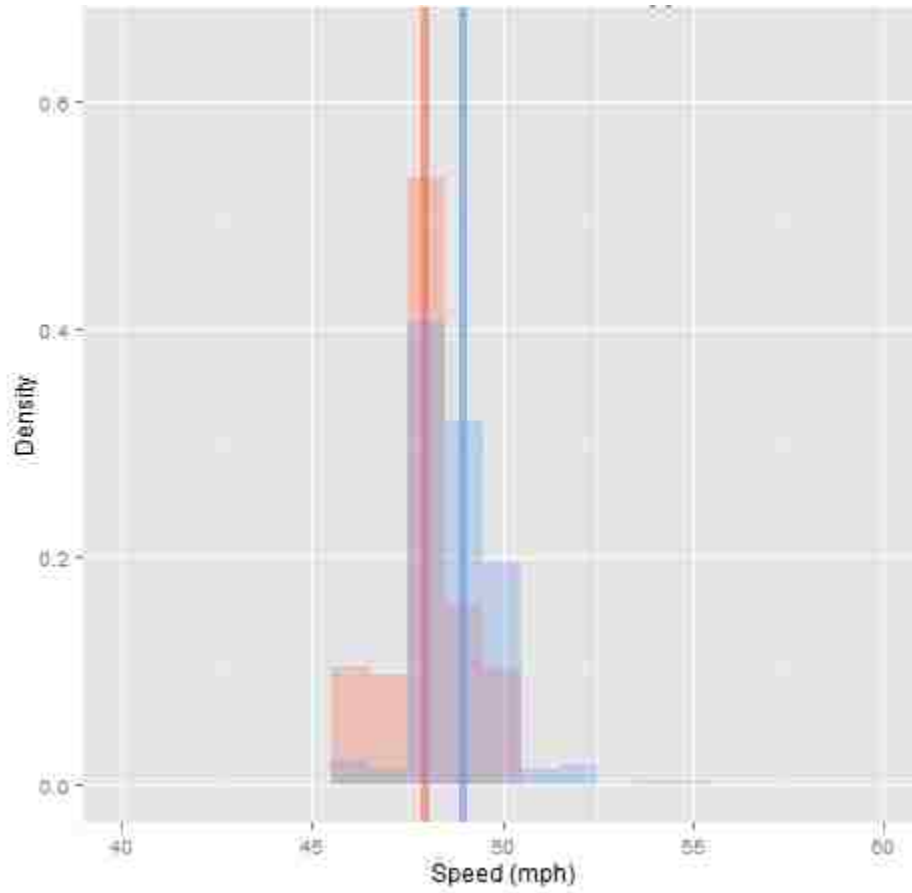


Figure E-7(b). 85th Percentile Speed Distribution for Approach 7, WB at 9000 South and 700 West, Sandy.

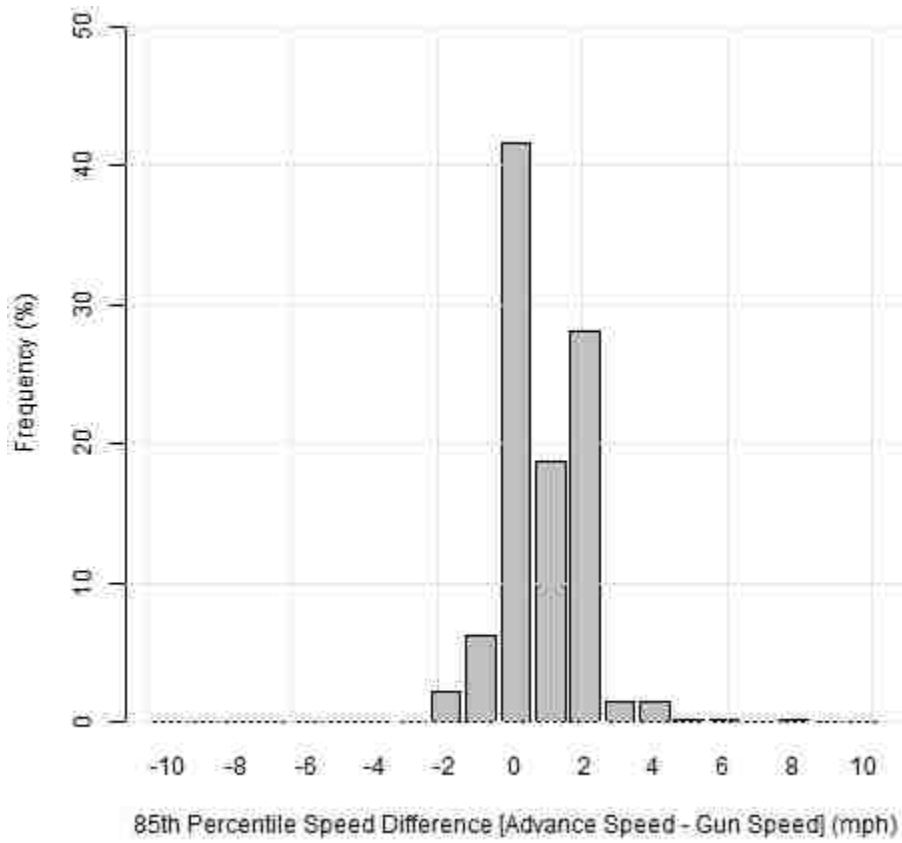


Figure E-7(c). Expected 85% Difference Distribution for Approach 7, WB at 9000 South and 700 West, Sandy.

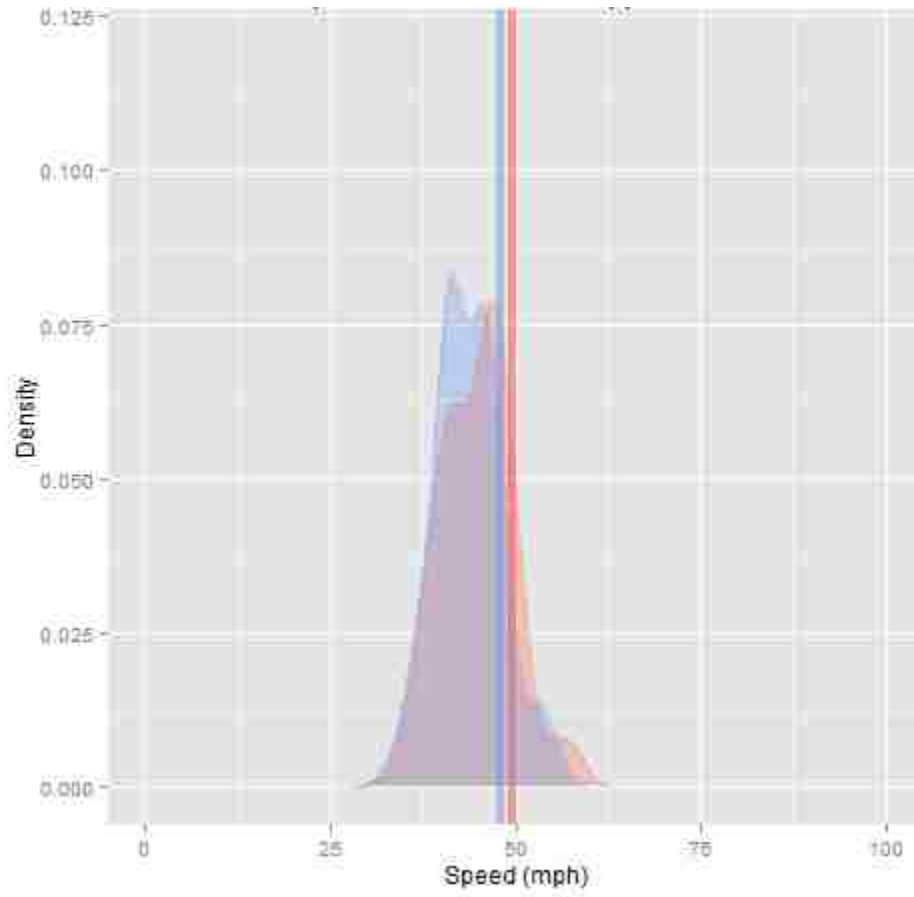


Figure E-8(a). Speed Distribution for Approach 8, WB at Geneva Rd and University Pkwy, Orem.

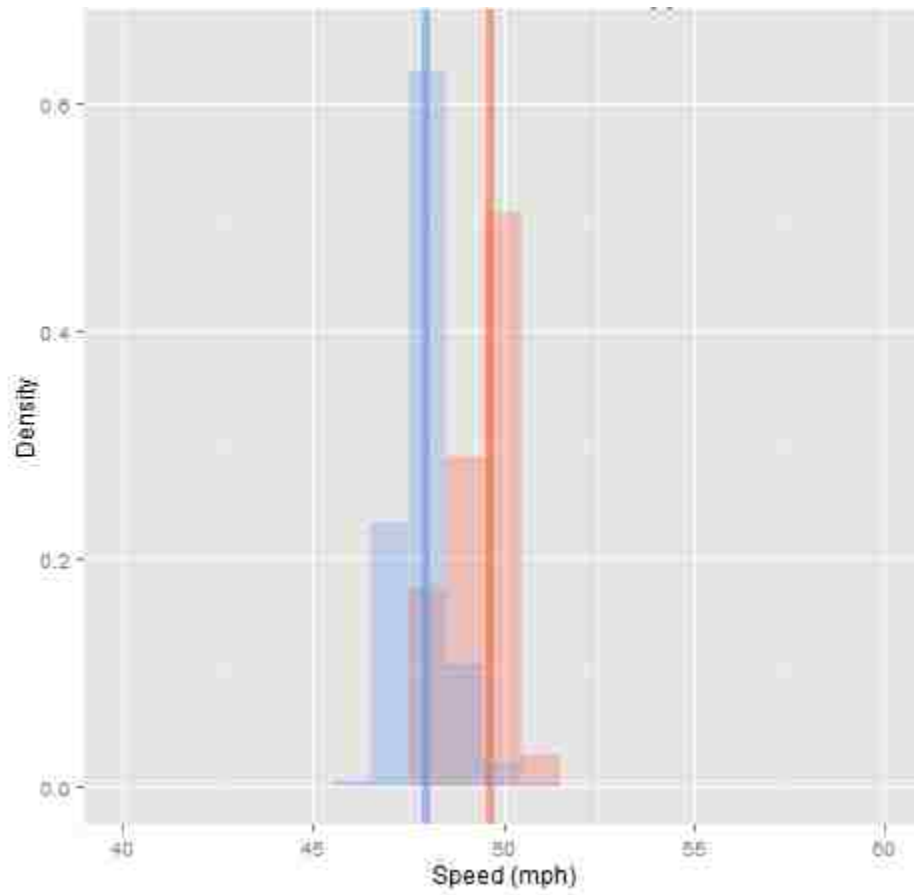


Figure E-8(b). 85th Percentile Speed Distribution for Approach 8, WB at Geneva Rd and University Pkwy, Orem.

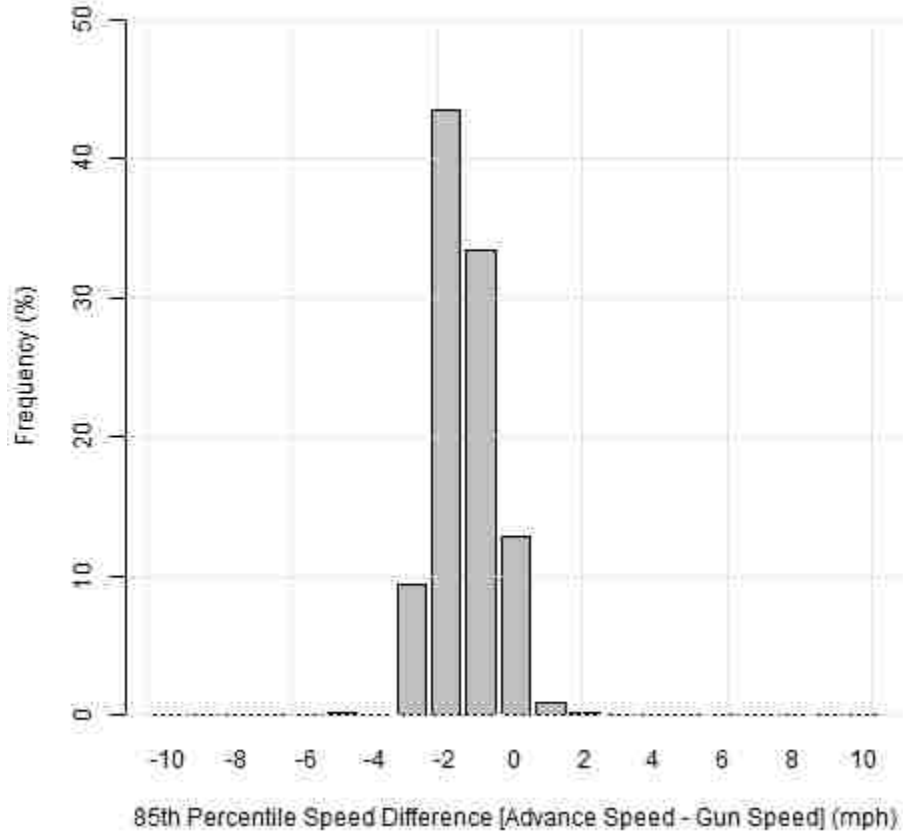


Figure E-8(c). Expected 85% Difference Distribution for Approach 8, WB at Geneva Rd and University Pkwy, Orem.